To the Graduate Council:

I am submitting herewith a dissertation written by Xingyuan Dong entitled "Theory of Electron-Capture Cross Section, Alignment, and Orientation in Low-Energy Collisions". I have examined the final copy of this dissertation for form and content and recommend that it be accepted in partial fulfillment of the requirements for the degree of Doctor of Philosophy, with a major in Physics.

Joseph H. Macek, Major Professor

We have read this dissertation
and recommend its acceptance:

Marianne Breinig

Accepted for the Council:

Associate Vice Chancellor
and Dean of The Graduate School

Theory of Electron-Capture Cross Section, Alignment, and Orientation in Low-Energy Collisions

A Dissertation
Presented for the
Doctor of Philosophy
Degree
University of Tennessee, Knoxville

Xingyuan Dong
May, 1994

Acknowledgements

I would like to express my deep gratitude to Dr. Joseph H. Macek for serving as my thesis advisor. He has always been frank, pleasant , open and available for help. His guidance, understanding, encouragement and sense of perspective have been a great source of enlightenment. I have also been given innumberable chances and immeasurable freedom to explore and discover on my own and use my knowledge to the full potential. I thank Dr. Macek for giving me an ideal working environment.

I would also like to thank the distinguished members on my committee, Professor Joachim E. Burgdoerfer, Professor Fredrerick A. Grimm, and Professor Marianne Breinig for their efforts and support in the progress of the thesis. I sincerely appreciate the helpful conversations with Dr. S. Yu Ovchinnikov for his help on several aspects of research presented in this thesis. I would like to thank Ivan Cordrey and Atef Titi for interactions that have formed an important part of my learning process. I wish to thank Dr. Paul Bergstrom for his invaluable assistance and thank James Sternberg for his help on the computer. I also wish to thank Dr. Sandra J. Ward for her help in many ways. I thank Professor Carolyn S. Carver for her help during writing my thesis. I also thank Merle Hancox, Maria Clark and Jeannette Lyons for their many considerations during the time of my work.

I want to thank my advisor, Professor Guozhu Ho in Nankai University, China, for his support and encouragement and helping me to get the opportunity to come to the U.S.A. to study. I also want to thank Nankai University for giving me a chance to come to America.

I also want to thank my dear husband Zhenwu Jiang and my two wonderful children Kanzhe, and Kanli for their understanding, endurance and invaluable support.

I also want to thank my family members in China, especially my father, who have sent me their spiritual support throughout my study.

Abstract

A Landau - Zener model with rotational and degenerate Stark - effect coupling is developed to calculate the partial and total cross sections of ionic states produced by collision of highly charged ions with neutral atoms. I apply this model to $C^{6+}+H(1s)$ collisions and obtain the total cross section and L-distributions. The results are compared with other calculations and available experimental data. I extend this single Landau-Zener crossing model to multiple Landau-Zener crossings and apply it to $O^{5+} + H(1s)$ and $C^{3+} + H(1s)$ collision processes. The total and partial cross sections are in agreement with available experimental data. I employ this model to calculate the mean value of atomic states produced by the $A^{Z_P+} + H(1s)$ collision process. I apply it to $C^{6+} + H(1s)$ and $B^{3+} + He$ collision processes and obtain the alignment and orientation parameters. When comparing the orientation parameter of $B^{3+} + He \rightarrow B^{2+}(2p) + He^{+}$ collisions with the experimental data, the result is very good.

Using the Demkov's contour integral expression for transition amplitudes, I derive a new model for the above collision process and apply it to $C^{6+}+H(1s)$ collisions. I obtain the total cross section. When comparing with the experimental data and other calculations, the result is excellent in the low velocity region.

Contents

1 Introduction 1

1.1 Electron transfer from neutral atoms to heavy multicharged ions.....1

1.2 Connection with the multiple crossing model of Demkov.....6

1.3 Theory of alignment and orientation of atomic states produced by the low-energy collision.....9

1.4 Plan of the thesis 9

2 Electron transfer from neutral atoms to full stripped heavy ions 12

2.1 Introduction.....12

2.2 Formulation 16

2.3 Modified method in very low-energy collisions.....28

2.4 Application to $C^{6+} + H(1s)$ collisions.....31

2.5 Extending Our Model to Multiple Landau-Zener Crossings.....35

2.6 Formula for no Rotational or no Stark-effect Coupling.....39

3 Extend the single Landau-Zener crossing model to the multiple Landau-Zener crossing model for partially charged heavy ions colliding with neutral atoms 43

3.1 Introduction 43

3.2 Formulation 44

3.3 Application to $O^{5+} + H(1s)$ and $C^{3+} + H(1s)$ Collisions.....47

4 Multiple crossing model of Demkov 59

4.1 Introduction 61

4.2 Formulation 61

4.3 Application to $C^{6+} + H(1s)$ Collisions.....67

5 Theory of alignment and orientation of atomic states produced by slow collisions of highly charged ions with neutral species 77

5.1 Introduction 77

5.2 Mean value of the irreducible tensors 78

5.3 Polarization of resonance fluorescence in the rotational coupling model 81

5.4 Application to $C^{6+} + H(1s)$ and $B^{3+} + He$ collisions 87

6 Conclusions 100

Bibliography 102

Appendices 107

A 0(4) group theory 108

B Relation between Euler angles and rotational angle 111

C Expression for submatrix $u_{nlm;Q}$ 115

D The represention of the amplitude and probability for multiple Landau-Zener crossing 117

E The represention of the amplitude and probability for partially charged ions colliding with hydrogen 125

F The nonlinear Hamilton 130

G The represention of the matrix $< j, m' | e^{iJ_x \phi} | j, m >$ 131

Vitae 133

List of Figures

Fig.1. Crossing of two molecular states.....2

Fig.2 Scheme for p-state during the collision.....5

Fig.3 Schematic adiabatic energy levels of the $A^{Z_P+}+H(1s)$ systems vs time.....14

Fig.4 Classical path of trajectory at low velocities region.....16

Fig.5 Classical path of trajectory at very low velocities region.....29

Fig.6 The value of the cross term of the probability with the factor $\sin[4j\alpha_{fi}+2\phi_s+2<Ea>]$.....29

Fig.7 Total cross section Q_n vs velocity for electron capture into $n=4$ level by fully stripped carbon ions.....33

Fig.8 Partial cross section $Q_{4,l}$ for electron capture into $n=4$ l-sublevels by fully stripped carbon ions in collision with $H(1s)$.....34

Fig.9 Partial cross section $Q_{4,3}$ for electron capture into $n=4$ $l=3$ sublevel by fully stripped carbon ions in collision with H(1s).....34

Fig.10 Schematic adiabatic energy levels for multistate of the $A^{Z_P+}+H(1s)$ systems vs time.....36

Fig.11 Schematic adiabatic energy levels of the $A^{q+}+H(1s)$ system vs time.....45

Fig.12 The total cross section Q for $O^{5+}+H(1s)$ collisions.....50

Fig.13 The partial cross sections for $O^{5+}+H(1s)$ collisions.....51

Fig.14 The cross section Q vs velocity for electron capture by C^{3+} ions.....54

Fig.15 The value of the matrix $<FA|\frac{\partial}{\partial R}|FB>$ vs the internuclear distance for $C^{3+}+H(1s)$ collision system.....55

Fig.16 The energy curves for the initial state and final state vs the internuclear distance for $C^{3+}+H(1s)$ collision system.....56

Fig.17 The cross section of the top-of-barrier model vs velocity for electron capture by C^{3+} 58

Fig.18 The total cross section for $C^{3+} + H(1s)$ collision system 59

Fig.19 The schematic angles between the nuclear distance vector $\vec{R}$ and unit vectors $\vec{n_1}$ and $\vec{n_2}$ 68

Fig.20 Effective energy levels of the $C^{6+} + H(1s)$ collision systems vs time 74

Fig. 21 The total cross section Q_n vs velocity for electron capture into $n = 4$ level by fully stripped carbon ions 76

Fig.22 The probability distribution of the crossing term with the factor $\cos \int_{t_i}^{t_f} [E_0(t) - E_n(t)]dt$ for $C^{6+} + H(1s)$ collision system at velocity $v = 22.8 \times 10^7 cm/sec$ 88

Fig.23 The probabilities, alignment, and orientation parameters as a function of impact parameter for $C^{6+} + H(1s)$ collision system at velocity $v = 0.5 \times 10^7 cm/sec$ 89

a) The probability P(b):

b) Alignment parameters A_0^{col} (b):

c) Alignment parameters A_{1+}^{col} (b):

d) Alignment parameters A_{2+}^{col} (b):

e) Orientation parameters O^{col} (b):

Fig.24 The probabilities, alignment, and orientation parameters as a function of impact parameter for $C^{6+} + H(1s)$ collision system at velocity $v = 22.8 \times 10^7 cm/sec$ 92

a) The probability P(b):

b) Alignment parameters A_0^{col}(b):

c) Alignment parameters A_{1+}^{col}(b):

d) Alignment parameters A_{2+}^{col}(b):

e) Orientation parameters O^{col}(b):

Fig.25 The integral alignment parameters (i.e. integrate over the impact parameters) as a function of velocities.....96

Fig.26 The orientation for 1.5-kev $B^{2+}(2p)$ ions produced by slow collision of $B^{3+} + He$.....98

Chapter 1

Introduction

1.1 Electron transfer from neutral atoms to heavy multicharged ions

Ion-atom collisions are an important subfield of atomic physics. Capture of an electron from neutral atoms by fully stripped heavy ions is a specific reaction that has received considerable theoretical and experimental attention in recent years. The interest stems in part from the importance of these charge transfer processes for various other fields of physics, for example, controlled magnetically confined fusion research[1,2,3] and astrophysics[4,5]. For the electron - capture processes, the large number of Rydberg states populated by such reactions hampers the *ab initio* computation of these processes and simple models have been sought. In addition, a solely numerical solution of any problem leaves a certain discontent, since the mechanism of the process studied often remains obscure. Therefore, it is desirable to obtain more analytical results although this is possible only under additional simplifications. Electron capture by highly charged projectiles in slow collisions, in which the velocity of atoms is substantially smaller than the velocity of the electrons in the atoms, makes it possible to introduce several valid approximations. Its basic framework is the adiabatic description employing the quasi - molecular states of the electron, accompanied by nonadiabatic transitions. This theory can be used to interpret various processes occurring in atomic collisions in gases, low-temperature plasmas, and electronic and ionic beams over a relatively wide energy range from

thermal energies to hundreds of electron volts[6].

The adiabatic approximation is one of the most widely used in physics at slow motion of a dynamic system. There have been several monographs and reviews on the adiabatic approximation and particularly on its applications to the atomic collisions[6,7], where it is used in calculations dealing with the processes of excitation, charge transfer, and ionization in the course of slow collisions of atoms when the motion of the nuclei can be regarded as classical. Let $\psi_1(\vec{r}, R)$ and $\psi_2(\vec{r}, R)$ be two electronic eigenfunctions of a molecule with stationary nuclei. The adiabatic approximation tells us that if the molecule is initially in state $\psi_1(\vec{r}, R)$, and R changes infinitely slowly from $R \gg R_0$ to $R \ll R_0$, then the molecule will remain in state $\psi_1(\vec{r}, R)$. R is the distance between nuclei and R_0 is the distance when the difference of adiabatic energy eigenvalues $\Delta E = E_1(R) - E_2(R)$ minimizes.

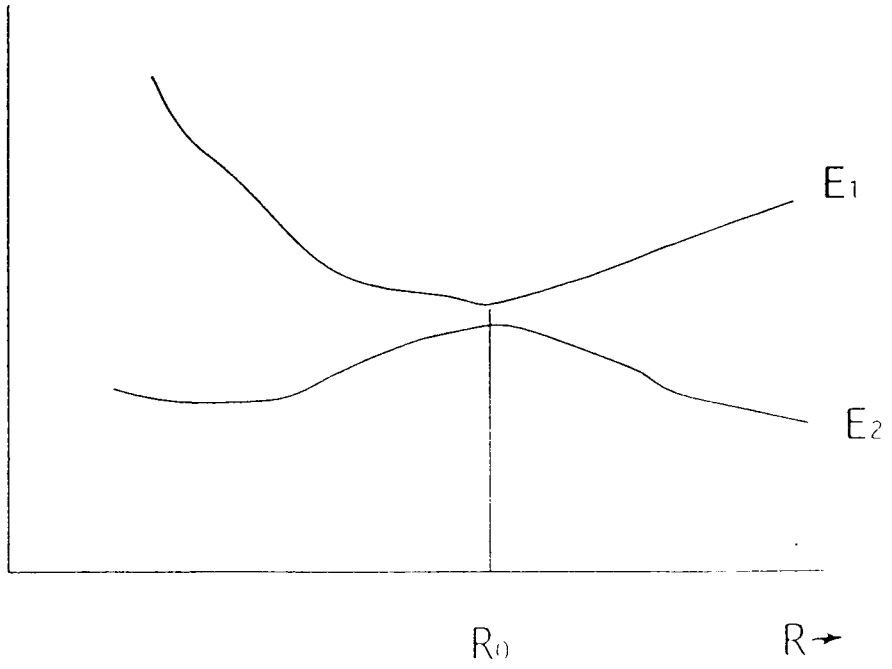


Fig.1. Crossing of two molecular states

However, if R changes with a finite velocity, the final state will be a linear combination[8]

$$\psi(\vec{r}, R) = A_1\psi_1(\vec{r}, R) + A_2\psi_2(\vec{r}, R). \quad (1)$$

Landau and Zener[8,9] modelled the above problem as a two-level system and solved the two coupled differential equations to determine non-adiabatic transitions. The two-level approximation has been further developed and the Landau-Zener formula has been made more precise by many papers[10,11]. Olson and Salop[12] employed a two-state curve-crossing mechanism to describe electron capture by highly charged ions. The diabatic potential curve correlating to the initial state A^{Z_P+} + B crosses several diabatic potential curves correlating to the final state $A^{(Z_P-1)+}(nlm)$ + B^+ formed by electron capture. For a n-manifold of n^2 eigenstates only one particular substate interacts significantly with the initial state at the crossing. This particular insight has been further developed by Taulbjerg[13] and forms the basis for his successful reaction-window analysis of low-energy ion-atom collisions. Despite this success, total cross sections in the original two-state theory are not in good accord with more elaborate calculations[14,15] and with the experiment[16]. The multistate calculations of Briggs and Vaaben[14] and Green, Shipsey, and Browne[15] show that all symmetry allowed nlm substates play a role in the capture process. A model of Abramov, Baryshnikov, and Lisitsa[17], which is similar to a model of Jaecks and co-workers[18], takes account of coupling between all of the degenerate substates approximately and obtains a total cross section in much better accord with more elaborate calculations than does the original two-state model[19].

The standard L-Z theory assumes that the collision system at the crossing point $R = R_0$ is traversed twice; once as the system passes along the classical path $\vec{R}(t)$

A and B separate ($t = t_f$). The system remains in adiabatic states at the all time except at $t = t_i$ and $t = t_f$. This gives an electron capture probability for each crossing equal to $p(1-p)$, where p is the probability of a transition at R_0.

In Ref. 18, Jaecks and co-workers point out that propagation between t_i and t_f is not adiabatic for degenerate states. They consider the effects of rotation coupling in the region (t_i,t_f). Rotational coupling among degenerate magnetic states implies that the symmetry axis of the state at t_i differs from that at t_f. Fig.2 shows schematic charge distributions of projectile p-states for successive positions along a classical straight line trajectory. Without rotational coupling Fig.(2a) the electron distribution follows the internuclear axis, and the propation between t_i and t_f is represented by a phase factor $\exp[i \int_{t_i}^{t_f} \Delta E(t)dt]$. With rotational coupling Fig.2(b) the electron charge doesn't follow the internuclear axis. In this case propagation between t_i and t_f includes a rotation function $d^l_{m,m'}(\theta)$ in addition to the usual phase factor. At large internuclear distances, when the two ions separate, the nlm sublevels are mixed by two effects: the rotational coupling and the Stark interaction due to the electric field of the residual ion. Therefore, I consider that the propagator could be a general matrix $U(t_i, t_f)$. For the general matrix I use Abramov's model[17] which includes the Stark effect. The Stark effect caused by the residual charge of the target after electron capture is strong enough to mix the various l substates for a given hydrogenic n state. I also extend this model to describe any number of n levels populated by multiple Landau - Zener crossings. In addition anisotropy parameters are computed for atomic states populated by electron capture.

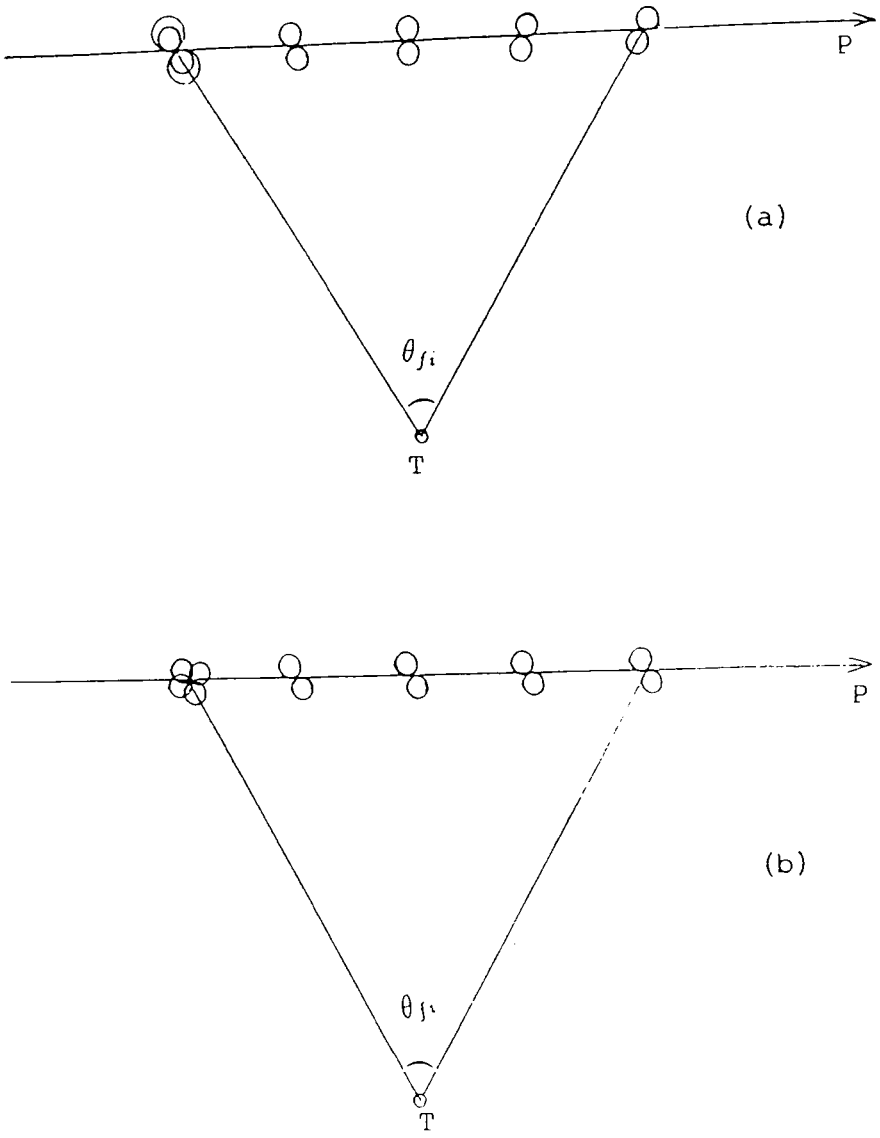


Fig.2. Scheme for p - state during the collision. (a) no rotational coupling between the degenerate states. (b) has rotational coupling between the degenerate states.

1.2 Connection with the multiple crossing model of Demkov

To represent the physical situation mathematically I construct a model involving a single state $|0>$ on the neutral target and a set of states $|A>$ with principle quantum number n on the ion after it has captured an electron. The set $|A>$ is further divided into a single state $|P>$ that couples to the state $|0>$ at time t_0 corresponding to the distance R_0, and a set of states $|Q>$ that do not so couple, but are coupled to $|P>$ at all times.

Corresponding to this division of the states there is a Hamiltonian matrix H of the form

$$H = \begin{pmatrix} H_{00} & H_{0P} & H_{0Q} \\ H_{P0} & H_{PP} & H_{PQ} \\ H_{Q0} & H_{QP} & H_{QQ} \end{pmatrix}, \tag{2}$$

where

$$H_{0Q} = H_{Q0} = 0,$$

$$H_{0P} = H_{P0} = const, \tag{3}$$

$$H_{00} = \alpha(t - t_0), \tag{4}$$

and H_{PP}, H_{PQ}, H_{QP}, H_{QQ}, are time-dependent block matrices to be determined later. For a final state with principle quantum number n, H_{PP} is a 1×1 matrix and H_{QQ} is a $(n^2 - 1) \times (n^2 - 1)$ matix. The parameter α is also a constant as in the standard Landau-Zener model.

At $t = t_0$ Landau-Zener transitions between channels 0 and P occur. These are described by the standard Landau-Zener transition matrix.

$$U^{LZ} = \begin{pmatrix} U_{00}^{LZ} U_{0P}^{LZ} 0 \\ U_{P0}^{LZ} U_{PP}^{LZ} 0 \\ 0 \quad 0 \quad 1 \end{pmatrix}, \tag{5}$$

where I represent the unit matrix in the subspace Q, and the other elements derive from two-state Landau-Zener theory.

The time-evolution matrix $U(t,t')$ for $t \neq t_0$ is approximated by

$$U(t,t') = \begin{pmatrix} \exp[-i\int_t^{t'} E_0(t")dt"] & 0 & 0 \\ 0 & U_{PP}(t,t')\, U_{PQ}(t,t') \\ 0 & U_{QP}(t,t')\, U_{QQ}(t,t') \end{pmatrix}, \tag{6}$$

where coupling to state $|0>$ is neglected for $t \neq t'$. The matrix $U_{AB}(t,t')$, where A, B represent indices P or Q, is determined by the model Hamiltonian of Eq.(4). It is supposed that the degenerate n - states have the energy $E_1(t)$ so that $U_{AB}(t,t')$ has the form

$$U_{AB}(t,t') = u_{AB}(t,t') \exp[-i\int_t^{t'} E_1(\tau)d\tau], \tag{7}$$

where some non-trivial models for $u_{AB}(t,t')$ will be introduced later. The time - evolution of the system through one crossing between $t = -\infty$ and $t' = 0$ is the product

$$U(0,-\infty) \approx U(0,t_0)U^{LZ}(t_0)U(t_0,-\infty). \tag{8}$$

The approximation in Eq.(8) consists in the neglect of the coupling matrix element H_{0P} for $t \neq t_0$. This approximation is standard in the Landau-Zener theory, which additionally takes the matrix $u_{AB}(t,t')$ equal to the unit matrix. The innovation in Ref. 18 is to use a non-diagonal matrix representing a rotation

$$u_{AB}(t,t') = d^{j}_{mm'}[\theta(t,t')], \tag{9}$$

where $\theta(t,t')$ is the angle through which the internuclear axis rotates between times t and t'. The innovation in my own work is to include the Stark-effect as well as rotation in the Hamiltonian[40] and in the matrix $u(t,t')$. The matrix elements in this case were computed by Abramov[17].

The Hamiltonian matrix elements are generally functions of time. If all except H_{00} are constant, then the model of Eq.(2) is easily transformed to the multiple - crossing model of Demkov and Osherov by diagonalizing the H matrix in the subspace spanned by P and Q. Upon transforming to this representation we have for H the expression

$$H' = \begin{pmatrix} H'_{00} & H'_{0A} \\ H'_{A0} & H'_{AA} \end{pmatrix}, \tag{10}$$

where H'_{AA} is diagonal, $H'_{00} = H_{00}$ varies linearly with time and H'_{0A} is a colum matrix of constants. This is just the multiple crossing model of Ref. (21). Because my submatrix is not constant with time, it is not possible to transform Eq.(2) to Eq.(10) exactly. In chapter 4 I show how the model of Eq.(2) is approximately transformed to the Demkov-Osherov model. Calculations are performed using this model and compared with available experimental data. Thus in my thesis I develop two models for multistate electron capture, namely the Landau-Zener model with rotational coupling and the Demkov-Osherov model. The two models are not equivalent: the Demkov-Osherov model applies when the eigenvalues of H_{AA} are well separated, while the Landau-Zener model works best when the eigenvalues are relatively close together.

1.3 Theory of alignment and orientation of atomic states produced by the low-energy collision

In collisions, electron charge clouds not only change size, they also change shape and rotate. Since the shape and circulation properties of excited states frequently reflect specific aspects of excitation processes, I compute these properties using my model. The shape of atomic states is given by "alignment" and the rotation by "orientation" parameters[22]. The study of alignment and orientation provides a more powerful tool to investigate details of electronic processes in atomic collision than does the simple determination of the probabilities and the cross sections for the same processes. Recently the study of polarization of atomic radiation emitted after impact excitation has yielded an enormous wealth of detailed information on the mechanism and dynamics of collisional excitation and energy transfer, both in electron and heavy particle impact studies.[23] In the work reported here I compute the mean value of irreducible tensors using the model of section 2.2 and 2.3, and obtain the general results for arbitrary irreducible tensors. Using these results I calculate the value of the linear polarization and the circular polarization for $C^{6+} + H(1s)$ collisions. I also apply this model to the $B^{3+} + He$ collision system and obtain the orientation parameter. Comparing the orientation parameter with the experimental data[24], we find good agreement with the experimental data of Ref. 24.

1.4 Plan of the thesis

I first present the formula for the electron capture cross section from neutral

atoms to fully stripped heavy ions in chapter 2. I use Abramov's general matrix $U(t_i, t_f)$ on the model of Ref.18 to obtain amplitudes and probabilities for electron capture from neutral atoms by fully stripped heavy ions in Sec. 2.2. In Sec. 2.3, I modify some parameters of the model, and obtain a modified model for electron capture in very low velocity regions. In Sec. 2.4, I apply the models of section 2.2 and 2.3 to the $C^{6+} + H(1s) \rightarrow C^{5+} + H^{+}$ collision process. I extend my single Landau-Zener crossing model to a multiple Landau-Zener crossings model in Sec. 2.5. In Sec.2.6, I discuss two special cases: one neglecting rotational coupling, and another neglecting the Stark - effect. For the latter, there are two cases in which we can neglect the Stark-effect: One is the $A^{Z_P+} + B^{-}$ collision, in which the fully stripped ions collide with negatively charged ions. The final states for this collision are $A^{(Z_P-1)+}(nlm) + B$ in which there is no Stark-effect even though the excited states of projectile are degenerate. Another is the $A^{q+} + B$ $(q < Z_P)$ collision, in which the partially stripped ions collide with neutral atoms. The final states for this collision is $A^{(q-1)+}(nlm) + B^{+}$ in which there is a Stark-effect but usually it is small compared with the energy difference between two close levels and can be neglected. I discuss the latter in chapter 3. In chapter 3, I extend the model of Ref.20 to the multiple Landau-Zener crossings for partially stripped projectiles. I obtain amplitudes and probabilities for electron capture from neutral atoms to partially stripped heavy ions in Sec.3.2. I apply the model of section 3.2 to O^{5+} + H and C^{3+} + H collision systems in Sec. 3.3. In chapter 4, I use the contour integral formula of Demkov and Osherov[21] to calculate the cross section for electron capture processes in low-energy collision. I apply this model to $C^{6+} + H(1s)$ collision system, and obtain amplitudes and probabilities for electron transfer in this alternative approximation. In chapter 5, I develop the theory of alignment and orientation in the Landau-Zener

model with rotational coupling. I apply this theory to the C^{6+} + H and B^{3+} + He collision systems. Comparing with the available experimental data, I find acceptable agreement.

Atomic units are used throughout this work unless stated otherwise. Additional technical details are given in appendices.

Chapter 2

Electron Transfer from Neutral Atoms to Full Stripped Heavy Ions

2.1 Introduction

In the approximation where the nuclei follow a classical path $\vec{R}(t)$, transitions between electronic states of colliding atoms or ions are described by the time-dependent Schrödinger equation[25]

$$H(\vec{R})\psi(\vec{r},t) = i\frac{\partial}{\partial t}\psi(\vec{r},t), \tag{11}$$

where $\vec{R} = \vec{R}(v,t)$ is the internuclear distance, v is the initial relative velocity of the nuclei, and $\vec{r}$ is the electron coordinate. In the straight line approximation

$$\vec{R}(t) = \vec{b} + \vec{v}t, \tag{12}$$

where b is the impact parameter. For a small velocity v the adiabatic approximation is appropriate and the electronic wavefunction $\psi(\vec{r},t)$ is expanded in molecular eigenstates $\phi(\vec{r},R)$,

$$\psi(\vec{r},t) = \sum_p A_p(t)\phi_p(\vec{r},R)\exp[-i\int^t E_p(R(vt'))dt'], \tag{13}$$

where $E_p(R)$ is the eigenvalues of equation

$$H(R)\phi_p(\vec{r},R) = E_p(R)\phi_p(\vec{r},R), \tag{14}$$

and $\phi_p(\vec{r}, R)$ are the corresponding eigenstates at fixed R. The well known electron translation factors $\exp[i\vec{v}.\vec{r}]$ were introduced by Bates and McCarroll[26] in collision treatments with separated atom bases to represent the relative motion of electrons belonging to their respective reactants. The form of translation factors, noncontroversial in separated-atom bases, has, however, continued to trouble treatments with molecular orbitals[27,28,29]. The hyperspherical procedure of Macek *et al*[30] and the Born-Oppenheimer procedure of Soloviev *et al*[31] have revealed that the use of these coordinates eliminates the need for translation factors in molecular processes. Therefore, I do not include the electron translation factors $\exp[i\vec{v}.\vec{r}]$ in my calculations. The probability of a transition from an initial molecular state $|0>$ at $t \rightarrow -\infty$ to a final state $|\phi_k>$ as $t \rightarrow +\infty$ is

$$P = lim_{t\rightarrow\infty}|A_k(t)|^2, \tag{15}$$

on the condition

$$lim_{t\rightarrow-\infty}A_k(t) = \delta_{k0}. \tag{16}$$

For systems of interest here the molecular eigenstates become atomic eigenstates as $|t| \rightarrow \infty$ so that P gives the desired probability for transition between atomic states. The probability P of the transition depends on the impact parameter b. Then the transition cross section

$$Q_k = 2\pi \int_0^\infty P(b)bdb. \tag{17}$$

The most important task is to compute the amplitude $A_k(b)$ of populating the $|\phi_k>$ state.

In our case, the reaction is

$$A^{Z_P+} + B \rightarrow A^{(Z_P-1)+}(nlm) + B^{+}. \tag{18}$$

A scheme of the relevant potential energy curves is shown in Fig. 3. Figure 3(a) is the classcial path of nuclei showing crossing R and figure 3(b) is a schematic adiabatic energy levels of the $A^{Z_P+} + H(1s)$ system vs time.

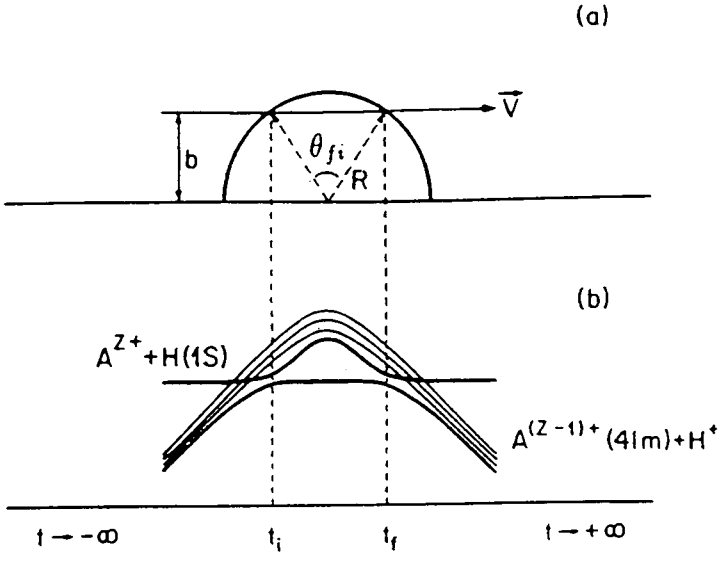


Fig.3. (a) Classical path showing crossing radius R and (b) Schematic adiabatic energy levels of the $A^{Z_P+} + H(1s)$ systems vs time.

Usually the initial channel, $A^{Z_P+} + B$, is slightly attractive at large internuclear distance owing to a polarization interaction between the ion and atom. In this section, I neglect this slight attraction in the initial channel and use the straight line approximation. The final states of $A^{(Z_P-1)+}$ (nlm) + B^{+} have repulsive Coulomb forms $(Z_P - 1)/R$ and cross the initial state. Strong coupling occurs at the crossing leading to electron transfer. The Landau-Zener probability of transition at the

potential crossing is given by[12]

$$P = \exp[-2\pi H_{12}^2/v_{rad}\Delta F], \tag{19}$$

where $v_{rad} = v(1 - b^2/R^2)^{1/2}$ is the radial velocity at the crossing R, R is the internuclear distance between nuclei at the two potential curve crossing point, H_{12} is one half the adiabatic splitting at the curve crossing R and ΔF the difference in slopes of the diabatic potential energy curves at R. The Landau-Zener model neglects the transition between all states except for two so that the transition cross section is equal to

$$Q_k = 2\pi \int_0^R 2P(1-P)bdb. \tag{20}$$

I employed this original two - state Landau - Zener model with rotational and degenerate Stark - effect coupling to obtain amplitudes and probabilities for capture to a nlm state in Sec. 2.2 for relative velocities below 30×10^7 cm/s. In the very low velocities region, I modified this model in Sec. 2.3. In Sec.2.4 I apply this model to the process

$$C^{6+} + H(1s) \rightarrow C^{5+}(nlm) + H^+, \tag{21}$$

and compare with available experimental data and previous results. I find satisfactory agreement with the L distributions computed by Green *et al.*[15] at low velocities, but find significant discrepancies as the relative velocity approaches the matching velocity.

2.2 Formulation

In the following I formulate my model for a bare projectile P of charge Z_P colliding with a hydrogen - like atom or ion of nuclear charge Z_T. I place the z'-axis along the initial velocity vector $\vec{v}$ and the x' axis in the scattering plane. The coordinate origin is placed at the target nucleus. The coordinate vector $\vec{r}$ represents the electron position with respect to the projectile and $\vec{R}(t)$ is the relative position of projectile and target nucleus. θ is the angle that $\vec{R}(t)$ makes with the initial velocity vector as shown in Fig.4. The Hamiltonian of the system is

$$H = -\frac{1}{2}\nabla^2 - \frac{Z_T}{|\vec{R}(t) - \vec{r}|} - \frac{Z_P}{r} + \frac{Z_T Z_P}{R(t)}. \tag{22}$$

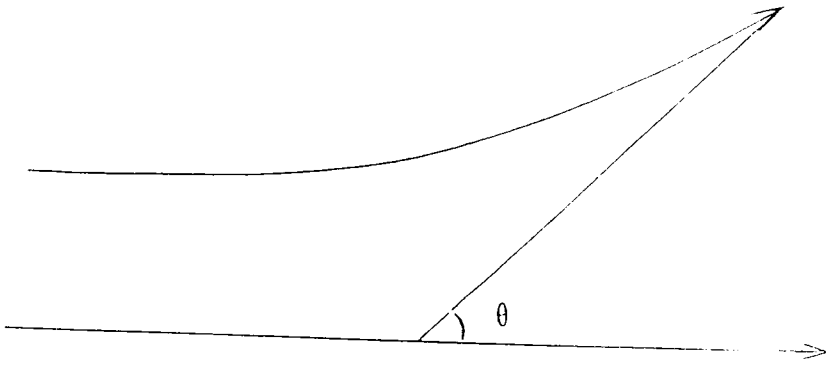


Fig. 4. Classical path of trajectory during the collision process.

In a rotating frame where the direction of $\vec{R}(t)$ is along the z-axis, the y-axis is

the axis of rotation. In the space-fixed frame the wavefunction ψ_f relates to the wavefunction in the rotating frame ψ_r according to

$$\psi_f = e^{-i\theta L_y}\psi_r. \tag{23}$$

The Hamiltonian of the rotating frame is

$$H_r = e^{i\theta L_y} H e^{-i\theta L_y} - \dot{\theta} L_y. \tag{24}$$

Then the $\vec{r}$ - dependent part of the interaction between the projectile P and the target T is taken to be

$$V_{int} = -\frac{Z_T}{|\vec{R} - \vec{r}|} - \dot{\theta} L_y + \frac{Z_T Z_P}{R}. \tag{25}$$

For R > r

$$\frac{1}{|\vec{R} - \vec{r}|} = \sum_l \frac{r^l}{R^{l+1}} P_l(\cos\theta), \tag{26}$$

where P_l is the l-order Legendre polynomial. The interaction potential of the second order approximation in the rotating frame is given by

$$V_{int} \approx -\frac{\vec{R}.\vec{r}}{R^3} - \dot{\theta} L_y + \frac{Z_T(Z_P - 1)}{R}. \tag{27}$$

The diagonal time-dependent factor $Z_T(Z_P$ - $1)/R$ contributes only to an overall phase factor so that it is omitted in the calculation of the submatrix $u_{nlm;Q}(t)$ but is included in the final expression. Then the interaction potential becomes

$$\begin{aligned} V_{int} &\approx -\frac{\vec{R}.\vec{r}}{R^3} - \dot{\theta} L_y \\ &= \frac{z}{R(t)^2} - \dot{\theta} L_y. \end{aligned} \tag{28}$$

In the semiclassical approximation, the heavy particle motion is described by a classical trajectory, the angle θ satisfies

$$R^2\dot{\theta} = -bv, \tag{29}$$

so that

$$V_{int} \approx -\frac{z - bvL_y}{R^2}, \tag{30}$$

where b is the impact parameter. I use the general method of Ref.17 and Ref.18 to write down the time - evolution matrix U(t,t') for the collision system. The time domain is divided into three regions, labeled I, II, and III, as illustrated in Fig. 3. According to Taulbjerg's reaction-window model, only one particular substate interacts significantly with the initial state $|0>$ at the crossing. I label this Stark state is $|Q>$. This state has a component of the dipole moment $<Q|\vec{r}|Q>$ along the direction of the electric field produced by the proton which is the largest of all of Stark substates. The crossing between the initial state $|0>$ and the single Stark state $|Q>$ occurs on the incoming part of the trajectory at t_i and the outgoing part at t_f. The times t_i and t_f separate the region I, II, and III.

The Stark eigenstates other than $|Q>$ are labeled by $|P>$. This partition of the degenerate Rydberg states of the ion with principle quantum number n is such that the space spanned by P+Q includes all nlm substates of the level n. Alternatively, the eigenstates can be written in the pseudospin representation $|j_1, m_1; j_2, m_2>$[32] with $j_1 = j_2 = (n-1)/2$ (see Apendix A) and $m = m_1 + m_2$. Both sets are complete in the subspace of the n level, but the latter is more convenient for computations since the long - range Stark coupling is diagonal in this representation.

I write the $U(\infty, -\infty)$ matrix using the Landau - Zener model at curve crossings, and employ the model of Ref.18 to compute $U(t, t')$ in the regions I, II, and III. I suppose the coupling between $|0>$ and $|Q>$ occurs only at the Landau - Zener

crossing and that $|Q>$ and $|P>$ are coupled at all times according to Eq.(30), but that $|P>$ does not couple directly to $|0>$. Then we have

$$U(\infty,-\infty) = U(\infty,t_f)U^{LZ}(t_f)U(t_f,t_i)U^{LZ}(t_i)U(t_i,-\infty), \tag{31}$$

where

$$U^{LZ}(t_i) = \begin{pmatrix} g & s^* & 0 & 0 & \cdots \\ -s & g & 0 & 0 & \cdots \\ 0 & 0 & 1 & 0 & \cdots \\ 0 & 0 & 0 & 1 & \cdots \\ \vdots & \vdots & \vdots & \vdots & \vdots \end{pmatrix}, \tag{32}$$

$$U(t,t') = \begin{pmatrix} U_{00}(t,t') & 0 & 0 & 0 & \cdots \\ 0 & U_{QQ}(t,t') & U_{QP_1}(t,t') & U_{QP_2}(t,t') & \cdots \\ 0 & U_{P_1Q}(t,t') & U_{P_1P_1}(t,t') & U_{P_1P_2}(t,t') & \cdots \\ 0 & U_{P_2Q}(t,t') & U_{P_2P_1}(t,t') & U_{P_2P_2}(t,t') & \cdots \\ \vdots & \vdots & \vdots & \vdots & \vdots \end{pmatrix}, \tag{33}$$

and

$$U^{LZ}(t_f) = \begin{pmatrix} g & -s & 0 & 0 & \cdots \\ s^* & g & 0 & 0 & \cdots \\ 0 & 0 & 1 & 0 & \cdots \\ 0 & 0 & 0 & 1 & \cdots \\ \vdots & \vdots & \vdots & \vdots & \vdots \end{pmatrix}. \tag{34}$$

In the reaction window model of Taulbjerg[13] the Landau - Zener parameters g and s are given by

$$g = e^{-\pi\gamma}, \tag{35}$$

$$\begin{aligned} s &= \frac{2\pi\gamma}{\Gamma(1+i\gamma)} \exp[-\frac{\pi\gamma}{2} + i\frac{\pi}{4} + i\gamma(ln\gamma - 1)] \\ &= |s|e^{i\phi_s + i\frac{\pi}{4}}, \end{aligned}$$

$$\phi_s = Im \ln \Gamma(1 - i\gamma) + \gamma(ln\gamma - 1), \tag{36}$$

$$\gamma = \frac{(9.13R)^2}{vZ_P(Z_P - 1)[1 - (b/R)^2]^{1/2}} \exp[-2.648R/\sqrt{Z_P}], \tag{37}$$

where v represents the relative velocity and R is the crossing radius. In addition, the Landau - Zener probability p is given by

$$p = |g|^2 = e^{-2\pi\gamma}, \tag{38}$$

and we have

$$|s|^2 = 1 - p. \tag{39}$$

The matrix U(t,t') is given by

$$U_{00}(t, t') = \exp[-i \int_t^{t'} E_0(\tau) d\tau], \tag{40}$$

$$U_{0i}(t, t') = U_{i0}(t, t') = 0, \qquad i \neq 0 \tag{41}$$

$$U_{ij}(t, t') = u_{ij}(t, t') \exp[-i \int_t^{t'} E_n(\tau) d\tau], \qquad i \neq 0, \quad j \neq 0. \tag{42}$$

Here $E_0(t)$ and E_n denote the energy of the diabatic states correlating to the initial state of the hydrogen - like atom and to the Rydberg level of the one - electron ion, respectively. The submatrix $u(t, t')$ which couples the Rydberg levels in the space spanned by P + Q is determined by the dynamics of the collision in an

approximation which represents the wave function of the system as a superposition of the degenerate substates of the Rydberg level n. A specific model for $u(t,t')$ will be given later.

I am interested in the element $U_{nlm;Q}(\infty,-\infty)$ equal to the amplitude $A_{nlm}(b)$ for populating state nlm by capture at an impact parameter b. It is found by carrying out the matrix multiplication in Eq.(31). The result is

$$\begin{aligned} A_{nlm}(b) = s^* g u_{nlm;Q}(\infty,t_f)\exp[-i\int_{-\infty}^{t_f} E_0(\tau)d\tau - i\int_{t_f}^{\infty} E_n(\tau)d\tau] \\ - s[(g-1)u_{Q;Q}(t_f,t_i)u_{nlm;Q}(\infty,t_f) + u_{nlm;Q}(\infty,t_i)] \\ \times \exp[-i\int_{-\infty}^{t_i} E_0(\tau)d\tau - i\int_{t_i}^{\infty} E_n(\tau)d\tau]. \end{aligned} \tag{43}$$

It remains to determine the matrix $u_{nlm;Q}$(t,t'). In the work of Jaecks *et al.*[18], this matrix was just a rotation matrix mixing eigenstates at the united atom limit. In my model it is necessary to take into account the electrostatic interaction of the H^+ ion with the electron in a Rydberg level of the $A^{(Z_P-1)+}$ ion. The submatrix $u(t,t')$ satisfies the equation:

$$i\frac{d}{dt}u(t,t') = V_{int}u(t,t'), \tag{44}$$

$$V_{int} = \frac{z - bvL_y}{R^2}. \tag{45}$$

Here $z = r\cos\theta$. This equation has been solved by many workers[17] employing the pseudospin representation. With $\vec{J}_1$ and $\vec{J}_2$ the pseudospin operators I have (see Apendix A)

$$u(t,t') = e^{i\alpha J_{1z}}e^{i\beta J_{1y}}e^{i\alpha J_{1z}}e^{-i\alpha J_{2z}}e^{i\beta J_{2y}}e^{-i\alpha J_{2z}}, \tag{46}$$

where α and β are Euler angles defined (see Appendix B) by

$$\omega(t,t') = -\frac{\Delta\theta(t,t')}{bv}[\ (3nZ_T/2Z_P)^2 + (bv)^2\ ]^{1/2}, \tag{47}$$

$$\tan\alpha(t,t') = \frac{3nZ_T}{2Z_P}[\ (3nZ_T/2Z_P)^2 + (bv)^2\ ]^{-1/2}\ \tan\frac{\omega(t,t')}{2}, \tag{48}$$

$$\cos\beta(t,t') = 1 - 2\frac{[\ bv\sin\frac{\omega(t,t')}{2}\ ]^2}{(3nZ_T/2Z_P)^2 + (bv)^2}. \tag{49}$$

Here $\Delta\theta(t,t')$ is the angle of the rotation of the internuclear axis during the time interval (t,t').

The state $|Q>$ refers to the pseudospin eigenstate,

$$|Q> = |j,j;j,-j>, \tag{50}$$

with $j_1 = j_2 =$ (n-1)/2. The conventional eigenstate $|nlm>$ relates to the pseudospin eigenstate according to the coupling scheme[32]

$$|nlm> = \sum_{m_1,m_2} |j,j;m_1,m_2\ ><\ j,j;m_1,m_2|lm\ >\ . \tag{51}$$

The matrix element $u_{nlm;Q}(t,t')$ is therefore given by

$$\begin{aligned} u_{nlm;Q}(t,t') &= <\ nlm|u(t,t')|j,j;j,-j\ > \\ &= \sum_{m_1,m_2} <\ j,j;m_1,m_2|lm\ ><\ j,j;m_1,m_2|u(t,t')|j,j;j,-j\ > \\ &= \sum_{m_1,m_2} <\ j,j;m_1,m_2|lm\ > u_{m_1,m_2;Q}(t,t'), \end{aligned} \tag{52}$$

where $<\ j,j;m_1,m_2|lm\ >$ is a Clebsch - Gordan coefficient. Recalling the definition of the rotation matrices $d^l_{m,m'}(\beta)$ and substituting Eq.(46) and Eq.(50) into the definition of $u_{m_1,m_2;Q}$ I have[20]

$$u_{m_1,m_2;Q} = e^{i(2j+m_1-m_2)\alpha} d^j_{m_1,j}(\beta) d^j_{m_2,-j}(\beta). \tag{53}$$

The rotation matrix elements that I need are given by

$$d^j_{m_1,j}(\beta) = (-1)^{(m_1-j)} d^j_{j,m_1}(\beta)$$
$$= (-1)^{(m_1-j)} \left[\frac{(2j)!}{(j+m_1)!(j-m_1)!}\right]^{1/2} \cos^{j+m_1}\frac{\beta}{2} \sin^{j-m_1}\frac{\beta}{2}$$
$$= (-1)^{(m_1-j)} \begin{pmatrix} 2j \\ j-m_1 \end{pmatrix}^{1/2} \cos^{j+m_1}\frac{\beta}{2} \sin^{j-m_1}\frac{\beta}{2}, \tag{54}$$

$$d^j_{m_2,-j}(\beta) = \begin{pmatrix} 2j \\ j-m_2 \end{pmatrix}^{1/2} \cos^{j-m_2}\frac{\beta}{2} \sin^{j+m_2}\frac{\beta}{2}, \tag{55}$$

so that

$$u_{nlm;Q} = \sum_{m_1,m_2} (-1)^{(m1-j)} e^{i(2j+m_1-m_2)\alpha} < j,j;m_1,m_2|lm >$$
$$\times \begin{pmatrix} 2j \\ j-m_1 \end{pmatrix}^{1/2} \begin{pmatrix} 2j \\ j-m_2 \end{pmatrix}^{1/2} (\cos\frac{\beta}{2}\sin\frac{\beta}{2})^{2j} \tan^{m-2m_1}\frac{\beta}{2}. \tag{56}$$

It is convenient to represent the binomial coefficients in terms of Clebsch - Gordan coefficients according to

$$\begin{pmatrix} 2j \\ j-m_1 \end{pmatrix}^{1/2} \begin{pmatrix} 2j \\ j-m_2 \end{pmatrix}^{1/2} = < j,m_1;j,m_2|2j,m > \left[\frac{(4j)!}{(2j+m)!(2j-m)!}\right]^{1/2}, \tag{57}$$

where $m = m_1 + m_2$. Then Eq.(56) may be written as

$$u_{nlm;Q}(t,t') = (-1)^{(\frac{m}{2}-j)} [e^{i\alpha}\cos\frac{\beta}{2}\sin\frac{\beta}{2}]^{2j} \left[\frac{(4j)!}{(2j+m)!(2j-m)!}\right]^{1/2}$$
$$\times \sum_{m_1,m_2} < l,m|j,j;m_1,m_2 > (ie^{i\alpha}\cot\frac{\beta}{2})^{(m_1-m_2)}$$
$$\times < j,j;m_1,m_2|2j,m > . \tag{58}$$

This sum has been evaluated by Biedenharn[33] (see Appendix C). To use his result I define the complex angle χ as

$$e^{i\chi} = ie^{i\alpha}\cot\frac{\beta}{2}. \tag{59}$$

According to Eq.(50) of Ref.33, the matrix element $u_{nlm;Q}$ is given by[34,35]

$$\begin{aligned} u_{nlm;Q}(t,t') = & i^{m-l}2^{-l}\sin^{-l}\chi[e^{i\alpha}\sin\beta\sin\chi]^{2j} \\ & \times\frac{(2j)!}{l!}\left[\frac{(2l)!(2l+1)!}{(l+m)!(l-m)!(2j-l)!(2j+l+1)!}\right]^{1/2} \\ & \times {}_2F_1(m-l,-m-l;\frac{1}{2}-l;\frac{1-\cos\chi}{2}). \end{aligned} \tag{60}$$

Using Eq.(15.3.29) of Ref.34 and Eq.(8.812) of Ref.35, I have

$$\begin{aligned} u_{nlm;Q}(t,t') &= (-1)^l < j,j;j,-j|l,0 > [e^{i2\alpha}\cos^2\frac{\beta}{2}+\sin\frac{\beta}{2}]^{2j} \\ &\times\left[\frac{(l-m)!}{(l+m)!}\right]^{1/2} P_l^m(i\cot\chi) \\ &= (-1)^l < j,j;j,-j|l,0 > [e^{i2\alpha}\cos^2\frac{\beta}{2}+\sin\frac{\beta}{2}]^{2j} d^l_{m,0}(\delta) \end{aligned} \tag{61}$$

where $P_l^m(i\cot\chi)$ is the associated Legendre function, $\cos\delta = i\cot\chi$, and $d^l_{m,0}(\delta)$ is a rotation function defined as Eq.(54). In this work I employ the complex associated Legendre function defined according to

$$P_l^m(x) = (1-x^2)^{m/2}\frac{d^m}{dx^m}P_l(x), \qquad m>0, \tag{62}$$

$$P_l^{-m}(x) = (-1)^m\frac{(l-m)!}{(l+m)!}P_l^m(x), \tag{63}$$

and $P_l(x)$ is the Legendre polynomial. I also note that

$$u_{Q;Q}(t,t') = e^{4j\alpha}\cos^{4j}\frac{\beta}{2}. \tag{64}$$

To express my result, I introduce Euler angles α and β with subscripts i, f, and fi corresponding to time intervals (∞, t_i), (∞, t_f), and (t_f, t_i), respectively. In addition, I introduce the complex angles ζ_{ii}, ζ_{ff}, and ζ_{if} given by

$$\zeta_{ab} = \delta_a - \delta_b^*, \qquad a, b = i, f. \tag{65}$$

I define the coefficients C_{nl}^f and C_{nl}^i as

$$\begin{aligned} C_{nl}^f = (-1)^l < \ j,j;j,-j|l,0 \ > [e^{i2\alpha_f}\cos^2\frac{\beta_f}{2} + \sin^2\frac{\beta_f}{2}]^{2j} \\ \times \left[s^* g \exp[-i\int_{-\infty}^{t_f} E_0(\tau)d\tau - i\int_{t_f}^{\infty} E_n(\tau)d\tau] \right. \\ \left. - s(g-1)\cos^{4j}\frac{\beta_{fi}}{2}\exp[i4j\alpha_{fi} - i\int_{-\infty}^{t_i} E_0(\tau)d\tau - i\int_{t_i}^{\infty} E_n(\tau)d\tau] \right], \end{aligned} \tag{66}$$

$$\begin{aligned} C_{nl}^i = (-1)^{l-1} s < \ j,j;j,-j|l,0 \ > [e^{i2\alpha_i}\cos^2\frac{\beta_i}{2} + \sin\frac{\beta_i}{2}]^{2j} \\ \times \exp[-i\int_{-\infty}^{t_i} E_0(\tau)d\tau - i\int_{t_i}^{\infty} E_n(\tau)d\tau], \end{aligned} \tag{67}$$

so that the amplitude $\mathrm{A}_{nlm}(\mathrm{b})$ is given by

$$A_{nlm}(b) = C_{nl}^f d_{m,0}^l(\delta_f) + C_{nl}^i d_{m,0}^l(\delta_i). \tag{68}$$

Eq.(68) is written in a form which exhibits the m - dependence of the amplitude explicitly. This m-dependence appears only in the rotation functions. I first construct the probablity $P_{nlm}(\mathrm{b})$

$$\begin{aligned} P_{nlm}(b) &= |A_{nlm}(b)|^2 \\ &= |C_{nl}^f|^2 |d_{m,0}^l(\delta_f)|^2 + |C_{nl}^i|^2 |d_{m,0}^l(\delta_i)|^2 \\ &+ [C_{nl}^f C_{nl}^{*i} d_{m,0}^l(\delta_f) d_{m,0}^{*l}(\delta_i) + c.c.]. \end{aligned} \tag{69}$$

where $c.c.$ denotes complex conjugate. I introduce the average integral $< Ea >$[36];

$$< Ea >= \int_b^R (E_0 - E_n)\frac{dR'}{\dot{R}'}, \tag{70}$$

where R is the crossing radius. Then

$$\int_{t_i}^{t_f} (E_0(t) - E_n(t))dt = 2 < Ea >, \tag{71}$$

and

$$\begin{aligned} |C_{nl}^f|^2 = & (1-p) < j,j;j,-j|l,0 >^2 (1-\sin^2\beta_f \sin^2\alpha_f)^{n-1} \\ & \times \left\{ p + (1+p-2\sqrt{p})\cos^{4(n-1)}\frac{\beta_{fi}}{2} \right. \\ & + 2\sqrt{p}(p-1)\cos^{2(n-1)}\frac{\beta_{fi}}{2} \\ & \left. \times \sin[2(n-1)\alpha_{fi} + 2\phi_s + 2 < Ea >] \right\}, \end{aligned} \tag{72}$$

$$|C_{nl}^i|^2 = (1-p) < j,j;j,-j|l,0 >^2 (1-\sin^2\beta_i \sin^2\alpha_i)^{n-1}, \tag{73}$$

$$\begin{aligned} C_{nl}^f C_{nl}^{*i} = & (1-p) < j,j;j,-j|l,0 >^2 \\ & \times [(e^{i2\alpha_f}\cos^2\frac{\beta_f}{2} + \sin^2\frac{\beta_f}{2})(e^{-i2\alpha_i}\cos^2\frac{\beta_i}{2} + \sin^2\frac{\beta_i}{2})]^{n-1} \\ & \times \left\{ p + (1+p-2\sqrt{p})\cos^{4(n-1)}\frac{\beta_{fi}}{2} \right. \\ & \times \left[e^{i2(n-1)\alpha_{fi}}(\sqrt{p}-1)\cos^{2(n-1)}\frac{\beta_{fi}}{2} \right. \\ & \left. \left. - \sqrt{p}\exp[-i(\pi/2 + 2\phi_s + 2 < Ea >]] \right\}. \end{aligned} \tag{74}$$

$\phi_s = Im \ln\Gamma(1-i\gamma) + \gamma(ln\gamma - 1)$ is the phase factor of Landau-Zener parameter s. Eq.(69) gives the LM distributions for a specific n level. Using the group property of the rotation function in Eq.(69) and summing over m

$$P_l(\cos\zeta_{ab}) = \sum_m d^l_{m,0}(\delta_a) d^{*l}_{m,0}(\delta_b), \tag{75}$$

where

$$\zeta_{ab} = \delta_a - \delta_b^*, \tag{76}$$

I obtain P_{nl}(b),

$$\begin{aligned} P_{nl}(b) &= |C_{nl}^f|^2 P_l(\cos\zeta_{ff}) + |C_{nl}^i|^2 P_l(\cos\zeta_{ii}) \\ &+ [C_{nl}^f C_{nl}^{*i} P_l(\cos\zeta_{fi}) + c.c.]. \end{aligned} \tag{77}$$

Summing over all substates gives the n-level probability

$$\begin{aligned} P_n(b) = (1-p)\Big\{\Big[p+1+(p-1)|u_{Q;Q}(t_f,t_i)|^2\Big] \\ + 2p|u_{Q;Q}(t_f,t_i)|\sin[4j\alpha(t_f,t_i) + 2\phi_s + 2 < Ea >]\Big\}. \end{aligned} \tag{78}$$

If I drop the term with the factor $\sin[4j\alpha(t_f,t_i)+2\phi_s+2<Ea>]$ of the probability $P_n(b)$, I have the probability computed directly by Abramov *et al*[17].

$$P_n(b) = (1-p)\left[p+1+(p-1)|u_{Q;Q}(t_f,t_i)|^2\right]. \tag{79}$$

The partial cross section for a sublevel l is

$$Q_{n,l} = 2\pi \int_0^R P_{n,l}(b) b db, \tag{80}$$

and the total cross section is

$$\begin{aligned} Q_n &= \sum_l Q_{n,l} \\ &= \sum_l 2\pi \int_0^R P_{n,l}(b) b db. \end{aligned} \tag{81}$$

I have used Eq.(80) and Eq.(81) to compute $Q_{n,l}$ and Q_n in the straight line approximation $R^2 = b^2 + v^2t^2$. This relatively simple expression for the l-partial cross

section is readily computed[20]. Indeed the computations are not much more difficult than those needed to compute the total cross section.

2.3 Modified method in very low-energy collision

In very low-energy collision(v< 0.5×10^7 cm/sec), electrons of the temporary quasi-molecule formed in the collision have sufficient time to adjust to the changing interatomic field as the nuclei approach and separate. As collision energies decrease below 1 eV/amu the ion-induced dipole attractive potential owing to a polarization interaction between the ion A^{+Z_P} and atom B in the initial channel is important. These effects can lead to an enhancement in the cross section that increases with decreasing collision energy. In order to explain the collision mechanism for reaction of Eq.(30). a scheme of the classical path of trajectory at very low velocities region is shown in Fig. 5. In the very low energy region, my calculation shows that the cross term in Eq.(78) with the factor $\sin[4j\alpha(t_f,t_i)+2\phi_s+2<Ea>]$ is very small and varies very rapid as shown in Fig.6. Therefore, I can drop it. Then I have the probability P_n for the n level

$$P_n=(1-p)[1+p+(p-1)|u_{Q;Q}(t_f,t_i)|^2], \tag{82}$$

here

$$|u_{Q;Q}(t_f,t_i)|^2=[1-\frac{(bv\sin\frac{\omega(t_f,t_i)}{2}}{(\frac{3nZ_t}{2Z_P})^2+b^2v^2}]^{2(n-1)}, \tag{83}$$

$$\frac{\omega(t_f,t_i)}{2}=-\frac{\Delta\theta(t_f,t_i)}{2bv}[(\frac{3nZ_t}{2Z_P})^2+(bv)^2]^{1/2}. \tag{84}$$

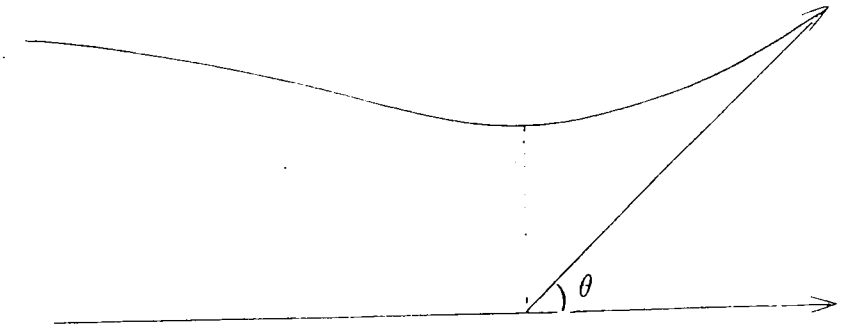


Fig. 5. Classical path of trajectory at very low velocity region.

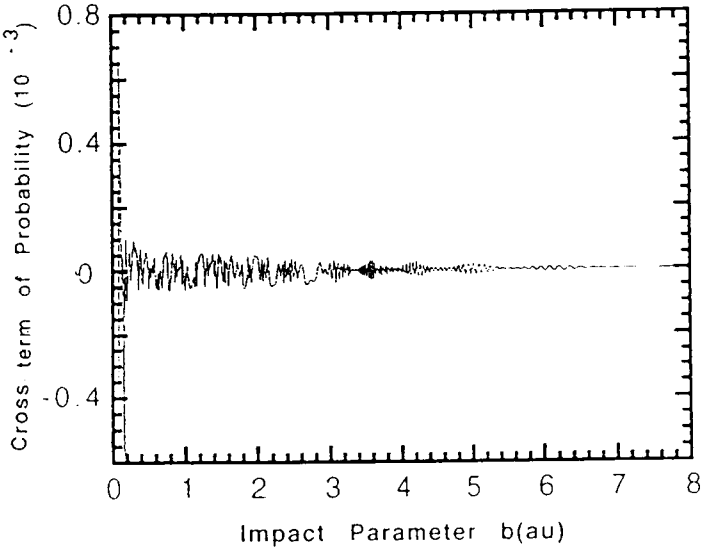


Fig.6 The value of the cross term of the probability with the factor $\sin[4j\alpha(t_f, t_i) + 2\phi_s + 2 < Ea >]$ for $C^{6+} + H \rightarrow C^{5+} + H^+$

In the straight line approximation, as shown in Fig. 3

$$\begin{aligned}\Delta\theta(t_f, t_i) &= \pi - 2\theta(\infty, t_f) \\ &= \pi - 2\sin^{-1}\frac{b}{R}.\end{aligned} \tag{85}$$

But in present case, the straight line approximation is no longer accurate as shown in Fig. 5. Because of the attraction of the polarization, the impact parameter b varies from 0 to b_{max} instead from 0 to R. For $A^{+Z_P} + B \rightarrow A^{+(Z_P-1)} + B^+$ collision system, b_{max} is

$$b_{max} = R\sqrt{1 + \frac{\alpha Z_p^2}{2R^4 E_\infty}}, \tag{86}$$

where α is a polarization factor and

$$E_\infty = \frac{1}{2}\mu v^2, \tag{87}$$

μ is the reduced mass of the collision sysytem. For the $A^{+Z_P} + H \rightarrow A^{+(Z_P-1)} + H^+$ collision system, $\alpha = 4.5$. For very low energy collision, the two potential curves at the avoided crossing point R do not cross exactly, therefore, the radial velocity is not equal to $v\sqrt{1 - (\frac{b}{R})^2}$, but equal to

$$v_{rad} = \frac{1}{2}(v_{rad1} + v_{rad2}), \tag{88}$$

here v_{rad1} is the radial velocity of the initial adiabatic curve at avoided crossing point R, and v_{rad2} is the radial velocity of the final adiabatic curve at avoided crossing point R. For a hydrogen target,

$$v_{rad1}^2 = v^2(1 - (\frac{b}{R})^2) + \frac{9Z_p^2}{4R^4 E_\infty}, \tag{89}$$

and

$$v_{rad2}^2 = v^2(1-(\frac{b}{R})^2) + \frac{9Z_p^2}{4R^4E_\infty} + \frac{\Delta E}{\mu}, \tag{90}$$

ΔE is the energy difference between the initial channel and the final channel at the avoided crossing point. I have modified the Landau - Zener parameter to be

$$\gamma = \frac{(9.13R)^2}{\frac{1}{2}(v_{rad1}+v_{rad2})Z_p(Z_p-1)} \exp[-2.648R/\sqrt{Z_P}]. \tag{91}$$

I apply these modified parameters to the C^{6+} + H(1s) collision system at velocities below 0.5×10^7 cm/sec in Sec. 2.4 and to C^{3+} + H(1s) and O^{5+} + H(1s) collision systems in Sec.3.3.

2.4 Application to C^{6+} + H(1s) collision

I apply my model to the C^{6+} + H(1s) $\rightarrow$ $C^{5+}(nlm)$ + H^+ capture process. As is known, in Ref. 20, only the $n = 4$ level is populated appreciably. The crossing radius R is determined from

$$\frac{Z_p-1}{R} - \frac{3n(n-1)}{2Z_PR^2} = \frac{Z_P^2}{2n^2} - \frac{1}{2}, \tag{92}$$

and I find

$$R = 7.88\ a.u. \tag{93}$$

As a check on my computations I compute $Q_n = \sum_l Q_{n,l}$ and compare this with the cross section obtained numerically by Green *et al*[15], Fritsch and Lin[38,39] and Salin[40]. Green *et al*[15] use the modified perturbed stationary states theory; Fritsch and Lin[38,39] use the atomic-orbital-expansion theory; and Salin's work is closely related to that of Green *et al* but includes the effect of Stark mixing. I use the Landau-Zener model with rotational and degenerate Stark-effect coupling which is

similar to Salin's model and obtain an analytical results. Figure 7 shows the total cross section as a function of velocity for C^{6+} Projectiles. The solid curve is my result, the dotted curve is the 33-state calculation of Green *et al.*[15], the $\triangle$ and the $\square$ are the results of Refs. 38 and 39, the $\oplus$ are from Ref.40, and the points are the experimental data of Ref. 16. The agreement is satisfactory, but the comparison does not provide a stringent test of the model. Figure 8 shows the L distributions which are the main result of our work. The most pronounced feature is the strong peaking of the $l = 3$ partial cross section near $v = 5 \times 10^7$ cm/s.

Figure 9 compares this $l = 3$ partial cross section with the multistate computations of Refs.15, 38, 39, and 40. Note that the rise towards a large $l = 3$ cross section at $v = 5 \times 10^7$ cm/s is agreement with their calculations but the rapid decrease with increasing velocity on the high-energy side of the peak is not. This indicates that my model is not reliable for L distributions above a velocity of 0.5 *a.u.* even though total cross sections are in good agreement with the multistate calculations. In comparison with the others' calculations, my L distributions are seen to be satisfactory for low velocities (below 5 $\times 10^7$ cm/s). Eq. (78), however, is only valid when a single n level is populated. Generally more than one n level is populated in capture reactions. My present model is readily extended to include any number of n levels populated by multiple Landau - Zener crossings.

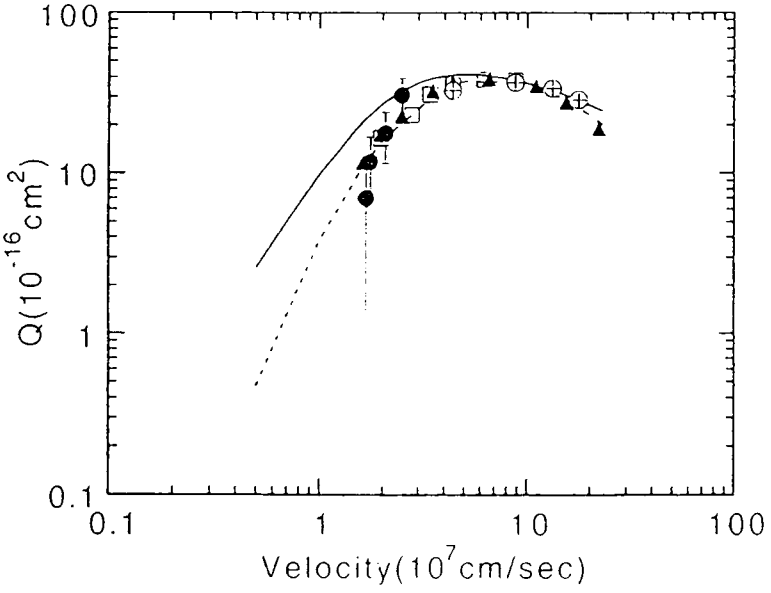


Fig. 7. Total cross section Q_n vs velocity for electron capture into $n = 4$ level by fully stripped carbon ions. The solid curve is the present calculation according to Eq.(73), the dashed curve is the 33-state calculation of Ref. 15, the ▲ are from Ref.38 and the □ are the results of Ref.39. the ⊕ are from Ref.40, and the points with error bars are experimental data of Ref. 16.

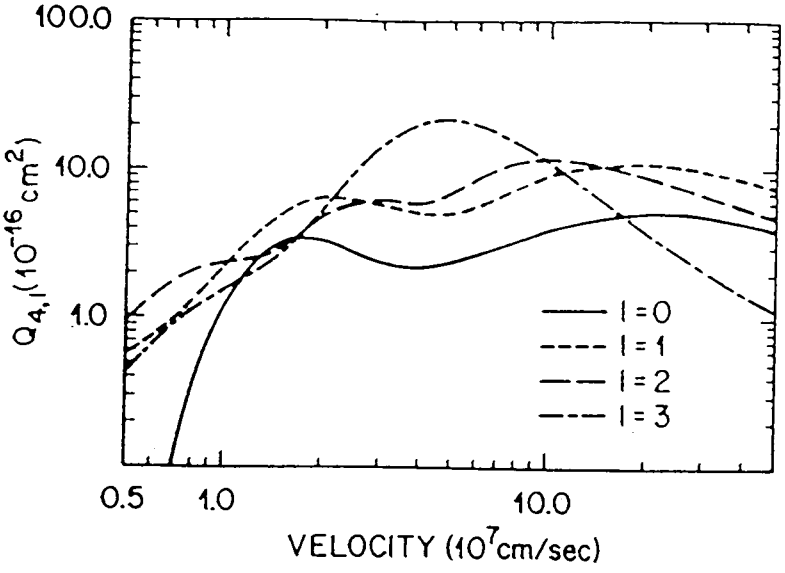


Fig. 8. Partial cross section $Q_{4,l}$ for electron capture into $n = 4$ l-sublevel by fully stripped carbon ions in collision with $H(1s)$.

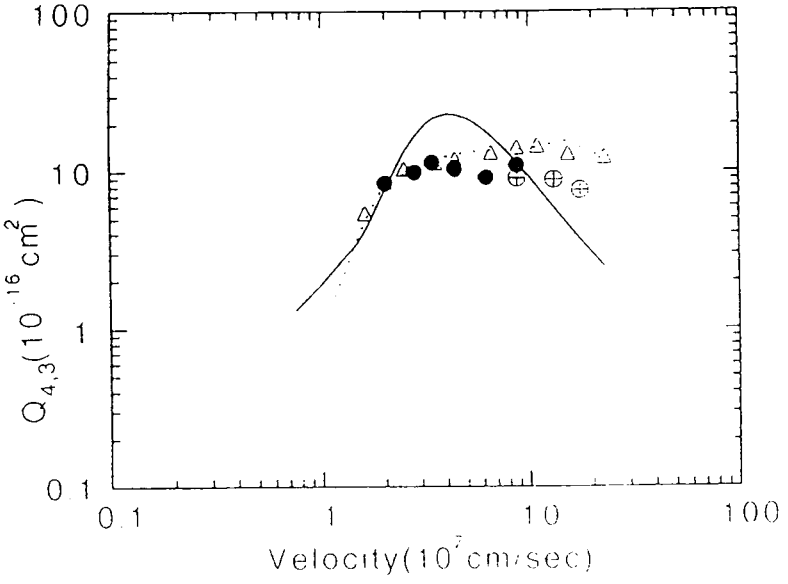


Fig. 9. Partial cross section $Q_{4,3}$ for electron capture into $n = 4$ $l = 3$ sublevel by fully stripped carbon ions in collision with $H(1s)$. The solid curve is the present calculation and the dashed curve is the 33 state calculation of Ref. 15, the Δ's are from Ref.38, the $\oplus$'s are from Ref. 39 and the $\bullet$ are from Ref. 40.

2.5 Multiple Landau-Zener crossings.

For highly charged bare projectiles, the initial states interact strongly with N final product states. Therefore, I extend the model of Sec.2.2 to the multiple Landau-Zener crossings. I still consider a bare projectile P of charge Z_P colliding with a one - electron ion of nuclear charge Z_T. The coordinate vector $\vec{r}$ represents the electron position with respect to projectile nucleus. The angle that the internuclear axis $\vec{R}$(t) makes with the initial velocity vector is denoted by θ. In a rotating frame where the direction of $\vec{R}$(t) is along the z - axis, the $\vec{r}$ - dependent part of the interaction between the projectile P and the target T is taken to be

$$V_{int} \approx -\frac{z - bvL_y}{R^2(t)}. \tag{94}$$

I employ the method of section 2.2 to write down the time - evolution matrix $U(t,t')$ for the collision system. The time domain is divided into 2N + 1 regions, labeled I, II,$\cdots$, 2N+1 as illustrated in Fig. 10. The crossing between the initial state $|0>$ with the Stark states $|Q_1>, |Q_2>, \cdots, |Q_k>, \cdots$, and $|Q_N>$ coupling to $|0>$ occurs on the incoming part of the trajectory at $t_{1i}, t_{2i}, \cdots, t_{ki}, \cdots$, and t_{Ni} and the outgoing part at $t_{1f}, t_{2f}, \cdots, t_{kf}, \cdots$, and t_{Nf}. The kth final level is the single Stark state

$$|Q_k> = |j_k, j_k; j_k, -j_k, >, \tag{95}$$

where $j_k = (n_k - 1)/2$, and n_k is the principal quantum of the k-level. The time $t_{1i}, t_{2i}, \cdots, t_{Ni}, t_{Nf}, \cdots$, and t_{1f} separate the regions I, II, $\cdots$, 2N+1.

The Stark eigenstates other than $|Q_k>$ are labeled by $|P_k>$. I suppose that coupling between $|0>$ and $|Q_k>$ occurs only at the Landau - Zener crossings and that $|Q_k>$ and $|P_k>$ are coupled at all times according to Eq.(94), but that $|P_k>$

does not couple directly to $|0>$. I also assume that there are not interferences between the k-level and J-level ($k \neq J$).

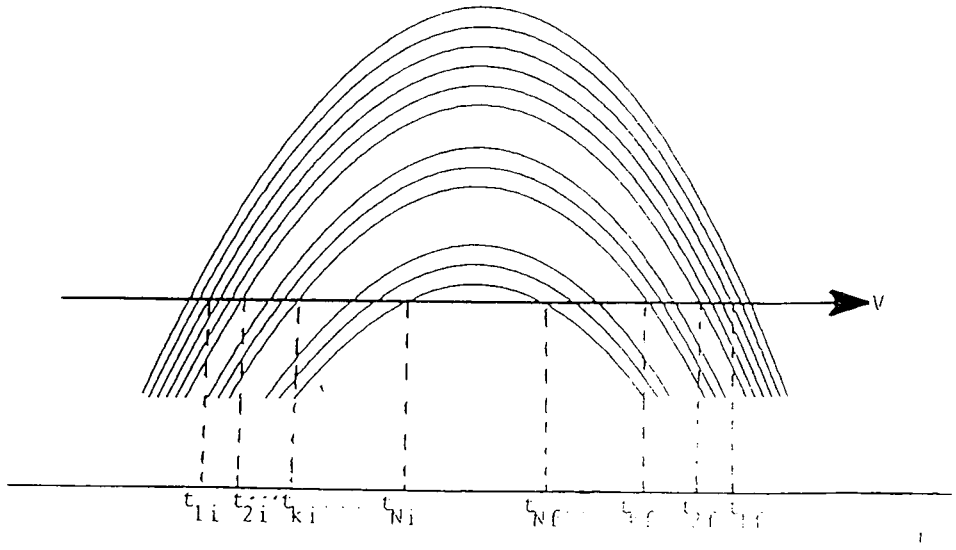


Fig. 10. Schematic adiabatic energy levels for multistate of the $A^{Z_P+} + H(1s)$ system vs time.

Refer to Eq.(31), I have

$$U(\infty, -\infty) = U(\infty, t_{1f})U^{LZ}(t_{1f})U(t_{1f}, t_{2f})U^{LZ}(t_{2f}) \cdots U^{LZ}(t_{Nf})$$
$$\times U(t_{Nf}, t_{Ni})U^{LZ}(t_{Ni}) \cdots U^{LZ}(t_{1i})U(t_{1i}, -\infty). \quad (96)$$

By carrying out the matrix multiplication in Eq.(96), the amplitude $A_{n_k l_k m_k}(b)$ for populating state $n_k l_k m_k$ by capture at impact parameter b is (see Appendix D)

$$A_{n_k l_k m_k}(b) = C^f_{n_k, l_n} d^{l_k}_{m_k, 0}(\delta_{kf}) + C^i_{n_k, l_n} d^{l_k}_{m_k, 0}(\delta_{ki}). \quad (97)$$

I get the probability $P_{n_k l_k m_k}(b)$

$$P_{n_k l_k m_k}(b) = |C^f_{n_k,l_k}|^2 |d^{l_k}_{m_k,0}(\delta_{kf})|^2 + |C^i_{n_k,l_k}|^2 |d^{l_k}_{m_k,0}(\delta_{ki})|^2 + \left[C^f_{n_k,l_n} C^{*i}_{n_k,l_n} d^{l_k}_{m_k,0}(\delta_{kf}) d^{*l_k}_{m_k,0}(\delta_{ki}) + c.c. \right]. \quad (98)$$

Using the group property of the rotation functions in Eq. (54) and summing over m_k to obtain $P_{n_k l_k}$(b), the probability $P_{n_k l_k}(b)$ is

$$P_{n_k l_k}(b) = |C^f_{n_k,l_k}|^2 P_{l_k}(\cos\zeta_{kff}) + |C^i_{n_k,l_k}|^2 P_{l_k}(\cos\zeta_{kii}) + \left[C^f_{n_k,l_n} C^{*i}_{n_k,l_n} P_{l_k}(\cos\zeta_{kfi}) + c.c. \right], \quad (99)$$

where

$$\zeta_{kab} = \delta_{ka} - \delta^*_{kb}, \qquad a, b = i, f. \quad (100)$$

As in my calculation in Sec.2.3, in the low velocities region, the term $\cos\int_{t_{ki}}^{t_{kf}} [E_0(\tau) - E_k(\tau)] d\tau$ varys veries rapidly so that I can drop it. Then I get

$$\begin{aligned}
P_{n_k l_k}(b) = & < j_k, j_k; j_k, -j_k | l_k, 0 >^2 (1-p_k) p_1 p_2 \cdots p_{k-1} \\
& \times \Big\{ \Big[(1 - \sin^2\beta_{kf} \sin^2\alpha_{kf})^{n_k - 1} p_k \Big[(p_{k+1} \cdots p_n)^2 \\
& + (1-p_N)^2 (p_{k+1} \cdots p_{N-1})^2 |u_{Q_N,Q_N}(t_{Nf}, t_{Ni})|^2 \\
& + (1-p_{N-1})^2 (p_{k+1} \cdots p_{N-2})^2 |u_{Q_{N-1},Q_{N-1}}(t_{(N-1)f}, t_{(N-1)i})|^2 \\
& + \cdots + (1-p_{k+2})^2 p^2_{k+1} |u_{Q_{k+2},Q_{k+2}}(t_{(k+2)f}, t_{(k+2)i})|^2 \\
& + (1-p_{k+1})^2 |u_{Q_{k+1},Q_{k+1}}(t_{(k+1)f}, t_{(k+1)i})|^2 \Big] \\
& + (\sqrt{p_k} - 1)^2 |u_{Q_k,Q_k}(t_{kf}, t_{ki})|^2 \Big] P_{l_k}(\cos\zeta_{kff}) \\
& + (1 - \sin^2\beta_{ki} \sin^2\alpha_{ki})^{n_k - 1} P_{l_k}(\cos\zeta_{kii}) \\
& + (\sqrt{p_k} - 1) \left[\left(e^{i2\alpha_{kf}} \cos^2\frac{\beta_{kf}}{2} + \sin^2\frac{\beta_{kf}}{2} \right)^{n_k - 1} \right. \\
& \times \left. \left(e^{-i2\alpha_{ki}} \cos^2\frac{\beta_{ki}}{2} + \sin^2\frac{\beta_{ki}}{2} \right) \right)^{n_k - 1} \\
& \times P_{l_k}(\cos\zeta_{kfi}) + c.c. \Big] \Big\},
\end{aligned}$$

$$1 \le k \le N-1, \quad (101)$$

where $P_l(x)$ denotes a Legendre polynomial. For the k-level in which the principal quantum number is n_k, the probability is

$$\begin{aligned}
P_{n_k}(b) = (1-p_k)p_1p_2\cdots p_{k-1}\Big\{p_k\Big[&(p_{k+1}\cdots p_N)^2 \\
&+(1-p_N)^2(p_{k+1}\cdots p_{N-1})^2|u_{Q_N,Q_N}(t_{Nf},t_{Ni})|^2 \\
&+(1-p_{N-1})^2(p_{k+1}\cdots p_{N-2})^2|u_{Q_{N-1},Q_{N-1}}(t_{(N-1)f},t_{(N-1)i})|^2 \\
&+\cdots(1-p_{k+2})^2p_{k+1}^2|u_{Q_{k+2},Q_{k+2}}(t_{(k+2)f},t_{(k+2)i})|^2 \\
&+(1-p_{k+1})^2|u_{Q_{k+1},Q_{k+1}}(t_{(k+1)f},t_{(k+1)i})|^2\Big] \\
&+1+(p_k-1)|u_{Q_k,Q_k}(t_{kf},t_{ki})|^2\Big\}, \\
&1\le k\le N-1,
\end{aligned} \tag{102}$$

and

$$P_{n_N}(b) = (1-p_N)p_1p_2\cdots p_{N-1}\Big\{p_N+1+(p_N-1)|u_{Q_N,Q_N}(t_{Nf},t_{Ni})|^2\Big\}. \tag{103}$$

The cross section for the populating state n_kl_k by capture at impact parameter b is

$$Q_{n_kl_k} = 2\pi\int_0^{R_k} P_{n_kl_n}(b)bdb, \tag{104}$$

and

$$Q_{n_k} = 2\pi\sum_{l_k=0}^{n_k-1}\int_0^{R_k} P_{n_kl_n}(b)bdb, \tag{105}$$

the total cross section is

$$Q = 2\pi\sum_{n_k=1}^{N}\sum_{l_k=0}^{n_k-1}\int_0^{R_k} P_{n_kl_n}(b)bdb. \tag{106}$$

2.6 Special cases: (1) no rotational coupling and (2) no Stark-effect.

It has been shown by Burgdörfer[41] that the mixing between substates can be very important. But in special cases, sometime we can neglect the interaction between substates. For convenience sake, I discuss these special cases only for the single n level. In section 2.2, I have obtained the general formulas of the amplitudes and probabilities for populating state nlm. The rotational coupling mixes the different m (magnetic quantum number) states. Stark-effect mixes the different l (angular quantum number) states. In the case of $\frac{3nZ_T}{2Z_P} \gg bv$, I can neglect the rotational coupling. From Eq.(49), the Euler angle

$$\beta(t,t') = 0. \tag{107}$$

As I assumed, only one particular Stark state $|Q>$ couples directly to the initial state $|0>$. When I neglect the rotational coupling, the charge transfer will be made to the same state $|Q>$ for incoming part at $t = t_i$ and outgoing part at $t = t_f$. The Stark eigenstates $|P>$ other than $|Q>$ are not coupled at all times with $|Q>$ and $|0>$. Therefore, this problem is reduced to the orignal two-state model. The amplitude for populating state nlm is

$$A_{nlm}(b) = 0, \qquad m \neq 0, \tag{108}$$

$$A_{nl0}(b) = g < l0|j,j;j,-j > \exp[i4j\alpha(\infty,t_f) - i\int_{-\infty}^{t_f} E_0(\tau)d\tau - i\int_{t_f}^{\infty} E_n(\tau)d\tau]$$
$$\times \left\{ s^* - s\exp[i4j\alpha_{f_i} + i\int_{t_i}^{t_f} [E_0(\tau) - E_n(\tau)]d\tau] \right\}. \tag{109}$$

The probability $P_{nl}(b)$ is

$$P_{nl}(b) = 2p(1-p) < l0|j,j;j,-j >^2 \times \{1 + \sin[4j\alpha_{fi} + 2\phi_s + 2 < Ea >]\}. \quad (110)$$

Where ϕ_s is the phase factor of the Landau-Zener parameter s. The probability $P_n(b)$ is

$$P_n(b) = \sum_l P_{nl}(b) = 2p(1-p)\{1 + \sin[4j\alpha_{fi} + 2\phi_s + 2 < Ea >]\}. \quad (111)$$

If I neglect the crossing term $\sin[4j\alpha_{fi} + 2\phi_s + 2 < Ea >]$, the probability $P_n(b)$ exactly equals to that of the original two-state theory.

Secondly, I will discuss neglecting the Stark - effect. There are two cases in which I neglect the Stark-effect: One is the $A^{Z_P+} + B^-$ collision, in which the fully stripped ions collide with one electron negative ions. The final states for this collision is $A^{(Z_P-1)+}(nlm) + B$ in which there is no Stark-effect but the excited states of projectile are degenerate. Another is the $A^{q+} + B$ $(q < Z_p)$ collision, in which the partially stripped heavy ions collide with neutral atoms. The final states for this collision is $A^{(q-1)+}(nlm) + B^+$ in which there is a Stark-effect but usually it is very small in comparison with the energy difference between two close states so that the Stark-effect can be neglected. I will discuss the latter case in chapter 3. In this chapter, I consider the collision system

$$A^{Z_P+} + B^- \rightarrow A^{(Z_P-1)+} + B. \quad (112)$$

From Eqs. (47), (48), and (49), the Euler angles are

$$\alpha(t,t') = 0, \quad (113)$$

$$\omega(t,t') = -\Delta\theta(t,t'), \tag{114}$$

$$\beta(t,t') = -\omega(t,t') = \Delta\theta(t,t'), \tag{115}$$

$$\cos\delta = -\cos\beta(t,t') = -\cos\Delta\theta(t,t'). \tag{116}$$

Where $\Delta\theta(t,t') = \theta(t') - \theta(t)$. The amplitude $A_{nlm}(b)$ is

$$\begin{aligned} A_{nlm}(b) = (-1)^{-l} < j,j;j,-j|l,0 > \left[\frac{(l-m)!}{(l+m)!}\right]^{1/2} \\ \times \left\{ s^* g P_l^m(-\cos\theta_f) \exp[-i\int_{-\infty}^{t_f} E_0(t)dt - i\int_{t_f}^{\infty} E_n(t)dt] \right. \\ - s\left[(g-1)\cos^{4j}\theta_{fi} P_l^m(-\cos\theta_f) + P_l^m(-\cos\theta_i)\right] \\ \left. \times \exp[-i\int_{-\infty}^{t_i} E_0(t)dt - i\int_{t_i}^{\infty} E_n(t)dt] \right\}, \end{aligned} \tag{117}$$

The rotation angles θ_f and θ_i are given in terms of the single angle $\theta_{fi} = \Delta\theta(t_f,t_i)$ by

$$\begin{aligned} \Delta\theta(t_f,t_i) &= \theta_i - \theta_f, \\ \theta_f &= (\pi - \theta_{fi})/2, \\ \theta_i &= (\pi + \theta_{fi})/2, \end{aligned} \tag{118}$$

the probability is

$$\begin{aligned} P_{nlm}(b) = (1-p) < j,j;j,-j|l,0 >^2 \frac{(l-m)!}{(l+m)!} \\ \times \left\{ [p + (\sqrt{p}-1)^2 \cos^{4(n-1)}\frac{\theta_{fi}}{2}]|P_l^m(-\cos\theta_f)|^2 + |P_l^m(-\cos\theta_i)|^2 \right. \\ + 2\sqrt{p}(\sqrt{p}-1)\cos^{2(n-1)}\frac{\theta_{fi}}{2}|P_l^m(-\cos\theta_f)|^2 \sin(2 < Ea > +2\phi_s) \\ + \left[(\sqrt{p}-1)\cos^{2(n-1)}\frac{\theta_{fi}}{2} P_l^m(-\cos\theta_f) P_l^{*m}(-\cos\theta_i) + c.c\right] \\ \left. - \sqrt{p}\left[P_l^m(-\cos\theta_f) P_l^{*m}(-\cos\theta_i) e^{i2 < Ea > +2\phi_s + i\frac{\pi}{2}} - c.c.\right] \right\}. \end{aligned} \tag{119}$$

Summing over m, the probability $P_{nl}(b)$ is

$$
\begin{aligned}
P_{nl}(b) &= (1-p) < j,j;j,-j|l,0>^2 \\
&\times \left\{ p+1+(\sqrt{p}-1)^2 \cos^{4(n-1)} \frac{\theta_{fi}}{2} \right. \\
&+ 2\sqrt{p}(\sqrt{p}-1) \cos^{2(n-1)} \frac{\theta_{fi}}{2} \sin(2 < Ea > +2\phi_s) \\
&+ 2\left[(\sqrt{p}-1) \cos^{2(n-1)} \frac{\theta_{fi}}{2} + \sqrt{p} \sin(2 < Ea > +2\phi_s) \right] \\
&\times \left. P_l(\cos\theta_{fi}) \right\} . \qquad (120)
\end{aligned}
$$

Eq.(120), in which there is no Stark-effect, is different from Eq.(110), in which there is no rotational coupling. For the no Stark-effect case, the rotational coupling still mixes the m-state so that the electron capture is not only from the coupling between $|Q>$ and $|0>$ but also is from the other Stark states $|P>$.

Chapter 3

Multiple Landau-Zener Crossings Model for Partially Stripped Heavy Ions Colliding with Neutral Atoms

3.1 Introduction

Capture of electrons from atomic hydrogen by partially multicharged ions is an important process in many practical applications[23]. The process is also of fundamental interest and for that reason several experimental groups have measured total cross sections for the production of H^+ ions in collisions of multicharged ions with H, especially in the low velocity ($v < 0.1 a.u.$) region. Many theoretical calculations[42-44] have been performed. For partially stripped incident ions, the Stark-effect when compared with the energy difference usually is very small,

$$\Delta_{pq} \gg \frac{< p|\vec{r}|q >}{R^2}, \tag{121}$$

so that I can neglect the Stark-effect coupling, where Δ_{pq} is the energy difference between p-state and q-state. Then the final states on the projectile are no longer degenerate in principal shells[13]. This means that there is a curve crossing for each particular subshell level. In this case, the number of such curve crossings is large. I have to extend our single Landau-Zener crossing model to the multiple Landau-Zener crossings to calculate the probabilities and cross sections. In section 3.2 I derive the new formula for partially stripped heavy ions colliding with a simple

one-electron target. I apply my modified model to $O^{5+} + H(1s)$ and $C^{3+} + H(1s)$ Collisions in Sec. 3.3. For the $C^{3+} + H(1s)$ Collision, at the higher velocities, I employ the top-of-barrier model of Pieksma and Ovchinnikov[7] and obtain very good results comparing with the recent experimental data[16,45,46].

3.2 Formulation

For the partially charged projectile, the final states are no longer degenerate. This means that there is a curve crossing for each l sublevel. Therefore, I have to extend the model of Sec. 2.2 to the multiple Landau-Zener crossings. I consider a partly charged projectile P of charge Z_P (the net charge $q < Z_P$) colliding with a one - electron ion of nuclear charge Z_T. The coordinate vector $\vec{r}$ represents the electron position with respect to projectile nucleus. The angle that the internuclear axis $\vec{R}$(t) makes with the initial velocity vector is denoted by θ. In a rotating frame where the direction of $\vec{R}$(t) is along the z - axis, the $\vec{r}$ - dependent part of the interaction between the projectile P and the target T is taken to be

$$V_{int} \approx -\dot{\theta} L_y. \tag{122}$$

From Eqs. (47), (48), and (49), the Euler angles are

$$\alpha = 0, \tag{123}$$

and

$$\beta(t, t') = \theta(t, t'). \tag{124}$$

According to the energy level data[47], the largest crossing radius corresponds to the highest angular quantum number for the same principal quantum number n,

and the s-state corresponds to the smallest crossing radius of the n level as shown in Fig. 11. I follow the general method of Sec. 2.2 to write down the time - evolution matrix $U(t,t')$ for the collision system. For the single level with principle quantum number n, the time domain is divided into 2n + 1 regions, labeled I, II,$\cdots$, 2n+1 as illustrated in Fig. 11. The crossing between the initial state $|0>$ with the states $|n-1,0>, |n-2,0>, \cdots, |l,0>, \cdots$, and $|S>$ coupling to $|0>$ occurs on the incoming part of the trajectory at $t_{(n-1)i}, t_{(n-2)i}, \cdots, t_{li}, \cdots$, and t_{Si} and the outgoing part at $t_{(n-1)f}, t_{(n-2)f}, \cdots, t_{lf}, \cdots$, and t_{Sf}. The time t_{li} and t_{lf} separate the region I, II, $\cdots, 2n+1$, where l is the angular quantum number.

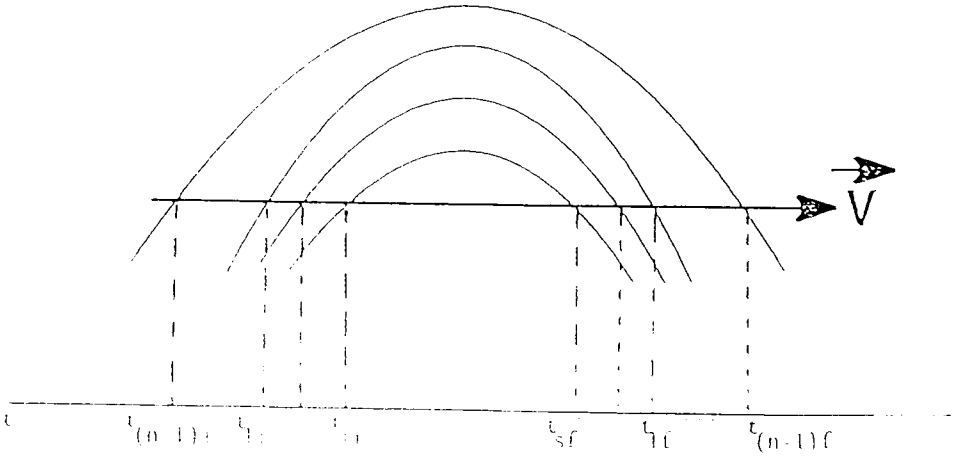


Fig. 11. Schematic adiabatic energy levels of the $A^{q+} + H(1s)$ system vs time.

I suppose that coupling between $|0>$ and $|l,0>$ occurs only at the Landau - Zener crossings and that $|l,0>$ and $|l,m>$ are coupled at all times according to

Eq.(122), but that $|l,m>|_{m\neq 0}$ does not couple directly to $|0>$, here $|0>$ denotes the initial state of the system. m is a magnetic quantum number. I also assume that there are no interferences between the l-sublevel and k-sublevel ($l \neq k$). For convenience sake, let $|S>$ represent s-state. Refer to Eq.(31), the time - evolution matrix $U(\infty,-\infty)$ is

$$U(\infty,-\infty) = U(\infty,t_{(n-1)f})U^{LZ}(t_{(n-1)f})U(t_{(n-1)f},t_{(n-2)f})U^{LZ}(t_{(n-2)f})\cdots U^{LZ}(t_{Sf})$$
$$\times U(t_{Sf},t_{Si})U^{LZ}(t_{Si})\cdots U^{LZ}(t_{(n-1)i})U(t_{(n-1)i},-\infty). \qquad (125)$$

By carrying out the matrix multiplication in Eq.(125), the amplitude $A_{nlm}(b)$ for the populating state nlm is (see Appendix E)

$$A_{nlm}(b) = C^f_{nl}d^l_{m,0}(\theta_f) + C^i_{nl}d^l_{m,0}(\theta_i), \qquad (126)$$

The amplitude for populating s-state is

$$A_s(b) = g_s g_1 g_2 \cdots g_{n-1}\exp[-i\int_{-\infty}^{t_{sf}} E_0(t)dt - i\int_{t_{sf}}^{\infty} E_s(t)dt]$$
$$\times\left\{s_s^* - s_s\exp[i\int_{t_{si}}^{t_{sf}}[E_0(t)-E_s(t)]dt]\right\}. \qquad (127)$$

The probability $P_{n,l,m}$(b)

$$P_{n,l,m}(b) = |C^f_{n,l}|^2|d^l_{m,0}(\theta_f)|^2 + |C^i_{n,l}|^2|d^l_{m,0}(\theta_i)|^2$$
$$+\left[C^f_{n,l}C^{*i}_{n,l}d^l_{m,0}(\theta_f)d^{*l}_{m,0}(\theta_i) + c.c.\right]. \qquad (128)$$

where c.c. denotes complex conjugate. In the low velocities region, it has been shown in chapter 2 that the term $\cos\int_{t_{li}}^{t_{lf}}[E_0(\tau)-E_l(\tau)]d\tau$ in comparison with value of the probability is very small and varies very rapidly so that I can drop it. Then I obtain

$$P_{n,l,m}(b) = (1-p_l)p_{l+1}p_{l+2}\cdots p_{n-1}\left\{\left[p_l(p_{l-1}p_{l-2}\cdots p_s)^2\right.\right.$$

$$+(1-p_s)^2(p_1\cdots p_{l-1})^2+(1-p_1)^2(p_2\cdots p_{l-1})^2|d^1_{0,0}(\theta_{1fi})|^2$$
$$+\cdots+(1-p_{l-2})^2p^2_{l-1}|d^{l-2}_{0,0}(\theta_{(l-2)fi})|^2$$
$$+(1-p_{l-1})^2|d^{l-1}_{0,0}(\theta_{(l-1)fi})|^2$$
$$+(\sqrt{p_l}-1)^2|d^l_{0,0}(\theta_{lfi})|^2\Big]\,|d^l_{m,0}(\theta_{lf})|^2+|d^{l_k}_{m_k,0}(\theta_{ki})|^2$$
$$-(\sqrt{p_l}-1)\left[d^l_{m,0}(\theta_{lf})d^{*l}_{m,0}(\theta_{ki})d^l_{0,0}(\theta_{lfi})+c.c.\right]\Big\},$$
$$1\le l\le n-1, \tag{129}$$

$$P_s(b)=2(1-p_s)p_sp_1p_2\cdots p_{n-1}. \tag{130}$$

Using the group property of the rotation functions in Eq. (54) and summing over m to obtain P_l(b), I have

$$P_{n,l}(b)=(1-p_l)p_{l+1}p_{l+2}\cdots p_{n-1}\Big\{p_l(p_{l-1}p_{l-2}\cdots p_s)^2$$
$$+(1-p_s)^2(p_1\cdots p_{l-1})^2+(1-p_1)^2(p_2\cdots p_{l-1})^2|d^1_{0,0}(\theta_{1fi})|^2$$
$$+\cdots+(1-p_{l-2})^2p^2_{l-1}|d^{l-2}_{0,0}(\theta_{(l-2)fi})|^2$$
$$+(1-p_{l-1})^2|d^{l-1}_{0,0}(\theta_{(l-1)fi})|^2$$
$$+(p_l-1)|d^l_{0,0}(\theta_{lfi})|^2+1\Big\}$$
$$1\le l\le n-1. \tag{131}$$

3.3 Application to $O^{5+}+H(1s)$ and $C^{3+}+H(1s)$ collisions

First, I apply this model to $O^{5+}+H(1s)$ capture process. From experimental data[16,46], the final states are mainly populated in the $n=4$ level. The electronic excited states are $4s, 4p$, and $4d$. From Ref. 47, I have the energy differences ΔE between $O^{5+}+H(1s)$ state and $O^{4+}(4l)+H^+$ states

$$\Delta E = \begin{cases} 0.3988 & 4s \\ 0.3361 \quad for & 4p \\ 0.3058 & 4d. \end{cases} \tag{132}$$

Using $R_l \approx \frac{q-1}{\Delta E}$, the crossing radii are

$$R_l \approx \begin{cases} 10.03 & 4s \\ 11.9 \quad for & 4p \\ 13.08 & 4d. \end{cases} \tag{133}$$

According to the Eqs. (130) and (131), I obtain the probabilities for $4s$, $4p$, and $4d$ states are

$$P_{4s} = 2(1-p_s)p_s p_p p_d, \tag{134}$$

$$P_{4p} = (1-p_p)p_d \left\{ p_p(p_s^2 + (1-p_s)^2) + 1 + (p_p - 1)|d^1_{0,0}(\theta_{pfi})|^2 \right\}, \tag{135}$$

and

$$\begin{aligned} P_{4d} = (1-p_d) \Big\{ & p_d \left[p_s^2 p_p^2 + (1-p_s)^2 p_p^2 + (1-p_p)^2 |d^1_{0,0}(\theta_{pfi})|^2 \right] \\ & + 1 + (p_d - 1)|d^2_{0,0}(\theta_{dfi})|^2 \Big\}. \end{aligned} \tag{136}$$

Here p_s, p_p, and p_d are Landau-Zener probabilities for $4s$, $4p$, and $4d$ states, respectively.

From the definition of the rotation function Eq. (54),

$$d^1_{0,0}(\theta_{pfi}) = \cos\theta_{pfi}, \tag{137}$$

and

$$d^2_{0,0}(\theta_{dfi}) = 1 - \frac{3}{2}\sin^2\theta_{dfi}. \tag{138}$$

In the straight line approximation,

$$\sin\theta_{pf} = \frac{b}{R_p}, \tag{139}$$

$$\sin\theta_{df} = \frac{b}{R_d}, \tag{140}$$

$$\theta_{pfi} = \pi - 2\theta_{pf}, \tag{141}$$

and,

$$\theta_{dfi} = \pi - 2\theta_{df}, \tag{142}$$

so that, I have

$$|d^1_{0,0}(\theta_{pfi})|^2 = |1 - 2\sin^2\theta_{pf}|^2, \tag{143}$$

and

$$|d^2_{0,0}(\theta_{dfi})|^2 = |1 - 6\sin^2\theta_{df}\cos^2\theta_{df}|^2. \tag{144}$$

Substituting Eqs.(143) and (144) into Eqs.(135) and (136), I have the total cross section

$$Q = 2\pi \sum_{s,p,d} \int_0^{R_k} P_{4k}(b) b db, \tag{145}$$

The total cross section is shown in Fig. 12. The solid curve is the present work, the dotted curve is from Ref. 48. The partial cross sections are shown in Fig. 13. The solid curve is the d-state, the dotted curve is the p-state and the dot-dashed curve is the s-state cross section of my calculations. The solid curve with points is the d-state partial cross section, the dotted curve with points is the p-state partial cross section, and the dot-dashed curve with points is the s-state partial cross section of Ref. 48. The partial cross sections are different from the calculation of Ref. 48 in the low energy region but in good agreement in the higher energy region. The total cross sections are acceptable agreement with the measurements of Havener *et al*[49] and the results of Andersson[48].

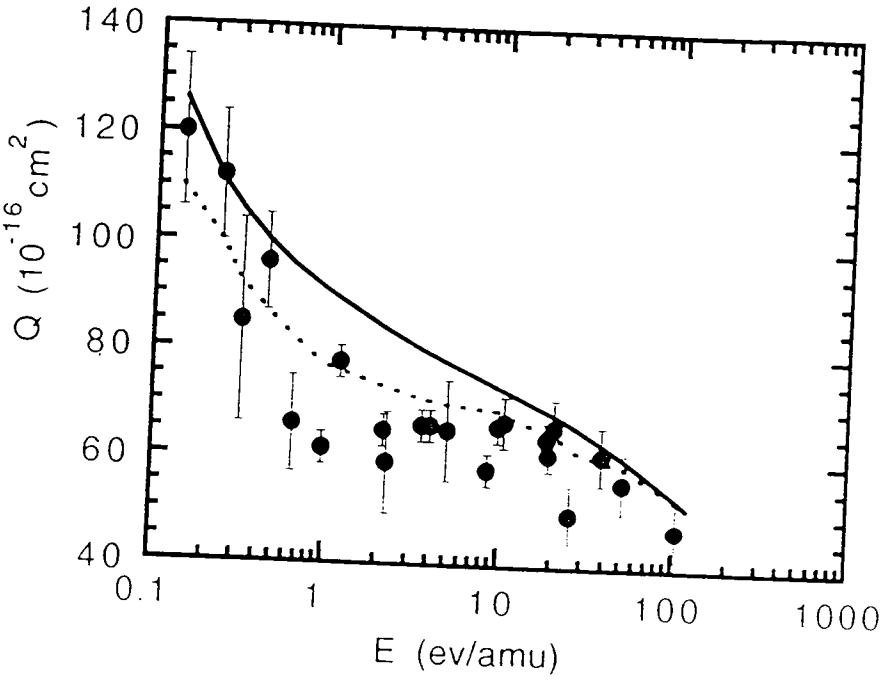


Fig.12 The total cross section for $O^{5+} + H(1s)$ collisions. The solid curve is present work, the dot curve is from Ref.48, and the points with error bars are experimental data of Ref.49.

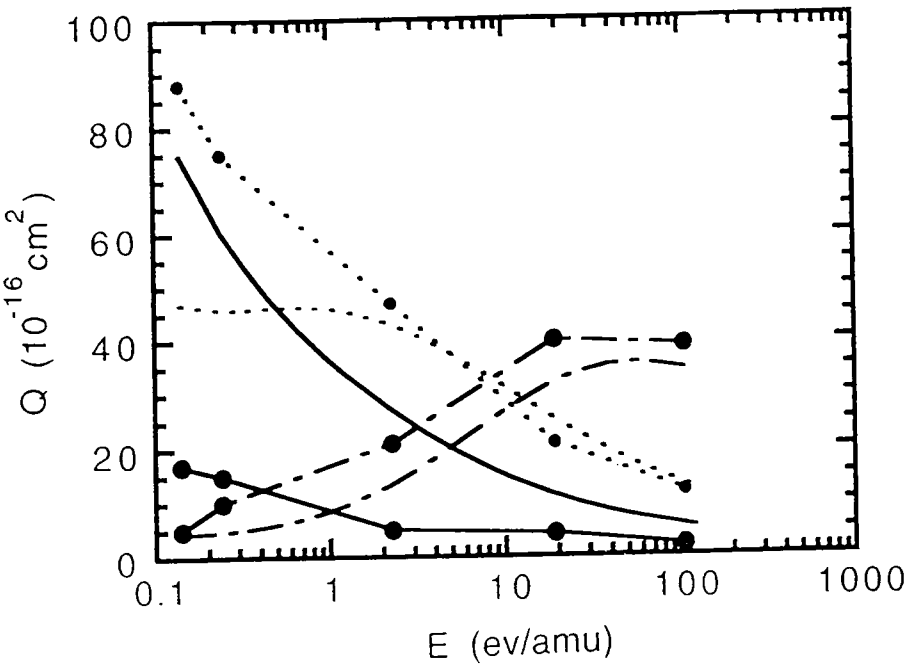


Fig.13 The partial cross sections for $O^{5+} + H(1s)$ collisions. The solid curve is the d-state, the dotted curve is the p-state and the dot-dashed curve is the s-state cross section of my calculations. The solid curve with points is the d-state partial cross section, the dotted curve with points is the p-state partial cross section, and the dot-dashed curve with points is the s-state partial cross section of Ref. 48.

Secondly, I apply this model to $C^{3+} + H(1s)$ capture process. From experimental data[16,49,50], the final states are mainly populated in the $n = 2$ and $n = 3$ levels. The electronic excited states are $2p, 3s, 3p$, and $3d$. From Ref. 47, I have the energy differences ΔE between $C^{3+} + H(1s)$ state and $C^{2+} + H^+$ states

$$\Delta E = \begin{cases} 1.031 & & 2\text{p} \\ 0.1734 & & 3\text{s} \\ 0.0735 & for & 3\text{p} \\ 0.0286 & & 3\text{d}. \end{cases}, \tag{146}$$

the correspond crossing radii are

$$R \approx \begin{cases} 1.9 & & 2\text{p} \\ 11.5 & & 3\text{s} \\ 26.5 & for & 3\text{p} \\ 69.7 & & 3\text{d}. \end{cases}. \tag{147}$$

From Eq. (147), the 2p state is far away from others so that I have the probability of final 2p state

$$P_{2p} \approx (1 - p_{2p})[p_{2p} + 1 + (p_{2p} - 1)\cos^2\theta_{2pfi}], \tag{148}$$

where θ_{2pfi} is the internuclear rotational angle between the time interval (t_{2pf}, t_{2pi}). It is shown in my calculation that the Landau-Zener probability p_{2p} is very small, and therefore, the probability of final 2p state is approximately

$$P_{2p} \approx 1 - \cos^2\theta_{2pfi}, \tag{149}$$

where

$$\theta_{2pfi} = \pi - 2\theta_{2pf}, \tag{150}$$

$$\sin\theta_{2pf} = b/R_{2p}, \tag{151}$$

final

$$P_{2p} = 4\frac{b^2}{R_{2p}^2}(1 - \frac{b^2}{R_{2p}^2}), \tag{152}$$

where R_{2p} is the crossing radius of the 2p state. The cross section of the 2p state is

$$\begin{aligned} Q_{2p} &= 2\pi \int_0^{R_{2p}} P_{2p}(b) b db \\ &= \frac{2}{3}\pi R_{2p}^2 = 7.5. \end{aligned} \tag{153}$$

According the Eqs. (130) and (131), the probabilities for $3s$, $3p$, and $3d$ states are

$$P_{3s} = 2(1 - p_{3s})p_{3s}p_{3p}p_{3d}, \tag{154}$$

$$P_{3p} = (1 - p_{3p})p_d \left\{p_{3p}[2p_{3s}^2 + 1 - 2p_{3s}] + 1 + (p_{3p} - 1)\cos^2\theta_{pfi}\right\}, \tag{155}$$

and

$$\begin{aligned} P_{3d} = (1 - p_{3d}) \Big\{ & p_{3d} \left[p_{3s}^2 p_{3p}^2 + (1 - p_{3s})^2 p_{3p}^2 \right. \\ & \left. + (1 - p_{3p})^2 \cos^2\theta_{pfi}\right] + 1 + (p_{3d} - 1)(1 - \frac{2}{3}\sin^2\theta_{dfi})^2 \Big\}. \end{aligned} \tag{156}$$

The total cross section for populating $2p, 3s, 3p, 3d$ states is shown in Fig. 14. My calculations show that the cross section departs from the experimental data at higher velocities, as would be expected in any Landau-Zener treatment.

Ovchinnikov[51] has calculated the matrix $< FA|\frac{\partial}{\partial R}|FB >$ which characterizes the interaction of adiabatic states for the $C^{3+} + H(1s)$ collision system. His calculation shows that the matrix $< FA|\frac{\partial}{\partial R}|FB >$ has two maxima at the crossing radii $R_c \approx 11.5a.u.$ and $R_c \approx 8.2a.u.$ as shown in Fig.15. As in my calculation, the first maximum point of $R_c \approx 11.5a.u.$ is the Landau-Zener crossing radius for populating the triplet 3s state. The second $R_c \approx 8.2a.u.$ relates to the eigenvalue in reaching the top-of-barrier. The potential energy surface for an electron in the field of two

positive charges has a saddle point where the net force on the electron vanishes. If an electron gets to this region and has zero velocity relative to the saddle point, it will stay there classically and will appear as a free electron of low energy in the laboratory frame. In the quantum theory an electron near the saddle point is represented by a transient molecular eigenstate of the electron in field of both target and projectile. Electron capture is then represented in terms of transitions between these transient molecular eigenstates. Solov'ev[52] has shown how to approximately compute these transitions employing the theory outlined in the textbook by Landau and Liftshitz[53].

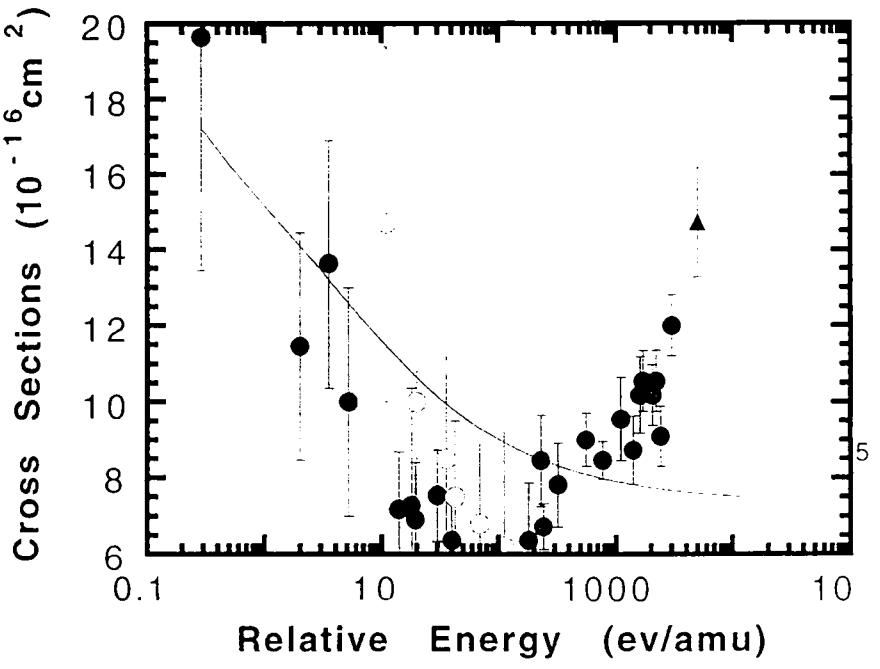


Fig.14 The cross section Q vs velocity for electron capture by C^{3+} ions, the points with error bars are experimental data of Refs. 49 and 50.

Since the Hamiltonian is an analytic function of the internuclear distance, the poten-

tial surfaces are different sheets of the same analytic function connected by branch points R where the curves cross exactly. Ovchinnikov[51] also computed the initial and final energy curves vs the internuclear distance as shown in Fig. 16.

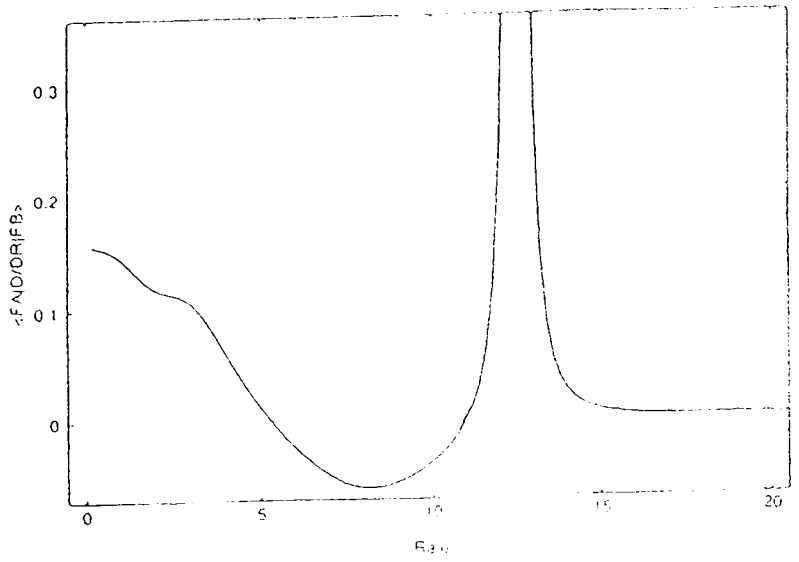


Fig.15 The value of the matrix $< FA|\frac{\partial}{\partial R}|FB >$ vs the internuclear distance for $C^{3+} + H(1s)$ collision system[51].

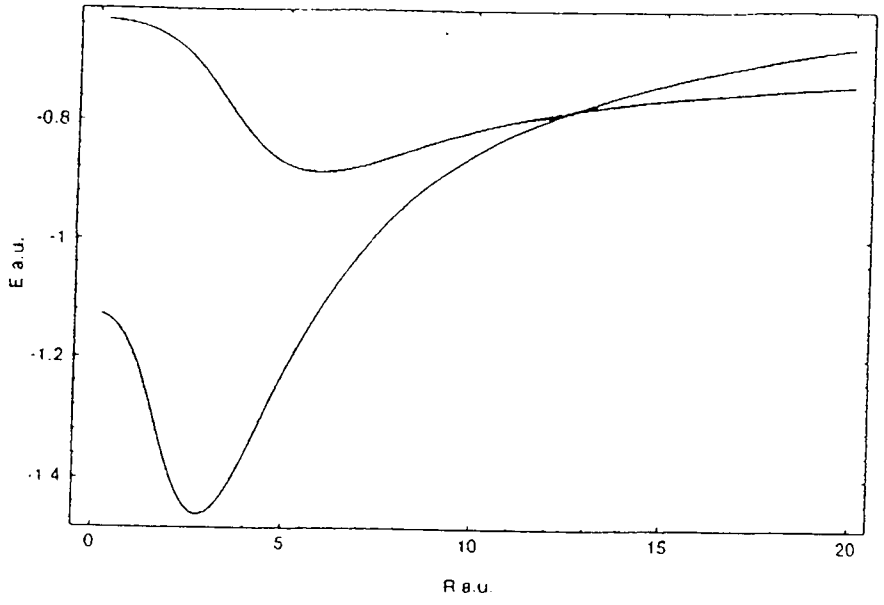


Fig.16 The energy curves for the initial state and final state vs the internuclear distance for $C^{3+} + H(1s)$ collision system[51].

These crossings R_c are called hidden crossings and determined by[52]

$$\Delta(E, R) = det\ (H(R) - EI) = 0, \tag{157}$$

where I is a unit matrix. There is a physical interpretation for the complex coordinate R_c. The real part of R_c indicates the region of internuclear distance where the transitions take place. The imaginary part of R_c determines the transition probability. Computations by Pieksma and Ovchinnikov[7] for $He^{2+} + H$ show that the top-of-barrier mechanism contributes substantially to electron capture for incident ion velocities between 1 and 2 atomic units. I employ this model for the $C^{3+} + H$

the work of Solov'ev[52], the expression for the transition amplitude of the nonlinear Hamilton is (see Appendix F)

$$A(b) = \frac{\sin[\pi\alpha/(n+\alpha)]}{\sin[\pi/(n+\alpha)]} \exp[-\Delta_{0f}/v_{rad}], \tag{158}$$

where

$$\Delta_{0f} = \frac{2}{3}\Delta E_{0f}\ ImR_c, \tag{159}$$

and $ImR_c = 4.5$, which is the width as shown in Fig.14. At $ReR_c = 8.2$, from Fig.15 $\Delta E_{of} = 0.1$. Substituting these values into Eq.(159) we have

$$\Delta_{0f} = 0.3. \tag{160}$$

For the nonlinear Hamilton the matrix $< FA|\frac{\partial}{\partial R}|FB >$ has simple form as[52]

$$\begin{aligned} < FA|\frac{\partial}{\partial R}|FB > &= \frac{i\alpha}{4}(\frac{1}{R-R_c} - \frac{1}{R-R_c^*}) \\ &= \frac{\alpha Im\ R_c}{2[(R-ReR_c)^2 + (Im\ R_c)^2]}, \end{aligned} \tag{161}$$

R_c^* denotes the complex conjugate of R_c, R_c is the complex crossing radius at the top-of-barrier. At $R = Re\ R_c$, the matrix $< FA|\frac{\partial}{\partial R}|FB >$ has the maximum 0.06 which can be obtained from Fig.14. Therefore, I have

$$\begin{aligned} < FA|\frac{\partial}{\partial R}|FB > |_{R=ReR} &= \frac{\alpha}{2Im\ R_c} \\ &= 0.06, \end{aligned} \tag{162}$$

substituting the value of $Im\ R_c$ into Eq.(162) I have

$$\alpha = 0.54. \tag{163}$$

Substituting the value of α, Δ_{0f}, and n=3 into Eq.(158), then I get the transition probability

$$p_{top} = |A_{pq}|^2$$
$$= (\frac{\sin[0.18\pi/1.18]}{\sin[\pi/3.54]})^2 \exp[-0.6/v_{rad}], \quad (164)$$

where $v_{rad} = v(1 - (\frac{b}{R})^2)^{1/2}$ is the radial velocity at the crossing. The cross section of the top-of-barrier theory is

$$Q_{top} = 2\pi \int_0^{ReR} 2p_{top}(1 - p_{top})bdb, \quad (165)$$

The figure 17 is the cross section of the model of the top-of-barrier.

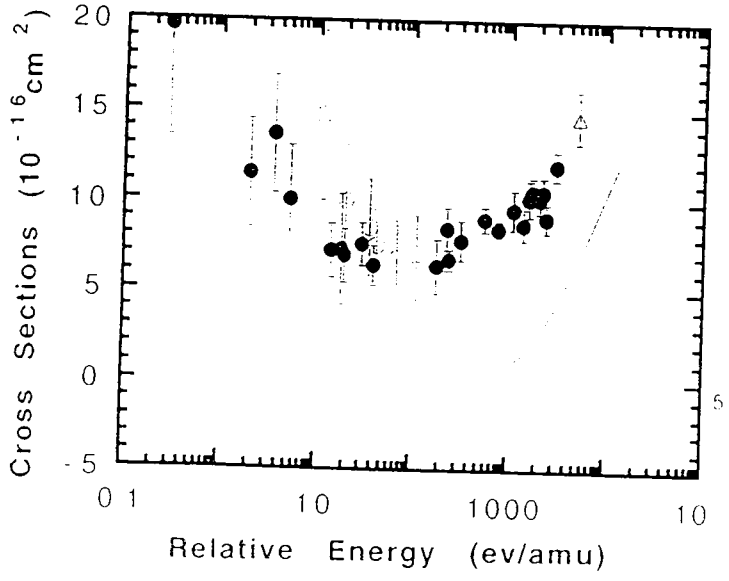


Fig. 17 The cross section of the top-of-barrier model vs velocity for electron capture by C^{3+}. The solid line is my present work for the top-of-barrier model, and the points with error bars are experimental data of Refs. 49, 50, and 54.

In the low velocity region, the cross section of the top-of-barrier is very small. It shows that the main capture process is following the Landau-Zener model in the lower velocity region, but in the higher velocity region the top-of-barrier process is the principal process. The figure 18 shows the total cross section in the energy region between $0.1eV/amu$ and $10^4eV/amu$. The solid line is the total cross section for $C^{3+}+H(1s) \rightarrow C^{2+}+H^+$ collision in my present work. The open points are from the measurement of Phaneuf[50], and the other points are from Havener[49]. Comparing with those experimental data, my calculation is very satisfactory.

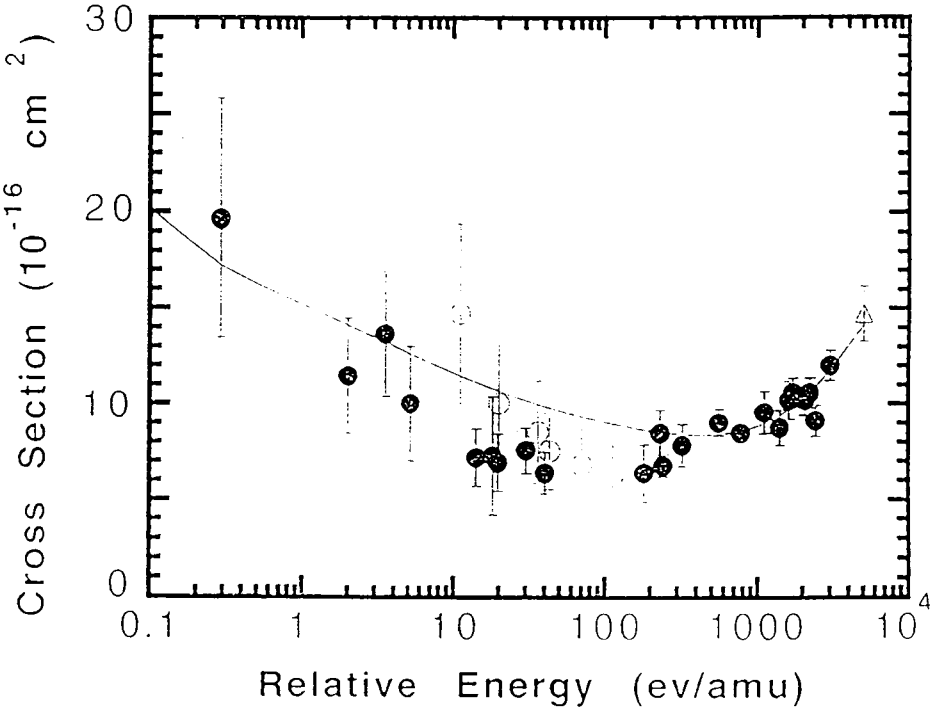


Fig.18 The total cross section for $C^{3+}+H(1s)$ collision system. The solid line is our present work, and the points with error bars are experimental data of Refs.49, 50, and 54.

From Ref. 54, the singlet 3s state has different crossing radius from the triplet

$3s$ state. After calculating the singlet $3s$ state and the triplet $3s$ state, I find the cross section of the singlet state is very small in comparsion with the cross section of the triplet state. Therefore, I do not include the cross section of the singlet state in my calculation.

Chapter 4

Multiple Crossings Model of Demkov

4.1 Introduction

As I have pointed[20] out, the two-state approximation turns out to be unsatisfactory in some cases. Based on the two-state model, Demkov and Osherov[21] used a contour integral to obtain the exact solution of the Schrödinger equation for a collision system in which the energy operator consists of a time - independent H_0 and a perturbation which depends linearly on time and is a projection operator onto a state $|\phi>$. The S-matrix for such a problem possesses the triangular property and decomposes into elementary Landau-Zener factors, each of which mixes only a pair of states. They also derived the S-matrix for other general cases. Demkov and Osherov[21] obtained the formula for transitions between bound electronic states, and from a bound state to continuum states. I employ their solution to my model and obtain a new approximate formula appropriate at low velocity for the A^{Z_P+} + H(1s) $\rightarrow$ $A^{(Z_P-1)+}$(nlm) + H^+ collision system in section 4.2 and apply it to collision C^{6+} + H(1s) $\rightarrow$ C^{5+}(nlm) + H^+. Results are compared with previous results in 4.3.

4.2 Formulation

Consider a bare projectile P of charge Z_p colliding with a one - electron ion of nuclear charge Z_T. The coordinate origin is placed at the projectile. The coordinate

vector $\vec{r}$ represents the electron position and $\vec{R}(t)$ is the relative position of projectile and target nucleus. θ is the angle that $\vec{R}(t)$ makes with the initial velocity. The interaction between the projectile P and the target T is taken to be

$$V_{int} = -\frac{\sqrt{(\frac{3nZ_T}{2Z_p})^2 + (bv)^2}}{R^2(t)}(\vec{n}_1.\vec{J}_1 - \vec{n}_2.\vec{J}_2), \tag{166}$$

here

$$\vec{n}_{1,2} = \frac{\frac{3nZ_T}{2Z_p}\hat{z} \mp bv\hat{y}}{\sqrt{(\frac{3nZ_T}{2Z_p})^2 + (bv)^2}}, \tag{167}$$

$$\dot{w} = \frac{\sqrt{(\frac{3nZ_T}{2Z_p})^2 + (bv)^2}}{R^2(t)}. \tag{168}$$

Writing the Hamiltonian in the rotating frame, I then have

$$H' = H'_0 - \dot{w}(t)(\vec{n}_1.\vec{J}_1 - \vec{n}_2.\vec{J}_2), \tag{169}$$

where H'_0 is the unperturbed part of Hamiltonian including the monopole term.

$$H'_0 = -\frac{1}{2}\Delta^2 - \frac{Z_P}{r} - \frac{Z_T(Z_P - 1)}{R}, \tag{170}$$

It is clear that H' is diagonal in the pseudo - spin representation

$$|\psi_i> = |j_1, m_{1i}>_{\vec{n}_1} \ |j_2, m_{2i}>_{\vec{n}_2}, \tag{171}$$

where the z-axis is determined by unit vectors $\vec{n}_1$ and $\vec{n}_2$, respectively. The corresponding eigenenergy is

$$\varepsilon_i(R) = E_n - \dot{w}(t)(m_{1i} - m_{2i}). \tag{172}$$

E_n is eigenvalue of H'_0. The H' - matrix in this representation then has the form

$$H' = \begin{pmatrix} h'_{00} & h'_{01} & h'_{02} & h'_{03} & \cdots \\ h'_{10} & \varepsilon_1 & 0 & 0 & \cdots \\ h'_{20} & 0 & \varepsilon_2 & 0 & \cdots \\ h'_{30} & 0 & 0 & \varepsilon_3 & \cdots \\ \vdots & \vdots & \vdots & \vdots & \cdots \end{pmatrix}. \tag{173}$$

where

$$h'_{00} =< 0|H'(t)|0 >, \tag{174}$$

$$h'_{0i} =< 0|H'(t)|\psi_i >, \tag{175}$$

and

$$\varepsilon_i =< \psi_i|H'(t)|\psi_i > . \tag{176}$$

I set

$$|\psi_i >= \exp[-i\int^t H'_0 dt]\ |\phi_i >, \tag{177}$$

then I have

$$\begin{aligned} i\frac{\partial}{\partial t}|\psi_i > &= H'_0 \exp[-i\int^t H'_0 dt]\ |\phi_i > + \exp[-i\int^t H'_0 dt]\ i\frac{\partial}{\partial t}|\phi_i > \\ &= E_n|\psi_i > + \exp[-i\int^t H'_0(t)dt] i\frac{\partial}{\partial t}|\phi_i >, \end{aligned} \tag{178}$$

$$< \psi_i|H'(t)|\psi_j >= (E_n + < \phi_i|H'(t)|\phi_j >)\delta_{ij}. \tag{179}$$

I define the effective Hamiltonian H

$$\begin{aligned} H &= \frac{H' - E_n I}{\dot{w}(t)} \\ &= \frac{1}{\dot{w}(t)}\frac{i\partial}{\partial t} = \frac{i\partial}{\partial w}, \end{aligned} \tag{180}$$

where I is an unit matrix. The effective H - matrix becomes

$$H = \begin{pmatrix} h_0 & h_1 & h_2 & h_3 & \cdots \\ h_1 & m_{21} - m_{11} & 0 & 0 & \cdots \\ h_2 & 0 & m_{22} - m_{12} & 0 & \cdots \\ h_3 & 0 & 0 & m_{23} - m_{13} & \cdots \\ \vdots & \vdots & \vdots & \vdots & \cdots \end{pmatrix}, \tag{181}$$

where $m_1(j) - m_2(j)$ are constants,

$$h_0 = \frac{h'_{00} - E_n}{\dot{w}(t)}, \tag{182}$$

and

$$h_j = \frac{h'_{0j}}{\dot{w}(t)}. \tag{183}$$

In the multiple crossing model of Demkov and Osherov[21], the Schrödinger equation is

$$(H_0 + |\phi > \beta t < \phi|)|\psi >= i\frac{\partial}{\partial t}\psi > . \tag{184}$$

The Hamiltonian of Demkov and Osherov[21] model represents a matrix of arbitrary size $(N-1) \times (N-1)$ and is given

$$H = \begin{pmatrix} \beta t & h_1 & h_2 & h_3 & \cdots \\ h_1 & \lambda_1 & 0 & 0 & \cdots \\ h_2 & 0 & \lambda_2 & 0 & \cdots \\ h_3 & 0 & 0 & \lambda_3 & \cdots \\ \vdots & \vdots & \vdots & \vdots & \cdots \end{pmatrix}, \tag{185}$$

where $\beta > 0$, h_i and λ_i are real constants $(i = 1, 2, \cdots, N)$. The probability at the Landau - Zener crossing is

$$p_j = e^{-2\pi \frac{h_j^2}{\beta}}. \tag{186}$$

According to their model, I define the new parameters g and s as

$$g_j = e^{-\pi\gamma_j}, \tag{187}$$

$$s_j = \sqrt{1 - |g_j|^2}, \tag{188}$$

and

$$\gamma_j = \frac{h_j^2}{\frac{dh_0}{dw}}, \tag{189}$$

the probability p_j at Landau-Zener crossing is given by

$$p_j = |g_j|^2 = e^{-2\pi\gamma_j}, \tag{190}$$

Using the new parameters g and s in the time-evolution matrix $U(t,t')$, the $U(\infty,-\infty)$ matrix is

$$\begin{aligned} U(\infty,-\infty) = & U(\infty,t_{1f})U^{LZ}(t_{1f})U(t_{1f},t_{2f})\cdots U(t_{Nf},t_{Ni}) \\ & \times U^{LZ}(t_{Ni})U(t_{Ni}t_{(N-1)i})\cdots U(t_{2i},t_{1i})U^{LZ}(t_{1i})U(t_{1i},-\infty), \end{aligned} \tag{191}$$

The amplitude $A_j(b)$ for the populating state $|\psi_j>$ by capture at an impact parameter b is found by carrying out the matrix multiplication in Eq.(191).

$$\begin{aligned} A_j(b) = & -s_j g_1 g_2 ... g_j \exp[-i\int_{-\infty}^{t_{ji}} E_0 dt - i\int_{t_{ji}}^{\infty} E_n dt - i(m_{1j}-m_{2j})B\vartheta_{ji}] \\ & + s_j^* g_1 g_2 ... g_j \exp[-i\int_{-\infty}^{t_{jf}} E_0 dt - i\int_{t_{jf}}^{\infty} E_n dt - i(m_{1j}-m_{2j})B\vartheta_{jf}] \\ & \times \Big[(g_{j+1}...g_N)^2 \\ & + (s_N g_{j+1}...g_{N-1})^2 \exp[-i\int_{t_{Ni}}^{t_{Nf}} (E_n - E_0)dt - i(m_{1N}-m_{2N})B\vartheta_{Nfi}] \end{aligned}$$

$$+ (s_{N-1}g_{j+1}...g_{N-2})^2 \exp[-i\int_{t_{N-1,i}}^{t_{N-1,f}}(E_n - E_0)dt - i(m_{1,N-1} - m_{2,N-1})B\vartheta_{(N-1)fi}]$$
$$+ \cdots + (s_{j+2}g_{j+1})^2 \exp[-i\int_{t_{j+2,i}}^{t_{j+2,f}}(E_n - E_0)dt - i(m_{1,j+2} - m_{2,j+2})B\vartheta_{(j+2)fi}]$$
$$+ s_{j+1}^2 \exp[-i\int_{t_{j+1,i}}^{t_{j+1,f}}(E_n - E_0)dt - i(m_{1,j+1} - m_{2,j+1})B\vartheta_{(j+1)fi}]\Big],$$
$$1 \leq j < N, \tag{192}$$

and

$$A_N(b) = g_1g_2...g_N \exp[-i\int_{-\infty}^{t_{Ni}} E_0dt - i\int_{t_{Ni}}^{\infty} E_ndt - i(m_{1N} - m_{2N})B\vartheta_{Ni}]$$
$$\times \Big[-s_N + s_N^* \exp[-i\int_{t_{Ni}}^{t_{Nf}}(E_n - E_0)dt - i(m_{1N} - m_{2N})B\vartheta_{Nfi}]\Big], \tag{193}$$

and ϑ_{ji} is the angle of the rotation of the internuclear axis during the time interval (∞, t_{ji}), ϑ_{jf} is the angle of the rotation of the internuclear axis during the time interval (∞, t_{jf}), and ϑ_{jfi} is the angle of the rotation of the internuclear axis during the time interval (t_{jf}, t_{ji}).

Upon squaring $A_j(b)$ and dropping terms with the rapidly varying factor $cos\int_{t'}^{t}(E_n - E_0)(\tau)d\tau$ I have

$$P_j(b) = |A_j|^2$$
$$= (1 - p_j)p_1p_2...p_j[1 + (1 - p_{j+1})^2 + (1 - p_{j+2})^2p_{j+1}^2 + \cdots$$
$$+ (1 - p_N)^2p_{j+1}^2...p_{N-1}^2 + p_{j+1}^2p_{j+2}^2...p_N^2],$$
$$1 \leq j < N, \tag{194}$$

and

$$P_N(b) = 2(1 - p_N)p_1p_2...p_N. \tag{195}$$

4.3 Application to C^{6+} + H(1s) Collisions

For $C^{6+} + H(1s) \rightarrow C^{5+}(nlm) + H^{+}$ collisions, only the $n = 4$ level is populated appreciably. For n=4, the $H'-$ matrix is

$$H' = \begin{pmatrix} h_0 & h'_1 & h'_2 & h'_3 & h'_4 & h'_5 & \cdots & h'_{16} \\ h'_1 & 3 & 0 & 0 & 0 & 0 & 0 & \cdots \\ h'_2 & 0 & 2 & 0 & 0 & 0 & 0 & \cdots \\ h'_3 & 0 & 0 & 2 & 0 & 0 & 0 & \cdots \\ h'_4 & 0 & 0 & 0 & 1 & 0 & 0 & \cdots \\ h'_5 & 0 & 0 & 0 & 0 & 1 & 0 & \cdots \\ \vdots & \vdots & \vdots & \vdots & \vdots & & & \vdots \\ h'_{16} & 0 & 0 & 0 & \cdots & 0 & 0 & -3 \end{pmatrix}. \tag{196}$$

where

$$\begin{aligned} h_0 &= \frac{\varepsilon_0 - \varepsilon_4 - 5/R}{\dot{w}(t)} \\ &= \frac{0.625R^2 - 5R}{\sqrt{(\frac{3nZ_T}{2Z_P})^2 + (bv)^2}}, \end{aligned} \tag{197}$$

$$\begin{aligned} h'_j &= < 1s(H)|H|\phi_i > \\ &= [\frac{5R - 1.125R^2}{\sqrt{(\frac{3nZ_T}{2Z_P})^2 + (bv)^2}} - (m_{1j} - m_{2j})] < 1s(H)|jm_1 >_{\vec{n}_1} |j, m_2 >_{\vec{n}_2} . \end{aligned} \tag{198}$$

The quantities $\varepsilon_0 = -\frac{1}{2}$ and $\varepsilon_4 = -\frac{9}{8}$ denote the energy of the electron states correlating to $1s$ state of hydrogen and to excited state of the one-electron carbon ion. Stark state $|j, m >_{\vec{R}}$ in the old rotating frame of my first model relates to the state $|j, m >_{\vec{n}}$ in the new rotating frame according to the coupling scheme

$$\begin{aligned} |j, m >_{\vec{n}} &= e^{iL_x\varphi}|j, m >_{\vec{R}} \\ &= \sum_{m'} < j, m'|[e^{iL_x\varphi}|j, m > |j, m' >_{\vec{R}}]. \end{aligned} \tag{199}$$

The transformation matrix is indicated in the appendix D. Eq.(410) gives

$$|j,m>_{\vec{n}}=\sum_{m'} e^{i(m-m')\frac{\pi}{2}} d^j_{m',m}(\varphi)|j,m'>_{\vec{R}}\,. \tag{200}$$

Then,

$$h'_j=[\frac{5R-1.125R^2}{\sqrt{1+(bv)^2}}-(m_{1j}-m_{2j})]\sum_{m'_1 m'_2}<1s(H)|j,m'_1;j,m'_2>_{\vec{R}}$$
$$\times\exp[i(m_1-m'_1+m'_2-m_2)\frac{\pi}{2}]d^j_{m'_1,m_1}(\varphi)d^j_{m_2,m'_2}(\varphi), \tag{201}$$

where φ is the angle between the vectors $\vec{R}$ (z-axis) and $\vec{n}_1$ and $\vec{n}_2$ as shown in Fig. 19.

$$\tan\varphi=\frac{bv}{3nZ_T/2Z_P}. \tag{202}$$

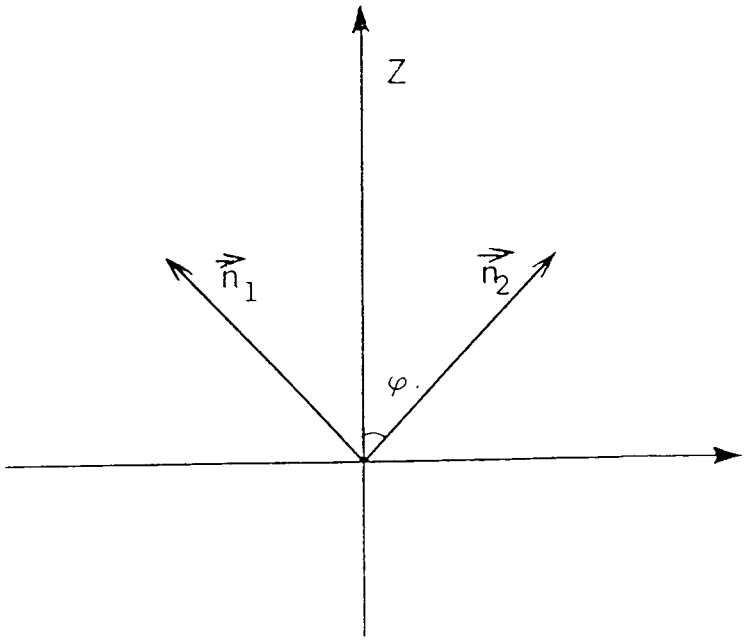


Fig.19 The schematic angles between z-axis and unit vectors $\vec{n_1}$ and $\vec{n_2}$.

Under the unitary transformation, Eq.(196) becomes

$$\underline{H} = \begin{pmatrix} h_0 & h_1 & \underline{h}_2 & 0 & \underline{h}_4 & 0 & \cdots & h_{16} \\ \underline{h}_1 & 3 & 0 & 0 & 0 & 0 & 0 & \cdots \\ \underline{h}_2 & 0 & 2 & 0 & 0 & 0 & 0 & \cdots \\ 0 & 0 & 0 & 2 & 0 & 0 & 0 & \cdots \\ \underline{h}_4 & 0 & 0 & 0 & 1 & 0 & 0 & \cdots \\ 0 & 0 & 0 & 0 & 0 & 1 & 0 & \cdots \\ \vdots & \vdots & \vdots & \vdots & \cdots & & & \\ h_{16} & 0 & 0 & 0 & \cdots & 0 & 0 & -3 \end{pmatrix}, \tag{203}$$

where

$$\underline{h}_2 = \sqrt{h_2'^2 + h_3'^2}, \tag{204}$$

$$\underline{h}_4 = \sqrt{h_4'^2 + h_5'^2 + h_6'^2}, \tag{205}$$

$$\underline{h}_7 = \sqrt{h_7'^2 + h_8'^2 + h_9'^2 + h_{10}'^2}, \tag{206}$$

$$\underline{h}_{11} = \sqrt{h_{11}'^2 + h_{12}'^2 + h_{13}'^2}, \tag{207}$$

$$\underline{h}_{14} = \sqrt{h_{14}'^2 + h_{15}'^2}, \tag{208}$$

and

$$\underline{h}_3 = \underline{h}_5 = \underline{h}_6 = \underline{h}_8 = \underline{h}_9 = \underline{h}_{10} = \underline{h}_{12} = \underline{h}_{13} = \underline{h}_{15} = 0. \tag{209}$$

I set

$$h_1 = h'_1,$$

$$h_2 = \underline{h}_2,$$

$$h_3 = \underline{h}_4,$$

$$h_4 = \underline{h}_7,$$

$$h_5 = \underline{h}_{11},$$

$$h_6 = \underline{h}_{14},$$

$$h_7 = h'_{16}. \tag{210}$$

The effective H-matrix becomes

$$\underline{H} = \begin{pmatrix} h_0 & h_1 & h_2 & h_3 & h_4 & h_5 & h_6 & h_7 \\ h_1 & 3 & 0 & 0 & 0 & 0 & 0 & 0 \\ h_2 & 0 & 2 & 0 & 0 & 0 & 0 & 0 \\ h_3 & 0 & 0 & 1 & 0 & 0 & 0 & 0 \\ h_4 & 0 & 0 & 0 & 0 & 0 & 0 & 0 \\ h_5 & 0 & 0 & 0 & 0 & -1 & 0 & 0 \\ h_6 & 0 & 0 & 0 & 0 & 0 & -2 & 0 \\ h_7 & 0 & 0 & 0 & 0 & 0 & 0 & -3 \end{pmatrix}. \tag{211}$$

Then the probability for populating $|j>$ state is

$$p_j(b) = \exp[-2\pi f_j(\omega)], \tag{212}$$

where

$$f_j(\omega) = \frac{h_j^2}{\frac{dh_0}{d\omega}}. \tag{213}$$

For the $C^{6+} + H \rightarrow C^{5+} + H^{+}$, the schematic effective adiabatic energy levels (diagonal elements of the H-matrix in Eq.(211)) of this collision are shown in Fig. 20. For small impact parameter b and low velocity, h_0 crosses $\varepsilon_i = -3, -2, -1$ four times as shown in Fig.20(a). As the value of bv increases, the crossing points between h_0 and $\varepsilon_i = -3, -2, -1$ become two as shown in Fig. 20(b). For the certain higher velocity and large impact parameter, there are no crossing points between h_0 and ε_{-3} as shown in Fig.20(c) and so on. If I include all of the above cases, then $U(\infty, -\infty)$ is

$$\begin{aligned} U(\infty,-\infty) = & U(\infty,t_{1f})U^{LZ}(t_{1f})U(t_{1f},t_{2f})\cdots U(t_{7f},t_{7i'}) \\ & \times U^{LZ}(t_{7i'}U(t_{7i'},t_{6i'})\cdots U(t_{5i'},t_{5f'})U^{LZ}(t_{5f'})\cdots \\ & \times U(t_{7f'}t_{7i})U^{LZ}(t_{7i})\cdots U(t_{2i},t_{1i})U^{LZ}(t_{1i})U(t_{1i},-\infty). \end{aligned} \tag{214}$$

According to section 4.2, it is easy to get the amplitudes and probability for populating the state j by capture at an impact parameter b by carrying out the matrix mulitiplication in Eq.(214). In my present model, the initial relative velocities are sufficiently high so that there are only two crossings between h_0 and $\varepsilon_j = -3, -2, -1$ as shown in Fig.20(b). So that I can simplify the equation (214) to

$$\begin{aligned} U(\infty,-\infty) = & U(\infty,t_{1f})U^{LZ}(t_{1f})U(t_{1f},t_{2f})\cdots U(t_{7f},t_{7i}) \\ & \times U^{LZ}(t_{7i})U(t_{7i}t_{6i})\cdots U(t_{2i},t_{1i})U^{LZ}(t_{1i})U(t_{1i},-\infty). \end{aligned} \tag{215}$$

From Eq.(215) , the amplitude for populating the $|j>$ state is

$$\begin{aligned} A_j(b) = & -s_j g_1 g_2 ... g_j \exp[-i\int_{-\infty}^{t_{j\prime}} E_0 dt - i\int_{t_{j\prime}}^{\infty} E_n dt - i\Delta m_j B\vartheta_{ji}] \\ & + s_j^* g_1 g_2 ... g_j \exp[-i\int_{-\infty}^{t_{jf}} E_0 dt - i\int_{t_{jf}}^{\infty} E_n dt - i\Delta m_j B\vartheta_{jf}] \\ & \times \left[(g_{j+1}\cdots g_7)^2 + \right. \end{aligned}$$

$$+(s_7 g_{j+1}...g_6)^2 \exp[i\int_{t_{7i}}^{t_{7f}}(E_0-E_n)dt - i\Delta m_7 B\vartheta_{7fi}]$$
$$+(s_6 g_{j+1}...g_5)^2 \exp[i\int_{t_{6,i}}^{t_{6,f}}(E_0-E_n)dt - i\Delta m_6 B\vartheta_{6fi}] + \cdots$$
$$+(s_{j+2}g_{j+1})^2 \exp[i\int_{t_{j+2,i}}^{t_{j+2,f}} E_0 dt - i\Delta m_{j+2} B\vartheta_{(j+2)fi}]$$
$$+ s_{j+1}^2 \exp[i\int_{t_{j+1,i}}^{t_{j+1,f}} E_0 dt - i\Delta m_{j+1} B\vartheta_{(j+1)fi}]\Big],$$
$$1 \le j \le 6, \tag{216}$$

and

$$A_7(b) = g_1 g_2 ... g_7 \exp[-i\int_{-\infty}^{t_{7i}} E_0 dt - i\int_{t_{ji}}^{\infty} E_n dt - i\Delta m_7 B\vartheta_{7i}]$$
$$\times\left[-s_7 + s_7^* \exp[i\int_{t_{7i}}^{t_{7f}} E_0 dt - i\Delta m_7 B\vartheta_{7fi}]\right], \tag{217}$$

where

$$B = \frac{\sqrt{(\frac{3nZ_t}{2Z_p})^2 + (bv)^2}}{bv}$$
$$\Delta m_j = m_{1j} - m_{2j}, \tag{218}$$

and ϑ_{ji} is the angle of the rotation of the internuclear axis during the time interval (∞, t_{ji}), ϑ_{jf} is the angle of the rotation of the internuclear axis during the time interval (∞, t_{jf}), and ϑ_{jfi} is the angle of the rotation of the internuclear axis during the time interval (t_{jf}, t_{ji}). In Eq.(217), if $j+k>7$, then $g_{j+k}=0$.

Upon squaring and dropping terms with the rapidly varying factor $cos\int_{t'}^{t}(E_0(\tau)-E_n(\tau))d\tau$ I have

$$P_j(b) = (1-p_j)p_1 p_2 \cdots p_j\left\{1 + (1-p_{j+1})^2 + (1-p_{j+2})^2 p_{j+1}^2 + \cdots\right.$$
$$\left. + (1-p_7)^2 p_{j+1}^2 \cdots p_6^2 + p_{j+1}^2 p_{j+2}^2 \cdots p_7^2\right\},$$
$$1 \le j \le 6, \tag{219}$$

and

$$P_7 = 2(1 - p_7)p_1 p_2 \cdots p_7. \tag{220}$$

The total cross section for $C^{6+} + H \rightarrow C^{5+} + H^+$ collision in $n = 4$ is shown in Fig.21.

The solid curve is the present calculation, the dashed curve is my previous calculation, the chained curve is the 33-state calculation of Ref.15 and the points with error bars are experimental data of Ref.16. Agreement between these models and the experimental data is good.

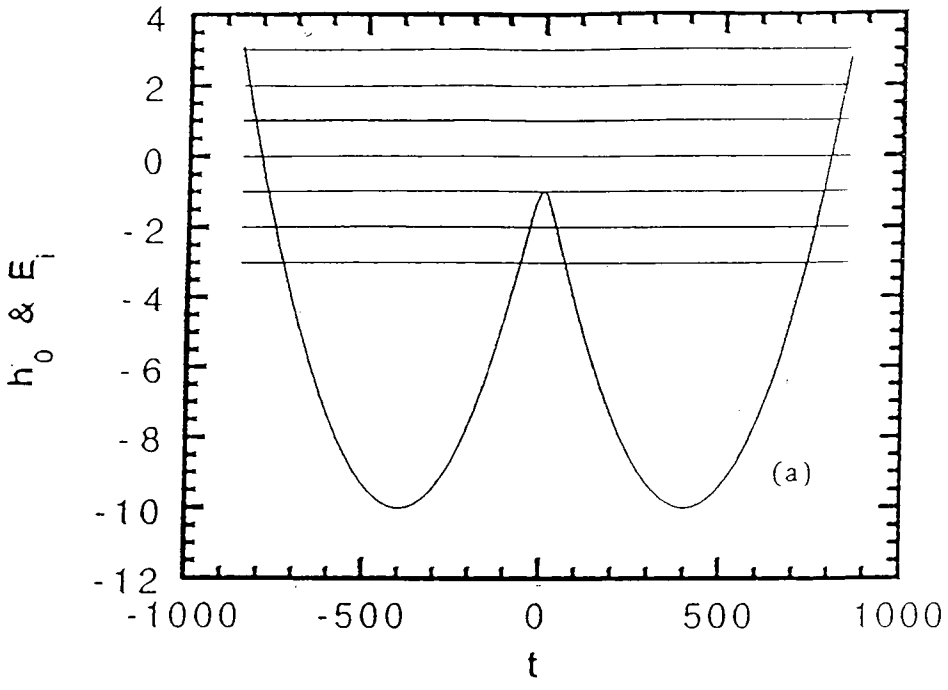


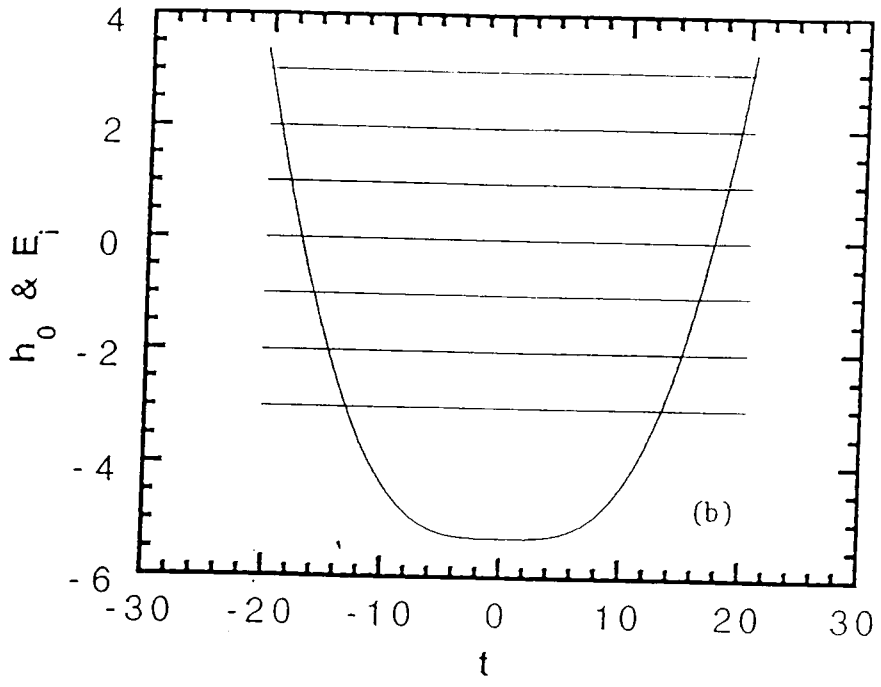
Fig.20 The effective energy levels of the $C^{6+} + H(1s)$ collision system vs time.

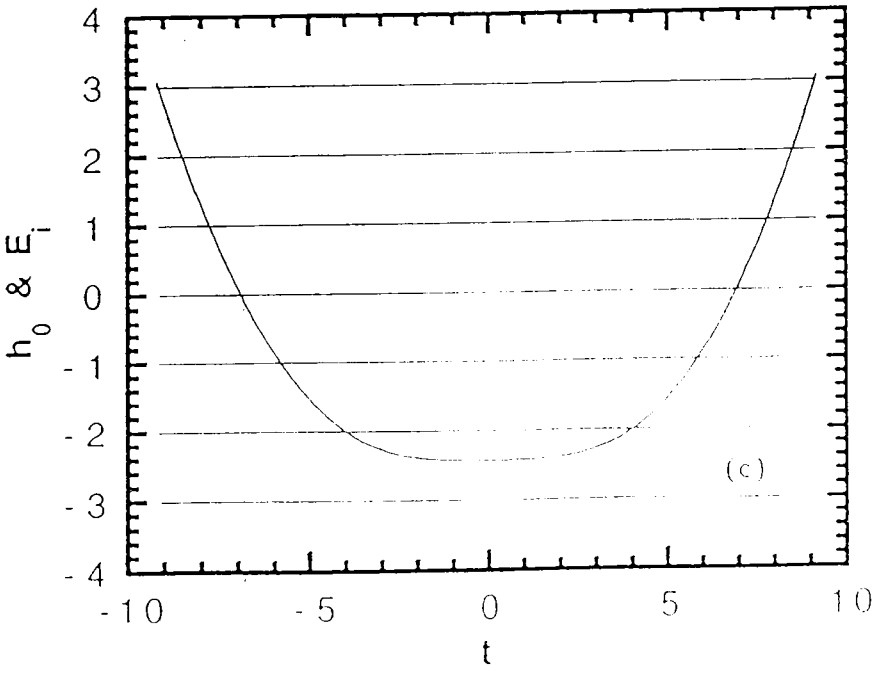
a) The relative velocity $v = 0.01 a.u.$ and the impact parameter $b = 0.2 a.u.$

b) The relative velocity $v = 0.4 a.u.$ and the impact parameter $b = 4 a.u.$

c) The relative velocity $v = 1. a.u.$ and the impact parameter $b = 4 a.u.$

Figure 20 (continued)





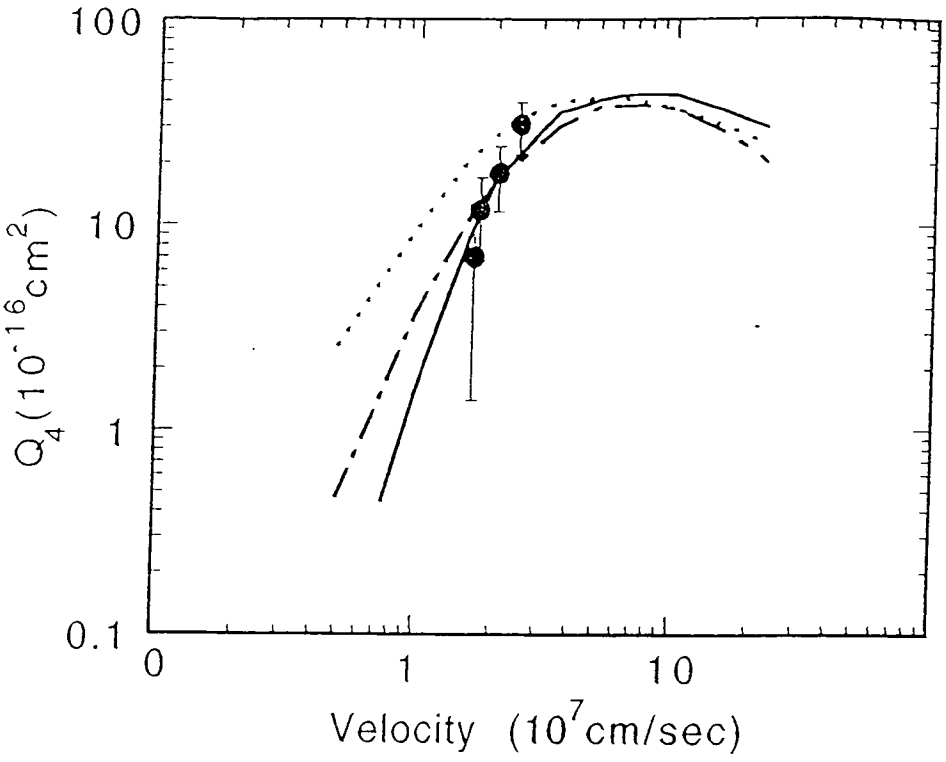


Fig. 21 Total cross section Q_n vs velocity for electron capture into the $n = 4$ level by fully stripped carbon ions. The solid curve is the present calculation, the dashed curve is my previous calculation, the chained curve is the 33-state calculation of Ref. 15, and the points with error bars are experimental data of Ref. 16.

My calculation shows that the Demkov's model not only can be used for a perturbation which depends linearly on time but also can be extended to the any interaction at the low energy collision system in which the effective H-matrix can be expressed in the form of the Demkov's model.

Chapter 5

Theory of Alignment and Orientation of Atomic States Produced by Slow Collisions of Highly Charged Ions with Neutral Species

5.1 Introduction

In a collision electron charge clouds not only change the size, they also change shape and rotate. The shape of atomic states is measured by the alignment parameter and the rotation is called the orientation parameter[22]. It is possible to carry out detailed experimental and theoretical studies of alignment and orientation of electronic charge clouds of atoms resulting from excitation or charge transfer during ion-atom collision processes. Such studies provide deeper insight into our understanding of excitation and charge-transfer collision dynamics in heavy-particle collisions than does the simple determination of probabilities or cross sections for the same processes. The study of the polarization of atomic radiation emitted after impact excitation has yielded much detailed information on the mechanism and dynamics of collisional excitation and energy transfer, both in electron and heavy particle impact studies[23]. In these studies, the beam of ions used to excite the atoms or ions provides a suitable quantization axis with respect to which the polarization of the fluorescent light of the excited atoms or ions is detected. From these data information on the density matrix of the excited atom or ion is extracted. This information can be expressed in terms of the mean value of irreducible tensors con-

structed from the angular momentum operators[55]. The commonly used Fano-Macek alignment and orientation parameters correspond to tensors of rank 2 and 1, respectively. In the work reported here I compute the mean value of irreducible tensors using the model of Macek and Dong[20]. I obtain the general result for arbitrary irreducible tensors in section 5.2. Values for tensors of rank 1 and 2, which are relevant to linear and circular polarization of fluorescent light are given in section 5.3. In section 5.4, I apply this theory to the processes

$$C^{6+} + H(1s) \rightarrow C^{5+}(nlm) + H^{+}, \tag{221}$$

$$B^{3+} + He(1s^2) \rightarrow B^{2+}(2p) + He^{+}(1s), \tag{222}$$

and

$$B^{3+} + He(1s^2) \rightarrow B^{2+}(2s) + He^{+}(1s). \tag{223}$$

I compare my results with the experimental data of Roncin *et al*[24].

5.2 Mean value of the irreducible tensors

From chapter 2, I have the amplitude $A_{nlm}(b)$ for populating the state nlm by capture at an impact parameter b

$$A_{nlm}(b) = C^{f}_{nl} d^{l}_{m,0}(\delta_f) + C^{i}_{nl} d^{l}_{m,0}(\delta_i), \tag{224}$$

where $d^{l}_{m,0}(\delta)$ is a rotation function[56,57,58]. In this work I employ complex associated Legendre function defined according to

$$P^{m}_{l}(x) = (1-x^2)^{m/2} \frac{d^m}{dx^m} P_l(x), \qquad m > 0 \tag{225}$$

$$P_l^{-m}(x) = (-1)^m \frac{(l-m)!}{(l+m)!} P_l^m(x), \tag{226}$$

and $P_l(x)$ is the Legendre polynomial. These functions are defined to agree with the definition of the rotation function[56,57,58]. The standard notation of Ref. 35 for the Legendre polynomials of complex argument is employed later.

All information on the behavior of a given system can be expressed in terms of mean values of suitably chosen operators[55,56,57]. The mean value of any operator Q is defined as

$$< |\hat{Q}| >= \sum_{m,m'} \rho_{m',m} < m|\hat{Q}|m' >, \tag{227}$$

Where $\rho_{m',m}$ is the density matrix element. In the present case I consider the unnormalized density matrix

$$\rho_{m',m}(b) = A_{nlm'}(b) A^*_{nlm}(b) \tag{228}$$

relevant to coincidence measurements where a single impact parameter b is singled out. Using Eq.(228) in Eq.(227) gives the mean value of an irreducible tensor $T_q^{[k]}$

$$< |T_q^{[k]}| >= \sum_{m,m'} A_{nlm'}(b) A^*_{nlm}(b) < lm|T_q^{[k]}|lm' > . \tag{229}$$

In order to use Eq.(224) azimuthal angles φ_f and φ_i are introduced and rotation function written in terms of spherical harmonic $Y_{lm}(\delta, \varphi)$ so that Eq.(224) becomes

$$A_{nlm}(b) = \sqrt{\frac{4\pi}{2l+1}} \left[C^f_{nl} Y_{lm}(\delta_f, \varphi_f) + C^i_{nl} Y_{lm}(\delta_i, \varphi_i) \right], \tag{230}$$

the angles φ_f and φ_i will be set to zero in the final expressions for alignment and orientation. Using Eq.(230) in Eq.(228) gives the mean value of an irreducible tensor $T_q^{[k]}$.

$$< |T_q^{[k]}| > = \frac{4\pi}{2l+1} \left\{ |C_{nl}^f|^2 \sum_{m,m'} Y_{lm'}(\delta_f, \varphi_f) Y_{lm}^*(\delta_f, \varphi_f) < lm|T_q^{[k]}|lm' > \right.$$
$$+ |C_{nl}^i|^2 \sum_{m,m'} Y_{lm'}(\delta_i, \varphi_i) Y_{lm}^*(\delta_i, \varphi_i) < lm|T_q^{[k]}|lm' >$$
$$\left. + \left[C_{nl}^f C_{nl}^{*i} \sum_{m,m'} Y_{lm'}(\delta_f, \varphi_f) Y_{lm}^*(\delta_i, \varphi_i) < lm|T_q^{[k]}|lm' > + c.c. \right] \right\}_{|\varphi_{f,i}=0} \quad (231)$$

The mean values are expressed in terms of the generic expression

$$\sum_{m,m'} Y_{lm}(\delta_1, \varphi_1) Y_{lm'}^*(\delta_2, \varphi_2) < nlm'|T_q^{[k]}|nlm > . \quad (232)$$

To compute this matrix element I note that an irreducible tensor operator $R_q^{[k]}$ which operates on the variables δ_2 and φ_2 obeys the equation

$$R_q^{[k]} Y_{lm}(\delta_2, \varphi_2) = \sum_{m'} Y_{lm'}(\delta_2, \varphi_2) < lm'|R_q^{[k]}|lm > . \quad (233)$$

By the Wigner - Eckart theorem[55] I can replace the matrix element $< lm'|R_q^{[k]}|lm >$ by $< lm'|T_q^{[k]}|lm >$. For a suitably normalized $R_q^{[k]}$ I then have

$$R_q^{[k]} Y_{lm}(\delta_2, \varphi_2) = \sum_{m'} Y_{lm'}(\delta_2, \varphi_2) < lm'|T_q^{[k]}|lm > \quad (234)$$

Upon multiplying by $Y_{lm}^*(\delta_1, \varphi_1)$ and summing over m I have

$$\sum_m Y_{lm}^*(\delta_1, \varphi_1) R_q^{[k]} Y_{lm}(\delta_2, \varphi_2) = R_q^{[k]} \sum_m Y_{lm}^*(\delta_1, \varphi_1) Y_{lm}(\delta_2, \varphi_2)$$
$$= \frac{2l+1}{4\pi} R_q^{[k]} P_l(\cos\zeta).$$
$$= \sum_{m',m} Y_{lm}^*(\delta_1, \varphi_1) Y_{lm'}(\delta_2, \varphi_2)$$
$$\times < nlm'|T_q^{[k]}|nlm >, \quad (235)$$

where

$$\cos\zeta = \cos^*\delta_1 \cos\delta_2 + \sin^*\delta_1 \sin\delta_2 \cos(\varphi_1 - \varphi_2). \quad (236)$$

Using Eq.(235) in Eq.(231) I obtain

$$< |T_q^{[k]}| > = \Big\{ \, |C_{nl}^f|^2 \, \hat{R}_q^{[k]} \, P_l(\cos\zeta_{ff}) + \, |C_{nl}^i|^2 \, \hat{R}_q^{[k]} \, P_l(\cos\zeta_{ii}) + [\, C_{nl}^f \, C_{nl}^{*i} \, \hat{R}_q^{[k]} \, P_l(\cos\zeta_{fi}) + c.c. \,] \Big\}_{\varphi_{f,i}=0}. \tag{237}$$

Eq.(237) is the desired expression which will be used in the next section to compute selected mean values relevant to collision excited states.

5.3 Polarization of resonance fluorescence in the rotational coupling model

I compute the alignment and orientation parameters. The alignment parameters are defined as

$$A_0^{col}(b) = \frac{< |3\hat{L}_z^2 - \hat{L}^2| >}{l(l+1)P_{nl}(b)}, \tag{238}$$

$$A_{1+}^{col}(b) = \frac{< |\hat{L}_x\hat{L}_z + \hat{L}_z\hat{L}_x| >}{l(l+1)P_{nl}(b)}, \tag{239}$$

$$A_{2+}^{col}(b) = \frac{< |\hat{L}_x^2 - \hat{L}_y^2| >}{l(l+1)P_{nl}(b)}. \tag{240}$$

The corresponding operator $\hat{R}_0^{[2]}$ is

$$\hat{R}_0^{[2]} = -3\frac{\partial^2}{\partial\varphi_2^2} - l(l+1). \tag{241}$$

Using Eq.(241) and the definition Eq.(237) in Eq.(235) I have

$$\begin{aligned} \hat{R}_0^{[2]} P_l(\cos\zeta) &= \Big[-3P_l''(\cos\zeta)\sin^2\delta_1^*\sin^2\delta_2\sin^2\varphi_2 \\ &\quad + 3P_l'(\cos\zeta)\sin\delta_1^*\sin\delta_2\cos\varphi_2 - l(l+1)P_l(\cos\zeta) \Big]_{|_{\varphi_2=0}} \\ &= 3P_l'(\cos\zeta)\sin\delta_1^*\sin\delta_2 - l(l+1)P_l(\cos\zeta). \end{aligned} \tag{242}$$

Substituting Eq.(242) into Eq.(235) and the result into Eq.(237) , I get the alignment parameter $A_0^{col}(b)$

$$A_0^{col}(b) = \frac{1}{l(l+1)P_{nl}(b)} \Big\{ |C_{nl}^f|^2 \left[3P_l'(\cos\zeta_{ff})|\sin\delta_f|^2 - l(l+1)P_l(\cos\zeta_{ff})\right] + |C_{nl}^i|^2 \left[3P_l'(\cos\zeta_{ii})|\sin\delta_i|^2 - l(l+1)P_l(\cos\zeta_{ii})\right] + \left[C_{nl}^f C_{nl}^{*i} \left(3P_l'(\cos\zeta_{fi})\sin\delta_i^* \sin\delta_f - l(l+1)P_l(\cos\zeta_{fi})\right) + c.c. \right] \Big\}. \quad (243)$$

The operator corresponding to $\hat{L}_x\hat{L}_z + \hat{L}_z\hat{L}_x$ is

$$\hat{R}_{1+}^{[2]} = 2\sin\phi_2 \frac{\partial}{\partial\phi_2}\frac{\partial}{\partial\delta_2} + 2\cot\delta_2\cos\phi_2\frac{\partial^2}{\partial\phi_2^2} + \cos\phi_2\frac{\partial}{\partial\delta_2} - \cot\delta_2\sin\phi_2\frac{\partial}{\partial\phi_2}, \quad (244)$$

I then have for the alignment parameter $A_{1+}^{col}(b)$

$$A_{1+}^{col}(b) = \frac{-1}{l(l+1)P_{nl}(b)} \Big\{ |C_{nl}^f|^2 \sin(\delta_f + \delta_f^*)\, P_l'(\cos\zeta_{ff}) + |C_{nl}^i|^2 \sin(\delta_i + \delta_i^*)\, P_l'(\cos\zeta_{ii}) + \left[C_{nl}^f C_{nl}^{*i} \sin(\delta_f + \delta_i^*)\, P_l'(\cos\zeta_{fi}) + c.c. \right] \Big\}. \quad (245)$$

The operator corresponding to $\hat{L}_x^2 - \hat{L}_y^2$ is

$$\hat{R}_{2+}^{[2]} = \Big\{ \cot\delta_2(\sin^2\phi_2 - \cos^2\phi_2)\frac{\partial}{\partial\delta_2} - (\sin^2\phi_2 - \cos^2\phi_2)\frac{\partial^2}{\partial\delta_2^2} + \cot^2\delta_2(\sin^2\phi_2 - \cos^2\phi_2)\frac{\partial^2}{\partial\phi_2^2} + 2\cot^2\delta_2\sin\phi_2\cos\phi_2\frac{\partial}{\partial\phi_2} - 4\cot\delta_2\sin\phi_2\cos\phi_2\frac{\partial}{\partial\phi_2}\frac{\partial}{\partial\delta_2} + \frac{2\sin\phi_2\cos\phi_2}{\sin^2\delta_2}\frac{\partial}{\partial\phi_2} \Big\}. \quad (246)$$

I have

$$\hat{R}_{2+}^{[2]} P_l(\cos\zeta) = \sin^2\zeta\ P_l''(\cos\zeta) - \sin^*\delta_1 \sin\delta_2\ P_l'(\cos\zeta), \quad (247)$$

so I have $A_{2+}^{col}(b)$

$$A_{2+}^{col}(b) = \frac{1}{l(l+1)P_{nl}(b)} \Big\{ |C_{nl}^{f}|^2 \ \Big[\sin^2\zeta_{ff}\ P_l^{''}(\cos\zeta_{ff}) - |\sin\delta_f|^2\ P_l^{'}(\cos\zeta_{ff})\Big] + |C_{nl}^{i}|^2 \ \Big[\sin^2\zeta_{ii}\ P_l^{''}(\cos\zeta_{ii}) - |\sin\delta_i|^2\ P_l^{'}(\cos\zeta_{ii})\Big] + \Big[\ C_{nl}^{f}\ C_{nl}^{*i}\ \Big[\sin^2\zeta_{fi}\ P_l^{''}(\cos\zeta_{fi}) - \sin^*\delta_i \sin\delta_f\ P_l^{'}(\cos\zeta_{fi})\Big] + c.c.\ \Big]\Big\}. \tag{248}$$

Since most standard computer programs for the associated Legendre functions of complex argument employ the definition

$$\mathcal{P}_l^m(z) = (z^2-1)^{m/2}\frac{d^m}{dz^m}P_l(z), \tag{249}$$

for complex z, Eq.(249) rather than Eq. (225) is used to express the group properties of the rotation function. For $m = even$ the two definitions are identitical, and Eq.(225) can be used directly in Eqs.(238) to Eq.(248). But for the orientation I must use the definition of Eq.(249). The orientation O_1^{col} is proportional to the mean value of $< |\hat{L}_y| >$.

$$O_1^{col} = \frac{< |\hat{L}_y| >}{l(l+1)P_{nl}(b)} \tag{250}$$

The corresponding operator $\hat{R}_q^{[k]}$ is

$$\hat{R}_y = i(-\cos\phi_2\frac{\partial}{\partial\delta_2} + \cot\delta_2\sin\phi_2\frac{\partial}{\partial\phi_2}), \tag{251}$$

and

$$\hat{R}_y P_l(\cos\zeta)|_{\varphi_2=0} = i\sin\zeta P_l^{'}(\cos\zeta). \tag{252}$$

According to the definition of Eq.(249), I get

$$\hat{R}_y P_l(\cos\zeta)|_{\phi_2=0} = \mathcal{P}_l^1(\cos\zeta). \qquad (253)$$

Substituting Eq.(253) to Eq.(237), the orientation parameter is

$$\begin{aligned} O_1^{col} &= \frac{< |\hat{L}_y| >}{l(l+1)P_{nl}(b)} \\ &= \frac{1}{l(l+1)P_{nl}(b)} \Big\{ |C_{nl}^f|^2 \, \mathcal{P}_l^1(\cos\zeta_{ff}) + |C_{nl}^i|^2 \, \mathcal{P}_l^1(\cos\zeta_{ii}) \\ &+ \Big[C_{nl}^f \, C_{nl}^{*i} \, \mathcal{P}_l^1(\cos\zeta_{fi}) + c.c. \Big] \Big\}. \end{aligned} \qquad (254)$$

More general irreducible tensors are given by Eq.(237). Here I have illustrated the use of Eq.(237) for tensors of rank 1 and 2.

In the case of $3nZ_T/2Z_P \gg bv$, I can neglect the rotational coupling. From chapter 2, I have

$$\begin{aligned} P_{nl}(b) &= 2p(1-p) < j, j; j, -j | l, 0 >^2 \\ &\times \left\{ 1 + \sin\left[4j\alpha_{fi} + 2\phi_s + \frac{2}{v} < Ea > \right] \right\}. \end{aligned} \qquad (255)$$

and

$$P_n(b) = 2p(1-p) \left\{ 1 + \sin\left[4j\alpha_{fi} + 2\phi_s + \frac{2}{v} < Ea > \right] \right\}. \qquad (256)$$

The single non - vanishing alignment parameter A_0^{col} has the value of -1, and the orientation vanishes. This means that the original two-state model can not get the orientation parameter.

From chapter 2, I know that there are two cases in which the Stark-effect can be neglected. For both cases, I have

$$\alpha(t, t') = 0, \qquad (257)$$

$$\omega(t,t') = \Delta\theta(t,t'), \tag{258}$$

$$\beta(t,t') = -\omega(t,t') = -\Delta\theta(t,t'), \tag{259}$$

$$\cos\delta = -\cos\beta(t,t') = -\cos\Delta\theta(t,t'), \tag{260}$$

where $\Delta\theta(t,t') = \theta(t') - \theta(t)$. For the first case, the final excited states on the projectile are degenerate, and the matrix element $u_{nlm;Q}(t,t')$ becomes

$$\begin{aligned} u_{nlm;Q}(t,t') &= (-1)^{-l} < j,j;j,-j|l,0 > \\ &\times \left[\frac{(l-m)!}{(l+m)!}\right]^{1/2} P_l^m[-\cos\Delta\theta(t,t')]. \end{aligned} \tag{261}$$

The rotation angles θ_f and θ_i are given in terms of the single angle $\theta_{fi} = \Delta\theta(t_f,t_i)$ by

$$\begin{aligned} \Delta\theta(t_f,t_i) &= \theta_i - \theta_f, \\ \theta_f &= (\pi - \theta_{fi})/2, \\ \theta_i &= (\pi + \theta_{fi})/2 \end{aligned} \tag{262}$$

and

$$\begin{aligned} P_{nl}(b) &= (1-p) < j,j;j,-j|l,0 >^2 \\ &\times \left\{ p + 1 + (\sqrt{p}-1)^2 \cos^{4(n-1)}\frac{\theta_{fi}}{2} \right. \\ &+ 2\sqrt{p}(\sqrt{p}-1)\cos^{2(n-1)}\frac{\theta_{fi}}{2}\sin(2 < Ea > +2\phi_s) \\ &\left. + 2\left[(\sqrt{p}-1)\cos^{2(n-1)}\frac{\theta_{fi}}{2} + \sqrt{p}\sin(2 < Ea > +2\phi_s)\right] P_l(\cos\theta_{fi}) \right\}. \end{aligned} \tag{263}$$

The alignment parameter is

$$\frac{<|3\hat{L}_z^2-\hat{L}^2|>}{l(l+1)P_{nl}(b)}=\frac{2(1-p)<j,j;j,-j|l,0>^2}{l(l+1)P_{nl}(b)}$$
$$\times\left[(\sqrt{p}-1)\cos^{2(n-1)}\frac{\theta_{fi}}{2}+\sqrt{p}\sin(2<Ea>+2\phi_s)\right]$$
$$\times\left[3P_l'(\cos\theta_{fi})\cos^2\frac{\theta_{fi}}{2}-l(l+1)P_l(\cos\theta_{fi})\right]. \qquad (264)$$

The orientation parameter is

$$\frac{<|\hat{L}_y|>}{l(l+1)P_{nl}(b)}=\frac{2(1-p)}{l(l+1)P_{nl}(b)}<j,j;j,-j|l,0>^2\mathcal{P}_l^1(\cos\theta_{fi})$$
$$\times\left[(\sqrt{p}-1)\cos^{2(n-1)}\frac{\theta_{fi}}{2}+\sqrt{p}\sin(2<Ea>+2\phi_s)\right]. \qquad (265)$$

For the second case, the final states on the projectile are no longer degenerate in the principal shells. This means that there is a curve crossing for each l-level. In this case, one has $3nZ_T/2Z_P \ll bv$ so that I neglect the Stark-effect. From chapter 3, the probability is

$$P_l(b)=|C_{n,l}^f|^2+|C_{n,l}^i|^2+\left[C_{n,l}^f C_{n,l}^{*i}P_l(\theta_{fi})+c.c.\right], \qquad (266)$$

where $P_l(\theta_{fi})$ is a Legendre Polynomial. The alignment parameter is

$$\frac{<3\hat{L}_Z^2-\hat{L}^2>}{l(l+1)P_{nl}(b)}=\frac{1}{l(l+1)P_{nl}(b)}[C_{nl}^f C_{nl}^{*i}+c.c.]$$
$$\times[3P_l'(\cos\theta_{fi})\cos^2\frac{\theta_{fi}}{2}-l(l+1)P_l(\cos\theta_{fi})]. \qquad (267)$$

The orientation parameter is

$$\frac{<|\hat{L}_y|>}{l(l+1)P_{nl}(b)}=\frac{1}{l(l+1)P_{nl}(b)}[C_{nl}^f C_{nl}^{*i}\mathcal{P}_l^1(\cos\theta_{fi})+c.c.]. \qquad (268)$$

Other components of the alignment tensors are easily computed but are not given here.

5.4 Application to $C^{6+} + H(1s)$ and $B^{3+} + He(1s^2)$ collisions

I apply my results to the C^{6+} + H(1s) $\rightarrow$ $C^{5+}(nlm)$ + H^+ and B^{3+} + $He(1s^2)$ $\rightarrow$ $B^{2+}(2p, 2s)$ + He^+ capture processes. As is known , for C^{6+} + H(1s), only the n=4 level is populated appreciably. The crossing radius is

$$R_c = 7.88 \tag{269}$$

I compute the probabilities, alignment parameters, and orientation parameters. Figure 22 show only the cross term with the factor $\cos \int_{t_i}^{t_f} [E_0(t) - E_n(t)]dt$ for the C^{6+} + H(1s) collision system at v=22.8×10^7 cm/sec. Comparing with the corresponding probability in the low velocity region the value of the cross term is very small, and oscillates very rapidly as shown in Fig. 6, so that I can drop the cross term. Otherwise, in the high velocity regions the values of the cross terms are not very small as shown in Fig. 21 so that I keep these terms in my calculations. Figure 23 and figure 24 show the probabilities, alignment, and orientation parameters as a function of impact parameter for the C^{6+} + H(1s) collision system at the velocity v=0.5×10^7 cm/sec and v=22.8×10^7 cm/sec, respectively. I drop the cross term with the rapidly varying factor $\cos \int_{t_i}^{t_f} [E_0(t) - E_n(t)]dt$ and without the denominators $l(l+1)P_{nl}(b)$ in the v=0.5×10^7 cm/sec calculation in Eqs. (238), (239), (240) and (254), but not in the v=22.8×10^7 cm/sec calculation.

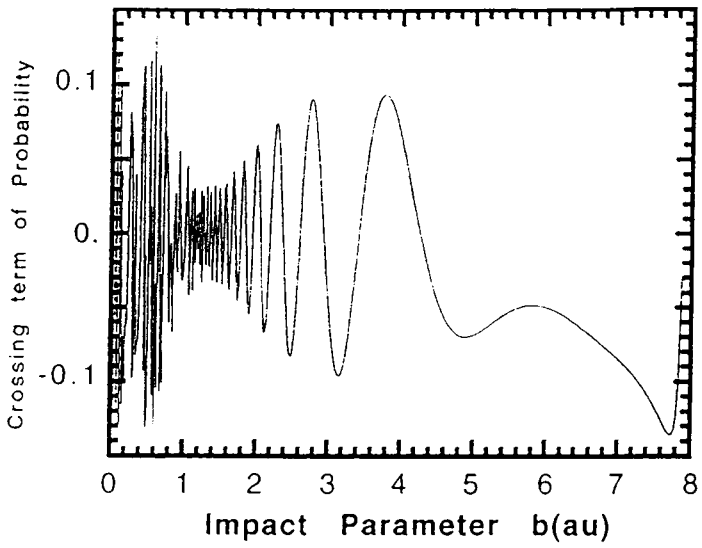


Fig. 22. The probability distribution of the cross term with the factor $\cos \int_{t_i}^{t_f} [E_0(t) - E_n(t)]dt$ for C^{6+} + H(1s) collision system at the velocity v=22.8×10^7 cm/sec.

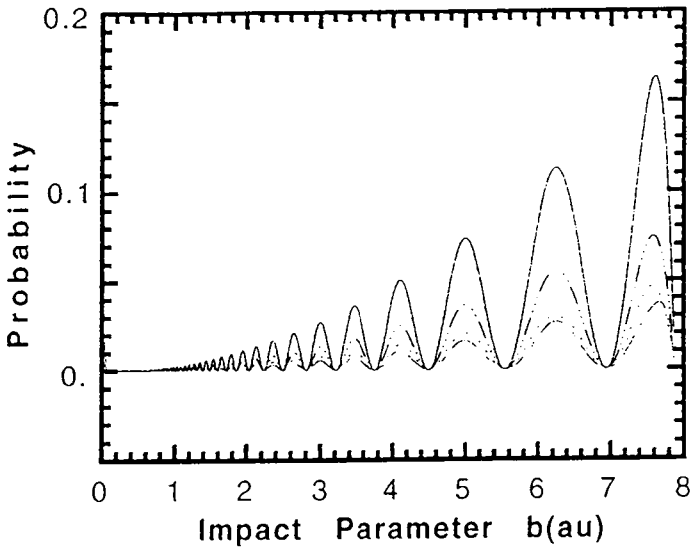


Fig. 23. The probabilities, alignment parameters, and orientation parameters as a function of impact parameter for C^{6+} + H(1s) collision system at the velocity v=0.5×10^7 cm/sec. a) The probability $P(b)$; solid line for n=4 state, dashed line for 4p, chain line for 4f, and dashed chain line for 4d substates, respectively.

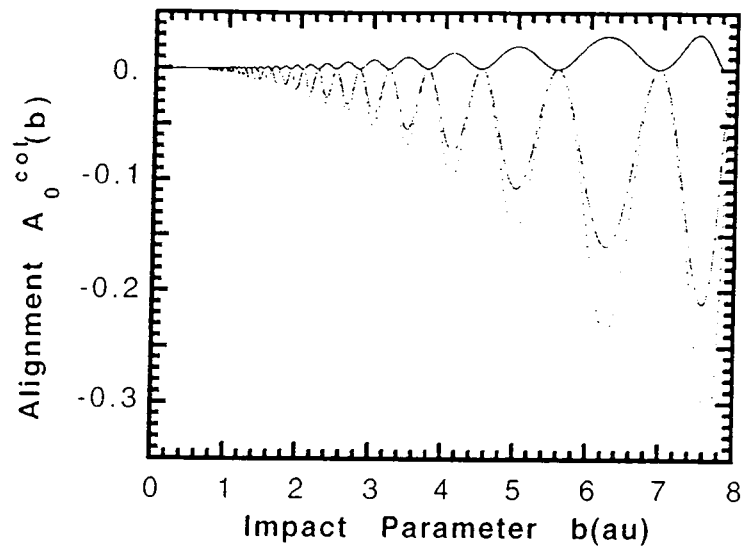
b) alignment parameter $A_0^{col}(b)$; solid lines for 4p state, dashed line for 4f, and chain line for 4d substates, respectively.

c) alignment parameter $A_{+1}^{col}(b)$; solid lines for 4p state, dashed line for 4f, and chain line for 4d substates, respectively.

d) alignment parameter $A_{+2}^{col}(b)$; solid lines for 4p state, dashed line for 4f, and chain line for 4d substates, respectively.

e) orientation $O^{col}(b)$; solid lines for 4p state, dashed line for 4f, and chain line for 4d substates, respectively.

Figure 23 (continued)



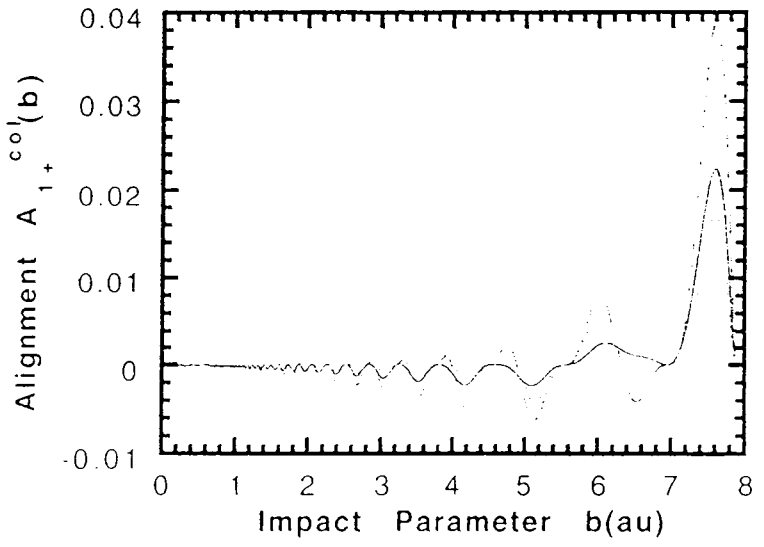
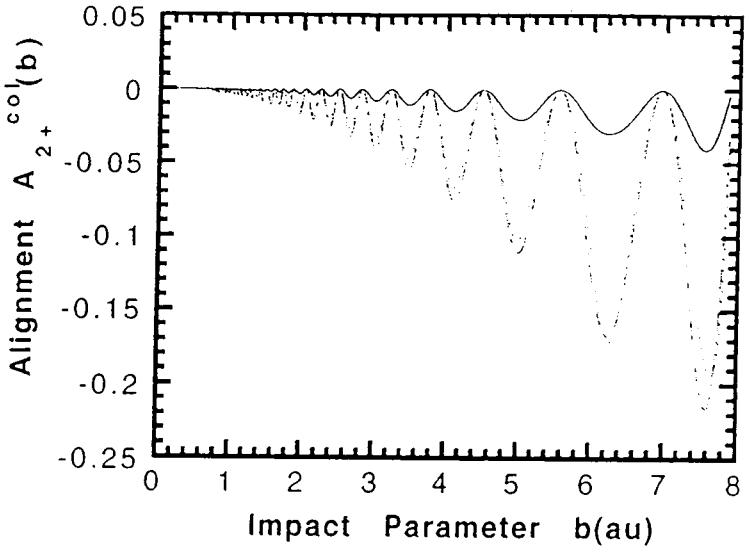
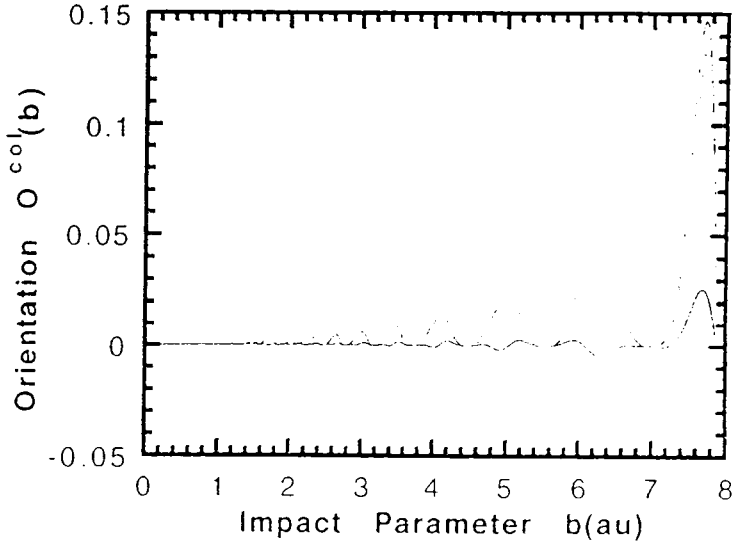


Figure 23 (continued)





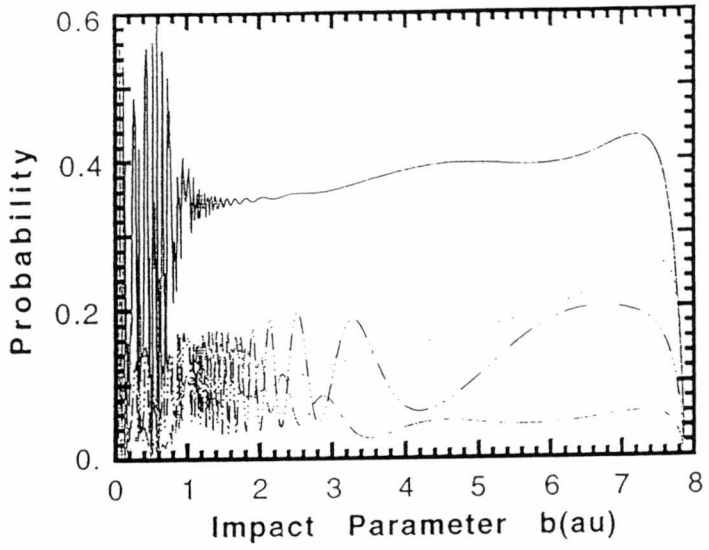


Fig.24 The probabilities, alignment, and orientation parameters as a function of impact parameter b for C^{6+} + H(1s) $\rightarrow$ $C^{5+}(nlm)$ + H^{+} collision system at v=22.8$\times$ 10^{7} cm/sec.

a) The probability $P(b)$; solid line for n=4 state, dashed line for 4p, chain line for 4f, and dashed chain line for 4d substates, respectively.

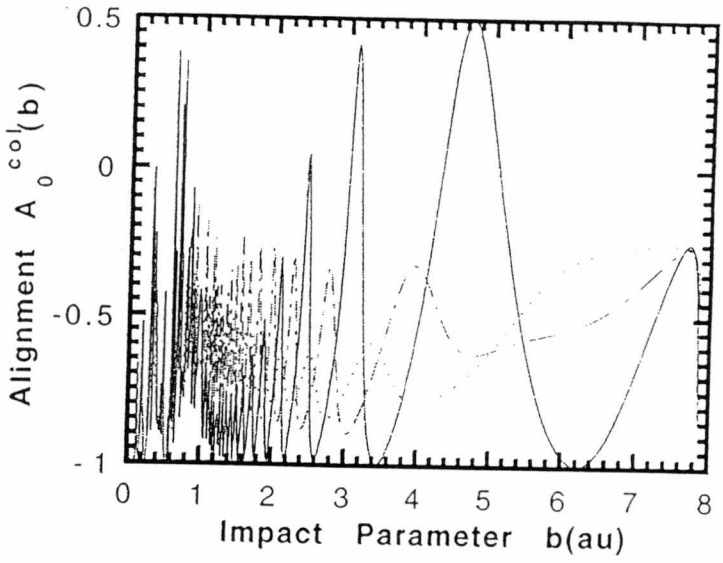
b) alignment parameter $A_0^{col}(b)$; solid lines for 4p state, dashed line for 4f, and chain line for 4d substates, respectively.

c) alignment parameter $A_{+1}^{col}(b)$; solid lines for 4p state, dashed line for 4f, and chain line for 4d substates, respectively.

d) alignment parameter $A_{+2}^{col}(b)$; solid lines for 4p state, dashed line for 4f, and chain line for 4d substates, respectively.

e) orientation $O^{col}(b)$; solid lines for 4p state, dashed line for 4f, and chain line for 4d substates, respectively.

Figure 24 (continued)



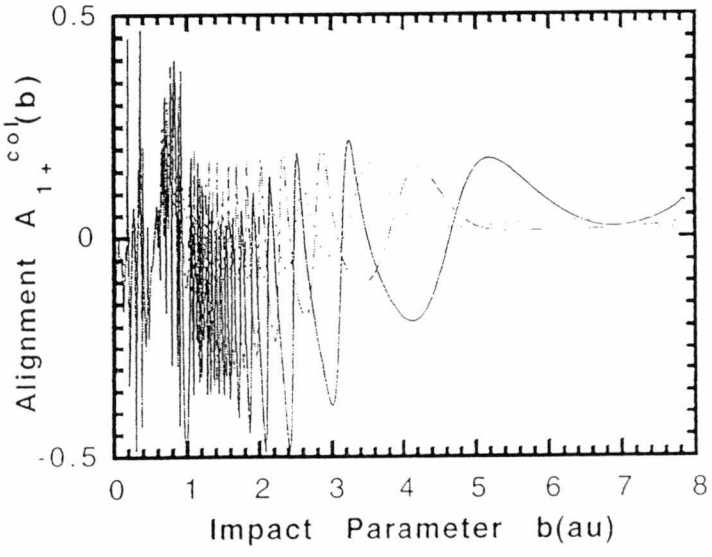
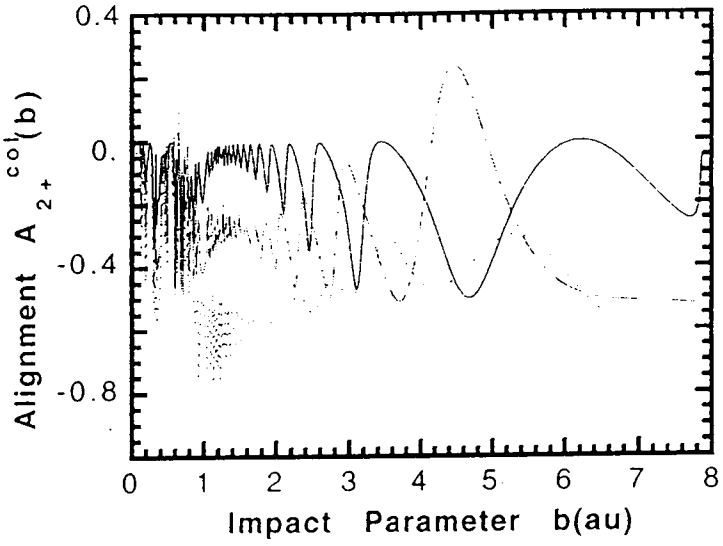


Figure 24 (continued)



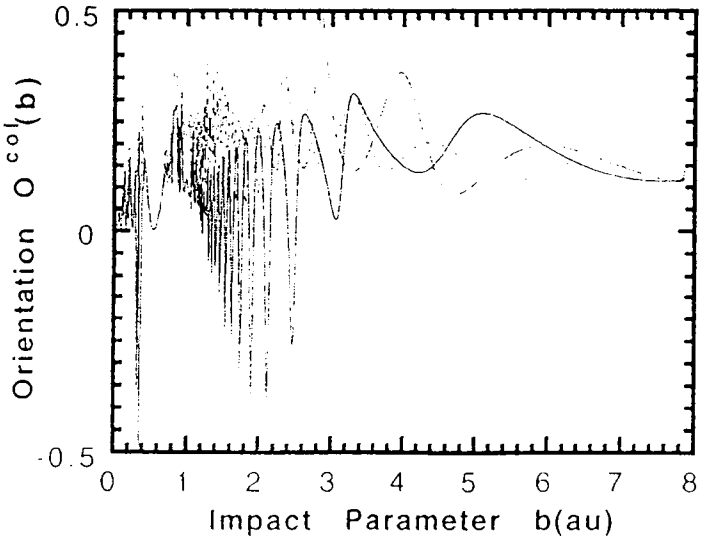


Figure 25 is the integral alignment parameter (i.e. integrate over the impact parameters) as a function of velocities.

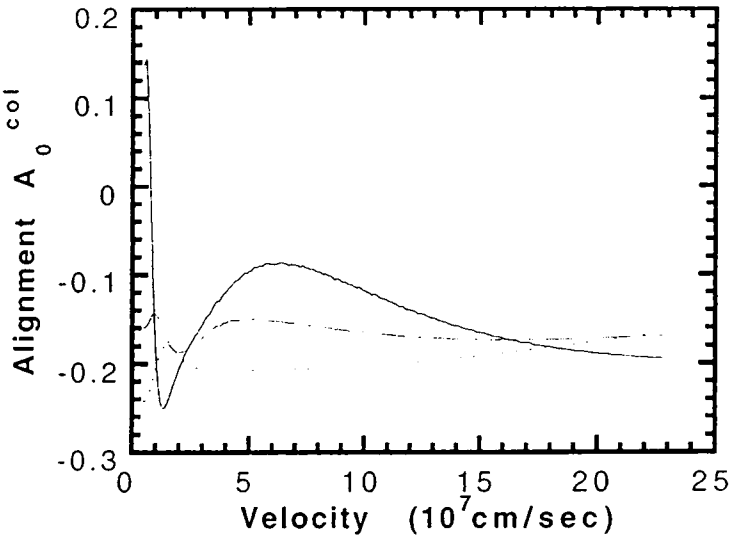


Fig. 25. The integral alignment parameter (i.e. integrate over the impact parameters) as a function of velocities. solid lines for 4p state, dashed line for 4f, and chain line for 4d substates, respectively.

As a check on my computations, I also calculate the circular polarization for B^{3+} + He collision system. For this case, I use the formula of the chapter 3 for partially charged ions. The final states for B^{2+} are $n = 2$ and $l = 1, 0$. The crossing radius for 2p states is 7.4a.u., and for 2s state is 4.5a.u.[24]. I neglect the Stark - effect in this collision. According Eqs.(126) and Eq.(127), the amplitude for electron - capture to 2s state is

$$A_{2s}(b) = g_s g_p \exp[-i \int_{-\infty}^{\infty} E_0(\tau) d\tau + i \int_{t_{s_1}}^{\infty} (E_0(\tau) - E_s(\tau)) d\tau]$$

$$\times \left\{ s_s^* - s_s \exp[i \int_{t_{si}}^{t_{sf}} (E_0(\tau) - E_s(\tau)) d\tau] \right\}, \tag{270}$$

the amplitude for electron - capture to 2p state is

$$A_{21_m}(b) = \left[C_{21}^f u_{21m}(\infty, t_{pf}) + C_{21}^i u_{21m}(\infty, t_{pi}) \right] \times \exp[-i \int_{-\infty}^{\infty} E_0(\tau) d\tau + i \int_{t_{pi}}^{\infty} (E_0(\tau) - E_p(\tau)) d\tau], \tag{271}$$

where g_s, s_s, g_p and s_p are the Landau - Zener parameters for 2s and 2p states, $E_0(\tau)$, $E_s(\tau)$, and $E_p(\tau)$ denote the energy of the diabatic states correlating of helium, 2s and 2p states of the three - electron boron ion, respectively. According the reaction-window analysis of Taulbjerg[13], the H_{12} should be modified as

$$H_{12} = (9.13 f_{nl}/\sqrt{q}) \exp[-1.324 R_c \alpha/\sqrt{q}), \tag{272}$$

where

$$\alpha = \sqrt{2I_t}, \tag{273}$$

I_t is the ionisation potential of the target.

The factor f_{nl}^{13} is

$$f_{nl} = (-1)^{n+l-1}(2l+1)^{1/2}\Gamma(n)\ [\Gamma(n+l+1)\Gamma(n-l)]^{-1/2}. \tag{274}$$

The coefficients C_{21}^f and C_{21}^i are

$$C_{21}^f = s_p^* g_p \left[p_s + (1-p_s) \exp[i2\phi_s + i \int_{t_{si}}^{t_{sf}} (E_0(\tau) - E_s(\tau)) d\tau] \right] - s_p(g_p - 1) u_0(t_{pf}, t_{pi}) \exp[i \int_{t_{pi}}^{t_{pf}} (E_0(\tau) - E_s(\tau)) d\tau], \tag{275}$$

where

$$(1-p_s) \exp[i2\phi_s] = s_s^2. \tag{276}$$

$$C_{21}^{i} = -s_p \exp[i \int_{t_{pi}}^{t_{pf}} (E_0(\tau) - E_s(\tau)) d\tau], \tag{277}$$

and

$$u_{21m}(t,t') = \begin{cases} \cos\theta(t,t') & m = 0 \\ \frac{\sqrt{2}}{2}\sin\theta(t,t') & m = 1 \\ -\frac{\sqrt{2}}{2}\sin\theta(t,t') & m = -1 \end{cases} . \tag{278}$$

The orientation is

$$\frac{< |L_y| >}{2P_{21}} = \frac{\sqrt{2}\, i(A_{211}A_{210}^{*} - c.c.)}{2(2|A_{211}(b)|^2 + |A_{210}(b)|^2)}. \tag{279}$$

Using the Bessel transform[59] for the very small angles

$$A_{21m}(\theta) = K(-i)^{m+1} \int_0^\infty A_{21m}(b) J_m(K\theta b) b db$$
$$K \approx [(\mu v)^2 - 2\mu\varepsilon_{lm}]^{1/2}. \tag{280}$$

with

$$\varepsilon_{lm} \ll \frac{1}{2}\mu v^2, \tag{281}$$

I have

$$A_{21m}(\theta) = (-i)^{m+1}\mu v \int_0^\infty A_{21m}(b) J_m(\mu v b\theta) b db. \tag{282}$$

Therefore, the amplitudes $A_{211}(\theta)$ and $A_{210}(\theta)$ are

$$A_{211}(\theta) = -\mu v \int_0^\infty A_{211}(b) J_1(\mu v b\theta) b db, \tag{283}$$

and

$$A_{210}(\theta) = -i\mu v \int_0^\infty A_{210}(b) J_0(\mu v b\theta) b db. \tag{284}$$

$J_1(\mu v b\theta)$ and $J_0(\mu v b\theta)$ are the first order and zero order Bessel functions. Substituting Eqs.(283) and (284) to Eq.(279), I have the orientation

$$O_1^{col}(\theta) = \frac{\sqrt{2}\, i(A_{211}(\theta)A_{210}^*(\theta) - c.c.)}{2(2|A_{211}(\theta)|^2 + |A_{210}(\theta)|^2)}. \tag{285}$$

Using Eq.(285) and $S(-\theta) = -S(\theta)$ I get the orientation for 1.5-kev $B^{2+}(2p)$ ions produced by slow collosion of $B^{3+} + He$ as shown in Fig.26. The solid curve is the present result. The • with error bars are experimental data from Ref.24. The o are from the relation $S(-\theta) = -S(\theta)$.

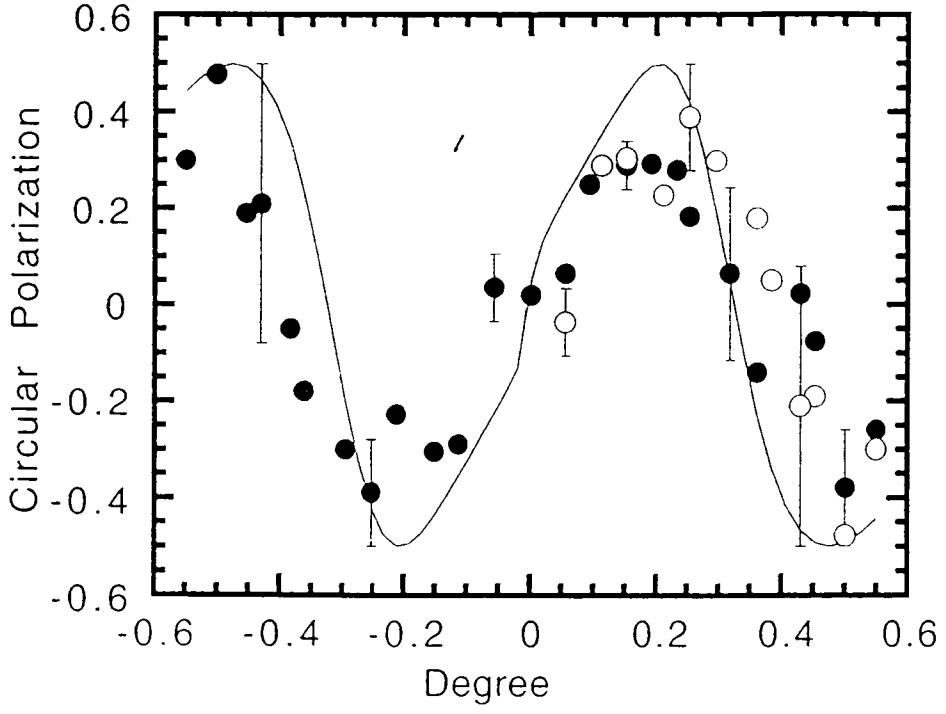


Fig. 26. The orientation for 1.5-kev $B^{2+}(2p)$ ions produced by slow collosion of $B^{3+} + He$. The solid curve is present result. The • with error bars are experimental data from Ref.24. The o with error bars are experimental data which are from the relation $S(-\theta) = -S(\theta)$.

Comparing my theoretical calculation with the experimental data of Ref.24, the

agreement is satisfactory in the small scattering angle region. I only include the Coulomb interaction between $B^{2+}(2p)$ and He^{+} ions, so that this approximate potential may cause the disagreement at large scattering angles.

My calculations and the figures show that my model is useful to get the alignment and orientation parameters.

Chapter 6
Conclusions

I combine the general formulation of Ref. 18 with the model of Ref. 17 to obtain a new model which is the Landau-Zener model with rotational and degenerate Stark - effect coupling, and obtain the electron transfer amplitudes and probabilities for populating the state nlm at impact parameter b. Using this theory I obtain the partial and total cross sections. The L-distributions provide a more stringent test of this model. My results show that L-distributions depart from those obtained by more exact calculations, but that the agreement is still good at velocities near and below the cross section maximum. At higher velocities discrepancies appear, as would be expected in any Landau-Zener treatment. Extending the single Landau-Zener crossing model, I obtain a model of the multiple Landau-Zener crossings. I apply the multiple Landau-Zener crossing model to partially charged heavy ions colliding with atoms at low velocities. At higher velocities (velocities higher than the velocity at the cross section maximum to 2 a.u.) I employ the top-of-barrier model to calculate the cross section and obtain a good result compared with other calculations and experimental data. Also, I have discussed two special cases: One is to neglect the rotational coupling. Within the Landau-Zener framework, the result is exactly equal to the original two-state model. Another is to neglect the degenerate Stark - effect coupling. I apply the later case to $A^{Z_P+} + B^-$ and $A^{q+} + B$ collision processes.

My electron capture amplitudes can be written in a form which exhibits the m-dependence explicitly. Because the m-dependence appears only in the rotation

functions, mean values of tensor operator are easily constructed. I have obtained a simple analytical formulation of the mean value for any rank of an irreducible tensor, especially, for alignment and orientation parameters. Application to $B^{3+} + He$ collision processes show that the orientation parameter is in good agreement with experimental data. My calculation shows that the Stark-effect and the rotational coupling are very important in the low energy collisions.

Bibliography

Bibliography

[1] J. E. Rice, E. S. Marmar, J. L. Terry, E. Källne and J. Källne, Phys. Rev. Lett. **56** 50(1986).

[2] R. J. Fonck, D. S. Darrow and K. P. Jähnig, Phys. Rev. A**29** 3288(1984).

[3] A. Boileau, M. Von Hellermana, L. D. Horton, J. Speuce and H. P. Summers, Plasma Phys. Controlled Fusion **31** 779(1989).

[4] A. Dalgarno, *Advances in Atomic and Molecular Physics* (edited by D. Bates and B. Bederson) 15 (Academic Press, London 1979).

[5] T. T. Heil, Nucl. Instrum Methods, B**23** 222(1987).

[6] E. E. Nikitin, S. Ya. Umanskii, *Theory of slow Atomic Collision* (1984).

[7] Marc Pieksma, and S. Yu Ovchinnikov, J. Phys. B: At. Mol. Opt. Phys. **24** 2699 (1991).

[8] L. Landau, Sow. Phys. **2** , 46(1932).

[9] C. Zener, Proc. Roy. Soc. A**137** , 696(1932).

[10] V. K. Bykhovskii, E. E. Nikitin and M. Ya. Ovchinnikova, Zh. Eksp. Teor. Fiz. **47** 750(1964) [Sov. Phys. _JETP **20**, 500 (1965)].

[11] E. E. Nikitin, Opt. Spektrosk. 13, 761 (1962).

[12] R. E. Olson and A. Salop,Phys. Rev. A**14** , 579(1976).

[13] Knud Taulbjerg, J. Phys. B**19** L367(1986).

[14] J. S. Briggs and J. Vaaben, J. Phys. B**15** L520(1982).

[15] T. A. Green, E. J. Shipsey, and J. C. Browne, Phys. Rev. A**25** 1364(1982).

[16] R. A. Phaneuf, I. Alvarez, F. W. Meyer, and D. H. Crandall, Phys. Rev. A**26** 1892(1982).

[17] V. A. Abramov, F. F. Baryshnikov, and V. S. Lisitsa, Zh. Eksp. Teor. Fiz. **74** 897(1978) [Sov. Phys. _ JETP **47**, 469(1979)].

[18] D. H. Jaecks, F. W. Erikson, W. de Rijk, and J. H. Macek, Phys. Rev. Lett. **35**, 723(1975).

[19] R. K. Janev, and H. Winter, Phys. Rept. **117**, 265(1985).

[20] J. Macek and X. Y. Dong, Phys. Rev. A**40** 95 (1989).

[21] Yu. N. Demkov, and V. I. Osherov, Zh. Eksp. Teor. Fiz. **53** 1589(1967) [Sov. Phys. _JETP **26**, 916(1968)].

[22] Joseph Macek, *Fundamental Processes in Energetic Atomic Collisions* (edited by H. O. Lutz, J. S. Briggs, and H. Kleinpoppin) (Plenum Publishing Corporation,1983). .

[23] Nils Andersen, Jean W. Gallagher, and Ingolf V. Hertel, Phys. Rep. **165** 1 (1988).

[24] P. Roncin, C. Adjouri, M. N. Gaboriaud, L. Guillemot, M. Barat, and N. Andersen, Phys. Rev. Lett. **65** 3261(1990).

[25] M. Born and R. Oppenheimer, Ann. Phys. (Leipzig)**84** 457 (1927).

[26] D. R. Bates and R. McCarroll, Proc. R. Soc. London Ser. A**245**, 175(1958).

[27] J. Macek and K. A. Jerjian, Phys. Rev. A**33**, 233(1986).

[28] J. B. Delos, Rev. Mod. Phys. **53**, 287(1981).

[29] R. T. Pack, Phys. Rev. A**32**, 2022(1985).

[30] J. Macek, M. Cavagnero, K. Jerjian, and U. Fano, Phys. Rev. A**35**, 3490(1987).

[31] E. A. Soloviev and S. I. Vinitzkn, J. Phys. B**18**, L557(1985).

[32] M. E. Rose *Elementary Theory of Angular Momentum* (edited by John Wiley & sons, Inc.) (1957)

[33] L. C. Biedenharn, J. Math. Phys. **2**, 433 (1961).

[34] *Handbook of Mathematical Functions* (edited by M. Abramowitz and I. A. Stegun) (Dover, New York, 1965).

[35] *Table of Integrals, Series, and Products*, (edited by I. S. Gradshyten and I. M. Ryshik) (Academic Press, Inc. 1980).

[36] William Lichten, Phys. Rev. **139** A27(1965).

[37] L. D. Landau and E. M. Lifshitz, *Mechanics* (third edition P31) (Pergamon Press).

[38] Wolfgang Fritsch and C. D. Lin, Phys. Rev. A**29** 3039 (1984).

[39] M. Kimura and C. D. Lin, Phys. Rev. A**32** 1357 (1985).

[40] A. Salin, J. Physique 45 671 (1984).

[41] J. Burgdörfer , Phys. Rev. A**24** 1756 (1981).

[42] S. Bienstock, T. G. Heil, C. Bottcher, and A. Dalgarno, Phys. Rev. A**45** 2850 (1982).

[43] L. F. Errea, B. Herrero, L. M*éndez*, and A. Riera, J. Phys. B: At. Mol. Opt. Phys. **24** 4061 (1991).

[44] L. Opradolce, L. Benmeuraiem, R. McCarroll, and R. D. Piacentini, J. Phys. B: At. Mol. Opt. Phys. **21** 503 (1987).

[45] F. G. Wilkie, R. W. McCullough, and H. B. Gilbody, J. Phys. B: At. Mol. Opt. Phys. **19** 239 (1986).

[46] C. C. Havener, W. S. Huq, H. F. Krause, P. A. Schulz, and R. A. Phaneuf, Phys. Rev. A**39** 1725(1989).

[47] Charlotte E. Moore *Atomic Energy Levels* (United States Department of Commerce National Bureau of Standards) (1949).

[48] L.R. Andersson, AIP CONFERENCE PROCEEDINGS 274, 16,1993 (paper presented at VIth International Conference on the Physics of Highly Charged Ions).

[49] C. C. Havener, F. W. Meyer, and R. A. Phaneuf, (paper presented at ICPEAC XVII, Brisbane, 1991).

[50] R. A. Phaneuf, and F. W. Meyer, Phys. Rev. A**17** 534(1977).

[51] Private Communication with S. Yu. Ovchinnikov.

[52] E. A. Solov'ev, Usp. Fiz. Nauk **157** 437 (1989).

[53] L. D. Landau and E. M. Lifshitz, *Quantum Mechanics.*

[54] R. A. Phaneuf, Phys. Rev. A**24** 1138(1981).

[55] U. Fano, and Joseph H. Macek, Rev. Mod. Phys. **45** 553(1973).

[56] D. M. Brink, and G. R. Satchler, *Angular Momentum.* (Clarendon, Oxford, 1968).

[57] U. Fano and G. Racah, *Irreducible Tensorial Sets.* (Academic Press. 1959).

[58] M. Weissbluth, *Atoms and Molecules.* (Academic Press. 1977).

[59] L. Wilets and S. J. Wallace, Phys. Rev. **169** 84 (1968).

[60] Charles J. Joachain, *Quantum Collision Theory*, (North-Holland,1987).

Appendices

Appendix A

O(4) group theory

With O(4) group theory, the Hamitonian H

$$H = \frac{1}{2}\nabla^2 - \frac{k}{r}, \tag{286}$$

The Runge - Lenz vector $\vec{A}$

$$\vec{A} = \frac{1}{2}(\vec{P} \times \vec{L} - \vec{L} \times \vec{P}) - \frac{k\vec{r}}{r}. \tag{287}$$

Here k = Z e^2. Z is the nuclear charge. The components of $\vec{A}$ and $\vec{L}$ commute with H. The various commutation relations are

$$[H\ L_i] = [H\ A_i] = 0, \tag{288}$$

$$[L_i\ L_j] = i\varepsilon_{ijk}L_k, \tag{289}$$

$$[L_i\ A_j] = i\varepsilon_{ijk}A_k, \tag{290}$$

$$[A_i\ A_j] = -2i\varepsilon_{ijk}\frac{L_k}{m}H, \tag{291}$$

e is the electron charge and m is the mass of the electron. In atomic units, $e = m = 1$. For a fixed energy subspace, H may be replaced by its eigenvalue E. I am interested in bound states only so that $E < 0$. If I define a new operator $\vec{K}$ by

$$\vec{K} = (-\frac{m}{2E})^{1/2}\vec{A}, \tag{292}$$

then I have the simple relationships

$$[L_i\ L_j] = i\varepsilon_{ijk}L_k, \tag{293}$$

$$[L_i\ K_j] = i\varepsilon_{ijk}K_k, \tag{294}$$

$$[K_i\ K_j] = i\varepsilon_{ijk}L_k. \tag{295}$$

I set

$$\vec{J}_1 = (\vec{L} + \vec{K})/2, \tag{296}$$

$$\vec{J}_2 = (\vec{L} - \vec{K})/2. \tag{297}$$

Then I have

$$[J_{1i}\ J_{1j}] = i\varepsilon_{ijk}J_{1k}, \tag{298}$$

$$[J_{2i}\ J_{2j}] = i\varepsilon_{ijk}J_{2k}, \tag{299}$$

$$[J_{1i}\ J_{2j}] = 0, \tag{300}$$

$$J_1^2 = j_1(j_1 + 1), \tag{301}$$

$$J_2^2 = j_2(j_2 + 1), \tag{302}$$

$$J_{1z} = m_1, \tag{303}$$

$$J_{2z} = m_2. \tag{304}$$

Here j_1, j_2, m_1 and m_2 are principal and magnetic quantum numbers of the operators $\vec{J}_1$ and $\vec{J}_2$. Because of $\vec{L}.\vec{A} = 0$, so that $\vec{L}.\vec{K} = 0$, I have

$$\begin{aligned} J_1^2 &= \frac{1}{4}(L^2 + K^2 + 2\vec{L}.\vec{K}) \\ &= \frac{1}{4}(L^2 + K^2 - 2\vec{L}.\vec{K}) \\ &= J_2^2, \end{aligned} \tag{305}$$

and I get $j_1 = j_2 = j$. For the fixed energy, from Eq.(291), I have

$$k^2 - A^2 = -2E(L^2 + 1), \tag{306}$$

$$A^2 = -2EK^2, \tag{307}$$

$$k^2 = -2E(L^2 + K^2 + 1), \tag{308}$$

$$\begin{aligned} L^2 + K^2 &= 4J^2 \\ &= (4j(j+1) + 1)^2 \\ &= (2j+1)^2, \end{aligned} \tag{309}$$

For the bound states, I have the energy

$$\begin{aligned} E &= -\frac{k^2}{2n^2} \\ &= -\frac{k^2}{2(2j+1)^2}, \end{aligned} \tag{310}$$

Final I get $j_1 = j_2 = \frac{n-1}{2}$.

Appendix B

Relation between Euler angles and rotational angle

For my case, the interaction potential

$$V_{int} = -\frac{z - bvL_y}{R^2}, \tag{311}$$

and the Runge - Lenz vector

$$\vec{r} = \frac{3nZ_T}{2Z_P}\vec{K}, \tag{312}$$

$$\vec{L} = \vec{J}_1 + \vec{J}_2, \tag{313}$$

$$\vec{K} = \vec{J}_1 - \vec{J}_2, \tag{314}$$

so I have

$$V_{int} = -\frac{1}{R^2}[(\frac{3nZ_T}{2Z_P}\hat{z} - bv\hat{y}).\vec{J}_1 - (\frac{3nZ_T}{2Z_P}\hat{z} + bv\hat{y}).\vec{J}_2]. \tag{315}$$

I define the unit vectors

$$\hat{n_1} = \frac{\frac{3nZ_T}{2Z_P}\hat{z} - bv\hat{y}}{\sqrt{(\frac{3nZ_T}{2Z_P})^2 + (bv)^2}}, \tag{316}$$

$$\hat{n_2} = \frac{\frac{3nZ_T}{2Z_P}\hat{z} + bv\hat{y}}{\sqrt{(\frac{3nZ_T}{2Z_P})^2 + (bv)^2}}, \tag{317}$$

and

$$\dot{\omega} = \frac{\sqrt{(\frac{3nZ_T}{2Z_P})^2 + (bv)^2}}{R^2(t)}. \tag{318}$$

The interaction potential is then written

$$V_{int} = -\dot{\omega}[\hat{n_1}.\vec{J_1} - \hat{n_2}.\vec{J_2}]. \tag{319}$$

Now $u(t,t')$ satisfies

$$i\frac{\partial}{\partial t}u(t,t') = V_{int}u(t,t'), \tag{320}$$

so I have

$$\begin{aligned} u(t,t') &= e^{-i\int V_{int}dt} \\ &= e^{i\omega(\hat{n_1}.\vec{J_1} - \hat{n_2}.\vec{J_2})}. \end{aligned} \tag{321}$$

Here

$$\begin{aligned} \omega &= \int \frac{\sqrt{(\frac{3nZ_T}{2Z_P})^2 + (bv)^2}}{R^2(t)}dt \\ &= \sqrt{(\frac{3nZ_T}{2Z_P})^2 + (bv)^2}\int \frac{1}{R^2(t)}dt. \end{aligned} \tag{322}$$

$$R^2\dot{\theta} = -bv, \tag{323}$$

so I have

$$\begin{aligned} \omega(t,t') &= -\sqrt{(\frac{3nZ_T}{2Z_P})^2 + (bv)^2}\int_{t'}^{t} \frac{\dot{\theta}}{bv}dt \\ &= \frac{\sqrt{(\frac{3nZ_T}{2Z_P})^2 + (bv)^2}}{bv}(\theta(t') - \theta(t)). \end{aligned} \tag{324}$$

The next step is to find the relationship between the Euler angles and ω, since I have

$$e^{i\omega\hat{n}.\vec{J}} = e^{i\alpha J_z} e^{i\beta J_y} e^{i\gamma J_z}. \tag{325}$$

For $\vec{J} = \frac{1}{2}\vec{\sigma} = \vec{S}$, where $\vec{\sigma}$ is the Pauli's matrix. I have

$$e^{i\frac{1}{2}\omega\hat{n}.\vec{\sigma}} = e^{i\frac{\alpha}{2}\sigma_z} e^{i\frac{\beta}{2}\sigma_y} e^{i\frac{\gamma}{2}\sigma_z}, \tag{326}$$

The left side of Eq.(326) is equal to

$$\begin{aligned} e^{i\frac{1}{2}\omega\hat{n}.\vec{\sigma}} &= \cos\frac{\omega}{2} + i(\hat{n}.\vec{\sigma})\sin\frac{\omega}{2} \\ &= \begin{pmatrix} \cos\frac{\omega}{2} + i\frac{3nZ_t}{2Z_P\sqrt{(\frac{3nZ_T}{2Z_P})^2+(bv)^2}}\sin\frac{\omega}{2} & -\frac{bv}{\sqrt{(\frac{3nZ_T}{2Z_P})^2+(bv)^2}}\sin\frac{\omega}{2} \\ \frac{bv}{\sqrt{(\frac{3nZ_T}{2Z_P})^2+(bv)^2}}\sin\frac{\omega}{2} & \cos\frac{\omega}{2} - i\frac{3nZ_t}{2Z_P\sqrt{(\frac{3nZ_T}{2Z_P})^2+(bv)^2}}\sin\frac{\omega}{2} \end{pmatrix} \end{aligned} \tag{327}$$

The right side of Eq.(326) is equal to

$$e^{i\frac{\alpha}{2}\sigma_z} e^{i\frac{\beta}{2}\sigma_y} e^{i\frac{\gamma}{2}\sigma_z} = \begin{pmatrix} \cos\frac{\beta}{2}e^{\frac{i}{2}(\alpha+\gamma)} & \sin\frac{\beta}{2}e^{\frac{i}{2}(\alpha-\gamma)} \\ -\sin\frac{\beta}{2}e^{-\frac{i}{2}(\alpha-\gamma)} & \cos\frac{\beta}{2}e^{-\frac{i}{2}(\alpha+\gamma)} \end{pmatrix}, \tag{328}$$

and I get

$$\begin{aligned} \cos\frac{\beta}{2}\cos\frac{(\alpha+\gamma)}{2} &= \cos\frac{\omega}{2}, \\ \cos\frac{\beta}{2}\sin\frac{(\alpha+\gamma)}{2} &= \frac{3nZ_T}{2Z_P\sqrt{(\frac{3nZ_T}{2Z_P})^2+(bv)^2}}\sin\frac{\omega}{2}, \\ \sin\frac{\beta}{2}\cos\frac{(\alpha-\gamma)}{2} &= -\frac{bv}{\sqrt{(\frac{3nZ_T}{2Z_P})^2+(bv)^2}}\sin\frac{\omega}{2}, \\ \sin\frac{\beta}{2}\sin\frac{(\alpha-\gamma)}{2} &= 0. \end{aligned} \tag{329}$$

I find $\alpha = \gamma$ and

$$\omega(t,t') = -\frac{\Delta\theta(t,t')}{bv}[\,(3nZ_T/2Z_P)^2 + (bv)^2\,]^{1/2}, \tag{330}$$

$$\tan\alpha(t,t') = \frac{3nZ_T}{2Z_P}[\,(3nZ_T/2Z_P)^2 + (bv)^2\,]^{-1/2}\ \tan\frac{\omega(t,t')}{2}, \tag{331}$$

$$\cos\beta(t,t') = 1 - 2\frac{[\,bv\sin\frac{\omega(t,t')}{2}\,]^2}{(3nZ_T/2Z_P)^2 + (bv)^2}. \tag{332}$$

These three equations give the Euler angles α, β, and γ in terms of the dynamical rotation parameter bv and the Stark - effect parameter $3nZ_T/2Z_P$.

Appendix C

In this appendix I simplify the matrix element

$$u_{nlm;Q}(t,t') = (-1)^{(\frac{m}{2}-j)}[e^{i\alpha}\cos\frac{\beta}{2}\sin\frac{\beta}{2}]^{2j}\left[\frac{(4j)!}{(2j+m)!(2j-m)!}\right]^{1/2}$$
$$\times\sum_{m_1m_2} < l,m|j,j;m_1,m_2 > (ie^{i\alpha}\cot\frac{\beta}{2})^{(m_1-m_2)}$$
$$\times < j,j;m_1,m_2|2j,m > \qquad (333)$$

Define

$$e^{i\chi} = ie^{i\alpha}\cot\frac{\beta}{2}, \qquad (334)$$

then,

$$\begin{aligned}
&\textstyle\sum_{m_1m_2} < l,m|j,j;m_1,m_2 > (ie^{i\alpha}\cot\frac{\beta}{2})^{(m_1-m_2)} < j,j;m_1,m_2|2j,m > \\
&= \sum_{m_1m_2} < l,m|j,j;m_1,m_2 > (e^{i\chi})^{(m_1-m_2)} < j,j;m_1,m_2|2j,m > \\
&= \sum_{m_1m_2} < l,m|(e^{i\chi})^{(\hat{J}_{1z}-\hat{J}_{2z})}|j,j;m_1,m_2 >< j,j;m_1,m_2|2j,m > \\
&= < l,m|(e^{i\chi})^{(\hat{J}_{1z}-\hat{J}_{2z})}|2j,m > \\
&= < l,m|(e^{i\chi})^{\hat{A}_3}|2j,m > . \qquad (335)
\end{aligned}$$

Here $\hat{A}_3 = \hat{J}_{1z} - \hat{J}_{2z}$. Define p=$j_1 + j_2$ = 2j, and q = $j_1 - j_2 = 0$. Using Eq.(50) of Ref. 33, I get

$$\begin{aligned}
< l,m|(e^{i\chi})^{\hat{A}_3}|2j,m > &= A^{[p,q]}_{l,m;2j,m}(\chi) \\
&= A^{[p,0]}_{l,m;p,m}(\chi) \\
&= A^{[p,0]}_{p,m;l,m}(\chi), \qquad (336)
\end{aligned}$$

with

$$A^{[p,0]}_{p,m;l,m}(\chi) = (2i)^{p-l}\frac{p!}{l!}\left[\frac{(p+m)!(p-m)!(2l)!(2l+1)!}{(l-m)!(l+m)!(2p)!(p-l)!(p+l+1)!}\right]^{1/2}$$
$$\times \sin^{p-l}\chi\, {}_2F_1(m-l,-m-l;\frac{1}{2}-l;\frac{1}{2}(1-\cos\chi)). \qquad (337)$$

Using Ref.34, Eq.(15.3.29)

$$ {}_2F_1(m-l,-m-l;\frac{1}{2}-l;\frac{1}{2}(1-\cos\chi))$$
$$= \cos^{l-m}\chi\, {}_2F_1(\frac{m-l}{2},\frac{m-l+1}{2};\frac{1}{2}-l;-\tan^2\chi), \qquad (338)$$

and Ref.35, Eq.8.812 of Gradshyten and Ryshik to write

$$ {}_2F_1(\frac{m-l}{2},\frac{m-l+1}{2};\frac{1}{2}-l;-\tan^2\chi)$$
$$= \frac{(-1)^m(l-m)!}{(2l-1)!!}(1+\cot^2\chi)^{-\frac{m}{2}}(i\cot\chi)^{m-l}P_l^m(i\cot\chi)$$
$$= \frac{(-1)^m i^{m-l}2^l l!(l-m)!}{(2l)!}\sin^l\chi\cos^{m-l}\chi P_l^m(i\cot\chi), \qquad (339)$$

I get

$$u_{nlm;Q} = (-1)^l(2j)![\frac{(2l+1)(l-m)!}{(l+m)!(2j-l)!(2j+l+1)!}]^{1/2}$$
$$\times (e^{i\alpha}\sin\beta\sin\chi)^{2j}P_l^m(i\cot\chi). \qquad (340)$$

Because

$$(2j)![\frac{(2l+1)}{(2j-l)!(2j+l+1)!}]^{1/2} =< j,j;j,-j|l,0 >, \qquad (341)$$

I have the desired expression

$$u_{nlm;Q} = (-1)^l < j,j;j,-j|l,0 > [\frac{(l-m)!}{(l+m)!}]^{1/2}(e^{i2\alpha}\cos^2\frac{\beta}{2}+\sin^2\frac{\beta}{2})^{2j}P_l^m(i\cot\chi)$$
$$= (-1)^l < j,j;j,-j|l,0 > (e^{i2\alpha}\cos^2\frac{\beta}{2}+\sin^2\frac{\beta}{2})^{2j}d^l_{m,0}(\delta). \qquad (342)$$

Here $d^l_{m,0}(\delta)$ is the rotation function, and $\cos\delta = i\cot\chi$. Because it involves a rotation function, standard angular momentum theory can be used to simplify formula involving $u_{nlm;Q}$.

Appendix D

The represention of the amplitude and probability for multiple Landau-Zener crossing

I employ the method of section 2.2 to write down the time - evolution matrix $U(t,t')$ for the collision system. The time domain is divided into 2N + 1 regions, labeled I, II,$\cdots$, 2N+1. The crossing between the initial state $|0>$ with the Stark states $|Q_1>, |Q_2>, \cdots, |Q_k>, \cdots$, and $|Q_N>$ coupling to $|0>$ occurs on the incoming part of the trajectory at $t_{1i}, t_{2i}, \cdots, t_{ki}, \cdots$, and t_{Ni} and the outgoing part at $t_{1f}, t_{2f}, \cdots, t_{kf}, \cdots$, and t_{Nf}. For the kth final level, the single Stark state

$$|Q_k>=|j_k, j_k; j_k, -j_k, >, \tag{343}$$

where $j_k = (n_k - 1)/2$, and n_k is the principal quantum of the k-level. The time $t_{1i}, t_{2i}, \cdots, t_{Ni}, t_{Nf}, \cdots$, and t_{1f} separate the regions I, II, $\cdots$, 2N+1.

The Stark eigenstates other than $|Q_k>$ are labeled by $|P_k>$. I suppose that coupling between $|0>$ and $|Q_k>$ occurs only at the Landau - Zener crossings and that $|Q_k>$ and $|P_k>$ are coupled at all times according to Eq.(28), but that $|P_k>$ does not couple directly to $|0>$. I also assume that there are not interferences between the k-level and J-level ($k \neq J$). Refer to Eq.(31), I have

$$\begin{aligned} U(\infty, -\infty) = & U(\infty, t_{1f}) U^{LZ}(t_{1f}) U(t_{1f}, t_{2f}) U^{LZ}(t_{2f}) \cdots U^{LZ}(t_{Nf}) \\ & \times U(t_{Nf}, t_{Ni}) U^{LZ}(t_{Ni}) \cdots U^{LZ}(t_{1i}) U(t_{1i}, -\infty). \end{aligned} \tag{344}$$

where

$$U^{LZ}(t_{ki}) = \begin{pmatrix} g_k & \underline{0} & s_k^* & 0 & \cdots & \cdots \\ \underline{0} & \underline{1} & \underline{0} & 0 & \cdots & \cdots \\ -s_k & \underline{0} & g_k & 0 & \cdots & \cdots \\ 0 & \underline{0} & 0 & 1 & 0 & \cdots \\ \vdots & & & & 1 & \\ \cdots & & & & & \ddots \end{pmatrix}, \tag{345}$$

$$U^{LZ}(t_{kf}) = \begin{pmatrix} g_k & \underline{0} & -s_k & 0 & \cdots & \cdots \\ \underline{0} & \underline{1} & \underline{0} & 0 & \cdots & \cdots \\ s_k^* & \underline{0} & g_k & 0 & \cdots & \cdots \\ 0 & \underline{0} & 0 & 1 & 0 & \cdots \\ \vdots & & & & 1 & \\ \cdots & & & & & \ddots \end{pmatrix}, \tag{346}$$

and

$$U(t,t') = \begin{pmatrix} U_{00}(t,t') & 0 & 0 & 0 & 0 & 0 & 0 & \cdots \\ 0 & U_{1_Q;1_Q}(t,t') & U_{1_Q;1_{P_1}}(t,t') & \cdots & 0 & 0 & 0 & \cdots \\ 0 & U_{1_{P_1};1_Q}(t,t') & U_{1_{P_1}1_{P_1}}(t,t') & \cdots & 0 & 0 & 0 & \cdots \\ \cdots & \cdots & \cdots & \cdots & \cdots & \cdots & \cdots & \cdots \\ 0 & 0 & 0 & 0 & U_{k_Q;k_Q}(t,t') & U_{k_Q;k_{P_1}}(t,t') & \cdots & 0 \\ 0 & 0 & 0 & 0 & U_{k_{P_1};k_Q}(t,t') & U_{k_{P_1};k_{P_1}}(t,t') & \cdots & 0 \\ \vdots & \vdots & \vdots & \vdots & \vdots & \vdots & \vdots & \vdots \end{pmatrix}, \tag{347}$$

here $\underline{0}$ denotes the number, which is equal to $\sum_{i=1}^{k-1} n_i^2$ of 0.

The Landau - Zener probability p_k is given by

$$p_k = |g_k|^2, \tag{348}$$

$$|s_k|^2 = 1 - p_k, \tag{349}$$

and

$$\begin{aligned} g_k &= \exp(-\pi\gamma_k), \\ s_k &= \frac{(2\pi\gamma_k)^{1/2}}{\Gamma(1+i\gamma_k)} \exp[-\frac{\pi\gamma_k}{2} + i\frac{\pi}{4} + i\gamma_k(\ln\gamma_k - 1)], \\ &= |s_k| e^{i\phi_{ks} + i\frac{\pi}{4}} \\ \gamma_k &= \frac{(9.13R_k)^2}{vZ_p(Z_p-1)[1-(\frac{b}{R_k})^2]} \exp(-1.324R_k/\sqrt{Z_P}). \end{aligned} \tag{350}$$

Where R_k is the crossing radius of k-level and ϕ_{ks} is the phase of s_k. The matrix $U(t,t')$ is given by

$$U_{00}(t,t') = \exp\left[-i\int_t^{t'} E_0(\tau)d\tau\right], \tag{351}$$

$$\begin{aligned} U_{0;k_i}(t,t') &= U(t,t')_{k_i:0} = 0, \\ & k \neq 0 \ \ and \ \ i = 1,2,\cdots n_k^2, \end{aligned} \tag{352}$$

$$\begin{aligned} U_{q_j;k_i}(t,t') &= U(t,t')_{k_i:q_j} = 0 \\ & k \neq q \neq 0 \ \ and \ \ i = 1,2,\cdots n_k^2, \ \ j = 1,2,\cdots n_q^2, \end{aligned} \tag{353}$$

and

$$U_{k_i;k_j}(t,t') = u_{k_i;k_j}(t,t') \exp\left[-i\int_t^{t'} E_k(\tau)d\tau\right], \qquad k \neq 0. \tag{354}$$

Here $E_0(t)$ and $E_k(t)$ denote the energy of the diabatic states correlating to the 1s state of one electron target and to the Rydberg level of ion, respectively. The submatrix u(t,t') is given by

$$\begin{aligned} u_{n_k,l_k,m_k;Q_k}(t,t') &= (-1)^{l_k} < j_k, j_k; j_k, -j_k | l_k, 0 > \\ &\times (e^{i2\alpha_k}\cos^2\frac{\beta_k}{2} + \sin^2\frac{\beta_k}{2})^{2j_k}\left[\frac{(l_k-m_k)!}{(l_k+m_k)!}\right]^{1/2} P_{l_k}^{m_k}(i\cot\chi_k) \\ &= (-1)^{l_k} < j_k, j_k; j_k, -j_k | l_k, 0 > \\ &\times (e^{i2\alpha_k}\cos^2\frac{\beta_k}{2} + \sin^2\frac{\beta_k}{2})^{2j_k} d^{l_k}_{m_k,0}(\delta_k), \end{aligned} \tag{355}$$

where $P_{l_k}^{m_k}(i\cot\chi_k)$ is the associated Legendre function, $d^{l_k}_{m_k,0}(\delta_k)$ is the rotation function, and α_k and β_k are the Euler angles defined by

$$\begin{aligned} \omega_k(t,t') &= -\frac{\Delta\theta_k(t,t')}{bv}[(3n_kZ_T/2Z_P)2 + (bv)^2]^{1/2}, \\ \tan\alpha_k(t,t') &= \frac{3n_kZ_T}{2Z_P}[(3n_kZ_T/2Z_P)2 + (bv)^2]^{-1/2}\tan\frac{\omega_k(t,t')}{2}, \\ \cos\beta_k(t,t') &= 1 - 2\frac{[bv\sin\frac{\omega_k(t,t')}{2}]^2}{(3n_kZ_T/2Z_P)^2 + (bv)^2}. \end{aligned} \tag{356}$$

Here $\Delta\theta_k(t,t')$ is the angle of the rotation of the internuclear axis of the k-level during the time interval (t,t'). I define the complex angle χ_k as

$$e^{i\chi_k} = ie^{i\alpha_k}\cot\frac{\beta_k}{2}, \tag{357}$$

and

$$\cos\delta_k = i\cot\chi_k. \tag{358}$$

For convenience, I set

$$\bar{u}_{Q_k;Q_k}(t_{kf},t_{ki}) = u_{Q_k;Q_k}(t_{kf},t_{ki})\exp\left[i\int_{t_{ki}}^{t_{kf}}[E_0(\tau) - E_k(\tau)]d\tau\right]. \tag{359}$$

To express my result, for k-level, I introduce Euler angles α_k and β_k with subscripts i, f and fi corresponding to time intervals (∞, t_{k_i}), (∞, t_{k_f}) and (t_{k_f}, t_{k_i}), respectively. In addition, I introduce the complex angles ζ_{kii}, ζ_{kff}, and ζ_{kif} given by

$$\zeta_{kab} = \delta_{ka} - \delta^*_{kb} \qquad a, b = i, f. \tag{360}$$

The amplitude $\mathrm{A}_{n_k l_k m_k}(\mathrm{b})$ for the populating state $n_k l_k m_k$ by capture at impact parameter b is

$$A_{n_k l_k m_k}(b) = C^f_{n_k, l_n} d^{l_k}_{m_k,0}(\delta_{kf}) + C^i_{n_k, l_n} d^{l_k}_{m_k,0}(\delta_{ki}), \tag{361}$$

where

$$\begin{aligned} C^f_{n_k,l_k} = {} & (-1)^{l_k} < j_k, j_k; j_k, -j_k | l_k, 0 > \exp[i \int_{t_{kf}}^{\infty} [E_0(t) - E_k(t)] dt] \\ & \times \left(e^{i2\alpha_{kf}} \cos^2 \frac{\beta_{kf}}{2} + \sin^2 \frac{\beta_{kf}}{2} \right)^{2j_k} \\ & \times g_1 g_2 \cdots g_{k-1} U_{0,0}(\infty, -\infty) \left\{ s^*_k g_k \left[(g_{k+1} \cdots g_N)^2 \right.\right. \\ & + (s_N g_{k+1} \cdots g_{N-1})^2 \bar{u}_{Q_N;Q_N}(t_{Nf}, t_{Ni}) \\ & + (s_{N-1} g_{k+1} \cdots g_{N-2})^2 \bar{u}_{Q_{N-1};Q_{N-1}}(t_{(N-1)f}, t_{(N-1)i}) \\ & + \cdots + s^2_{k+2} g^2_{k+1} \bar{u}_{Q_{k+2};Q_{k+2}}(t_{(k+2)f}, t_{(k+2)i}) \\ & \left.\left. + s^2_{k+1} \bar{u}_{Q_{k+1};Q_{k+1}}(t_{(k+1)f}, t_{(k+1)i}) \right] - s_k (g_k - 1) \bar{u}_{Q_k;Q_k}(t_{kf}, t_{ki}) \right\}, \end{aligned} \tag{362}$$

and

$$\begin{aligned} C^i_{n_k,l_k} = {} & (-1)^{l_k+1} < j_k, j_k; j_k, -j_k | l_k, 0 > \left(e^{i2\alpha_{kf}} \cos^2 \frac{\beta_{kf}}{2} + \sin^2 \frac{\beta_{kf}}{2} \right)^{2j_k} \\ & \times s_k g_1 g_2 \cdots g_{k-1} U_{0,0}(\infty, -\infty) \exp[i \int_{t_{ki}}^{\infty} [E_0(t) - E_k(t)] dt], \\ & 1 \le k \le N-1, \end{aligned} \tag{363}$$

$$C^f_{n_N,l_N} = (-1)^{l_N} < j_N, j_N; j_N, -j_N | l_N, 0 > \exp[i \int_{t_{Nf}}^{\infty} [E_0(t) - E_N(t)] dt]$$
$$\times \left(e^{i2\alpha_{Nf}} \cos^2 \frac{\beta_{Nf}}{2} + \sin^2 \frac{\beta_{Nf}}{2} \right)^{2j_N} g_1 g_2 \cdots g_{N-1} U_{0,0}(\infty, -\infty)$$
$$\times [s^*_N g_N - s_N(g_N - 1)\tilde{u}_{Q_N;Q_N}(t_{Nf}, t_{Ni})] , \tag{364}$$

and

$$C^i_{n_N,l_N} = (-1)^{l_N+1} < j_N, j_N; j_N, -j_N | l_N, 0 > \exp[i \int_{t_{Ni}}^{\infty} [E_0(t) - E_N(t)] dt]$$
$$\times \left(e^{i2\alpha_{Nf}} \cos^2 \frac{\beta_{Nf}}{2} + \sin^2 \frac{\beta_{Nf}}{2} \right)^{2j_N}$$
$$\times s_N g_1 g_2 \cdots g_{N-1} U_{0,0}(\infty, -\infty). \tag{365}$$

I get the probability $P_{n_k l_k m_k}$(b)

$$P_{n_k l_k m_k}(b) = |C^f_{n_k,l_k}|^2 |d^{l_k}_{m_k,0}(\delta_{kf})|^2 + |C^i_{n_k,l_k}|^2 |d^{l_k}_{m_k,0}(\delta_{ki})|^2$$
$$+ \left[C^f_{n_k,l_n} C^{*i}_{n_k,l_n} d^{l_k}_{m_k,0}(\delta_{kf}) d^{*l_k}_{m_k,0}(\delta_{ki}) + c.c. \right] . \tag{366}$$

Using the group property of the rotation functions in Eq. (50) and summing over m_k to obtain $P_{n_k l_k}$(b), the probability $P_{n_k l_k}(b)$ is

$$P_{n_k l_k}(b) = |C^f_{n_k,l_k}|^2 P_{l_k}(\cos \zeta_{kff}) + |C^i_{n_k,l_k}|^2 P_{l_k}(\cos \zeta_{kii})$$
$$+ \left[C^f_{n_k,l_n} C^{*i}_{n_k,l_n} P_{l_k}(\cos \zeta_{kfi}) + c.c. \right] , \tag{367}$$

where ζ_{kii}, ζ_{kff} and ζ_{kfi} are defined in Eq.111

As my calculation in Sec.2.2, in the low velocities region, the term $\cos \int_{t_{ki}}^{t_{kf}} [E_0(\tau) - E_k(\tau)] d\tau$ varys veries rapidly so that I can drop it. Then I get

$$P_{n_k l_k m_k}(b) = < j_k, j_k; j_k, -j_k | l_k, 0 >^2 (1 - p_k) p_1 p_2 \cdots p_{k-1}$$
$$\times \left\{ \left[(1 - \sin^2 \beta_{kf} \sin^2 \alpha_{kf})^{n_k - 1} p_k \left[(p_{k+1} \cdots p_n)^2 \right. \right. \right.$$
$$\left. \left. \left. + (1 - p_N)^2 (p_{k+1} \cdots p_{N-1})^2 |u_{Q_N,Q_N}(t_{Nf}, t_{Ni})|^2 \right. \right.$$

$$
\begin{aligned}
&+(1-p_{N-1})^2(p_{k+1}\cdots p_{N-2})^2|u_{Q_{N-1},Q_{N-1}}(t_{(N-1)f},t_{(N-1)i})|^2\\
&+\cdots+(1-p_{k+2})^2p_{k+1}^2|u_{Q_{k+2},Q_{k+2}}(t_{(k+2)f},t_{(k+2)i})|^2\\
&+(1-p_{k+1})^2|u_{Q_{k+1},Q_{k+1}}(t_{(k+1)f},t_{(k+1)i})|^2\Big]\\
&+(\sqrt{p_k}-1)^2|u_{Q_k,Q_k}(t_{kf},t_{ki})|^2\Big]\,|d^{l_k}_{m_k,0}(\delta_{kf})|^2\\
&+(1-\sin^2\beta_{ki}\sin^2\alpha_{ki})^{n_k-1}|d^{l_k}_{m_k,0}(\delta_{ki})|^2\\
&+(\sqrt{p_k}-1)\left[\left(e^{i2\alpha_{kf}}\cos^2\frac{\beta_{kf}}{2}+\sin^2\frac{\beta_{kf}}{2}\right)^{n_k-1}\right.\\
&\times\left(e^{-i2\alpha_{ki}}\cos^2\frac{\beta_{ki}}{2}+\sin^2\frac{\beta_{ki}}{2})\right)^{n_k-1}\\
&\left.\times\ d^{l_k}_{m_k,0}(\delta_{kf})d^{*l_k}_{m_k,0}(\delta_{ki})u_{Q_k,Q_k}(t_{kf},t_{ki})+c.c.\right]\Big\},\\
&\qquad 1\le k\le N-1,
\end{aligned}
\tag{368}
$$

$$
\begin{aligned}
P_{n_Nl_Nm_N}(b)&=(1-p_N)<j_N,j_N;j_N,-j_N|l_N,0>^2\\
&\times p_1p_2\cdots p_{N-1}\Big\{(1-\sin^2\beta_{Nf}\sin^2\alpha_{Nf})^{n_N-1}\\
&\times\Big[p_N+(\sqrt{p_N}-1)^2|u_{Q_N,Q_N}(t_{Nf},t_{Ni})|^2\Big]\,|d^{l_N}_{m_N,0}(\delta_{Nf})|^2\\
&+(1-\sin^2\beta_{Ni}\sin^2\alpha_{Ni})^{n_N-1}||d^{l_N}_{m_N,0}(\delta_{Ni})|^2\\
&+(\sqrt{p_N}-1)\left[\left(e^{i2\alpha_{Nf}}\cos^2\frac{\beta_{Nf}}{2}+\sin^2\frac{\beta_{Nf}}{2}\right)^{n_N-1}\right.\\
&\times\left(e^{-i2\alpha_{Ni}}\cos^2\frac{\beta_{Ni}}{2}+\sin^2\frac{\beta_{Ni}}{2})\right)^{n_N-1}\\
&\left.\times\ d^{l_N}_{m_N,0}(\delta_{Nf})d^{*l_N}_{m_N,0}(\delta_{Ni})u_{Q_N,Q_N}(t_{Nf},t_{Ni})+c.c.\right]\Big\}.
\end{aligned}
\tag{369}
$$

Summing over m_k, I find

$$
\begin{aligned}
P_{n_kl_k}(b)&=<j_k,j_k;j_k,-j_k|l_k,0>^2\,(1-p_k)p_1p_2\cdots p_{k-1}\\
&\times\Big\{\Big[(1-\sin^2\beta_{kf}\sin^2\alpha_{kf})^{n_k-1}p_k\,\Big[(p_{k+1}\cdots p_n)^2\\
&+(1-p_N)^2(p_{k+1}\cdots p_{N-1})^2|u_{Q_N,Q_N}(t_{Nf},t_{Ni})|^2
\end{aligned}
$$

$$
\begin{aligned}
&+(1-p_{N-1})^2(p_{k+1}\cdots p_{N-2})^2|u_{Q_{N-1},Q_{N-1}}(t_{(N-1)f},t_{(N-1)i})|^2\\
&+\cdots+(1-p_{k+2})^2p_{k+1}^2|u_{Q_{k+2},Q_{k+2}}(t_{(k+2)f},t_{(k+2)i})|^2\\
&+(1-p_{k+1})^2|u_{Q_{k+1},Q_{k+1}}(t_{(k+1)f},t_{(k+1)i})|^2\Big]\\
&+(\sqrt{p_k}-1)^2|u_{Q_k,Q_k}(t_{kf},t_{ki})|^2\Big]\,P_{l_k}(\cos\zeta_{kff})\\
&+(1-\sin^2\beta_{ki}\sin^2\alpha_{ki})^{n_k-1}P_{l_k}(\cos\zeta_{kii})\\
&+(\sqrt{p_k}-1)\left[\left(e^{i2\alpha_{kf}}\cos^2\frac{\beta_{kf}}{2}+\sin^2\frac{\beta_{kf}}{2}\right)^{n_k-1}\right.\\
&\times\left.\left(e^{-i2\alpha_{ki}}\cos^2\frac{\beta_{ki}}{2}+\sin^2\frac{\beta_{ki}}{2})\right)^{n_k-1}\right.\\
&\times\left.P_{l_k}(\cos\zeta_{kfi})+c.c.\right]\Big\}\,,\\
&\qquad 1\le k\le N-1,
\end{aligned}
\tag{370}
$$

where $P_l(x)$ denotes a Legendre polynomial. For the k-level, the probability is

$$
\begin{aligned}
P_{n_k}(b)=&(1-p_k)p_1p_2\cdots p_{k-1}\Big\{p_k\Big[(p_{k+1}\cdots p_N)^2\\
&+(1-p_N)^2(p_{k+1}\cdots p_{N-1})^2|u_{Q_N,Q_N}(t_{Nf},t_{Ni})|^2\\
&+(1-p_{N-1})^2(p_{k+1}\cdots p_{N-2})^2|u_{Q_{N-1},Q_{N-1}}(t_{(N-1)f},t_{(N-1)i})|^2\\
&+\cdots(1-p_{k+2})^2p_{k+1}^2|u_{Q_{k+2},Q_{k+2}}(t_{(k+2)f},t_{(k+2)i})|^2\\
&+(1-p_{k+1})^2|u_{Q_{k+1},Q_{k+1}}(t_{(k+1)f},t_{(k+1)i})|^2\Big]\\
&+1+(p_k-1)|u_{Q_k,Q_k}(t_{kf},t_{ki})|^2\Big\}\,,\\
&\qquad 1\le k\le N-1,
\end{aligned}
\tag{371}
$$

and

$$
P_{n_N}(b)=(1-p_N)p_1p_2\cdots p_{N-1}\Big\{p_N+1+(p_N-1)|u_{Q_N,Q_N}(t_{Nf},t_{Ni})|^2\Big\}\,.
\tag{372}
$$

Appendix E

The represention of the amplitude and probability for partially charged ions colliding with hydrogen

Refer to Eq.(31), the time - evolution matrix $U(\infty,-\infty)$ is

$$U(\infty,-\infty)=U(\infty,t_{(n-1)f})U^{LZ}(t_{(n-1)f})U(t_{(n-1)f},t_{(n-2)f})U^{LZ}(t_{(n-2)f})\cdots U^{LZ}(t_{Sf})$$
$$\times U(t_{Sf},t_{Si})U^{LZ}(t_{Si})\cdots U^{LZ}(t_{(n-1)i})U(t_{(n-1)i},-\infty). \tag{373}$$

where

$$U^{LZ}(t_{li})=\begin{pmatrix} g_l & \underline{0} & s_l^* & 0 & \cdots\cdots \\ \underline{0} & \underline{1} & \underline{0} & 0 & \cdots\cdots \\ -s_l & \underline{0} & g_l & 0 & \cdots\cdots \\ 0 & \underline{0} & 0 & 1 & 0\ \cdots \\ \vdots & & & & 1 \\ \cdots & & & & \ddots \end{pmatrix}, \tag{374}$$

$$U^{LZ}(t_{lf})=\begin{pmatrix} g_l & \underline{0} & -s_l & 0 & \cdots\cdots \\ \underline{0} & \underline{1} & \underline{0} & 0 & \cdots\cdots \\ s_l^* & \underline{0} & g_l & 0 & \cdots\cdots \\ 0 & \underline{0} & 0 & 1 & 0\ \cdots \\ \vdots & & & & 1 \\ \cdots & & & & \ddots \end{pmatrix}, \tag{375}$$

and

$$U(t,t') = \begin{pmatrix} U_{00}(t,t') & 0 & 0 & 0 & 0 & 0 & 0 \cdots \\ 0 & U_{n-1,0;n-1,0}(t,t')\, U_{n-1,0;n-1,1}(t,t') \cdots & & & 0 & 0 & 0 \cdots \\ 0 & U_{n-1,1;n-1,0}(t,t')\, U_{n-1,1;n-1,1}(t,t') \cdots & & & 0 & 0 & 0 \cdots \\ \cdots & \cdots & \cdots & \cdots & \cdots & \cdots & \cdots\cdots \\ 0 & 0 & 0 & 0\ U_{l,0;l,0}(t,t')\, U_{l,0;l,1}(t,t') \cdots & & & 0 \\ 0 & 0 & 0 & 0\ U_{l,1;l,0}(t,t')\, U_{l,1;l,1}(t,t') \cdots & & & 0 \\ \vdots & \vdots & \vdots & \vdots & \vdots & \vdots & \vdots\ \vdots \end{pmatrix}, \tag{376}$$

here $\underline{0}$ denots the number, which is equal to $\sum_{i=n-1}^{l-1} 2i+1$ of 0.

The Landau - Zener probability p_l is given by

$$p_l = |g_l|^2, \tag{377}$$

$$|s_l|^2 = 1 - p_l, \tag{378}$$

and

$$\begin{aligned} g_l &= \exp(-\pi\gamma_l), \\ s_l &= \frac{(2\pi\gamma_l)^{1/2}}{\Gamma(1+i\gamma_l)} \exp[-\frac{\pi\gamma_l}{2} + i\frac{\pi}{4} + i\gamma_l(\ln\gamma_l - 1)], \\ &= |s_l| e^{i\phi_{ls} + i\frac{\pi}{4}} \\ \gamma_l &= \frac{(9.13R_l)^2}{vZ_p(Z_p-1)[1-(\frac{b}{R_l})^2]} \exp(-1.324R_l/\sqrt{Z_P}). \end{aligned} \tag{379}$$

Where R_l is the crossing radius of l-sublevel and ϕ_{ls} is the phase of s_l. The matrix $U(t,t')$ is given by

$$U_{00}(t,t') = \exp\left[-i\int_t^{t'} E_0(\tau)d\tau\right], \tag{380}$$

$$U_{0;l_i}(t,t') = U_{l_i;0}(t,t') = 0,$$
$$l \neq 0 \ \ and \ \ i = 1,2,\cdots 2k+1, \tag{381}$$

$$U_{l_j;k_i}(t,t') = U_{k_i;l_j}(t,t') = 0$$
$$k \neq l \neq 0 \ \ and \ \ i = 1,2,\cdots 2k+1, \ \ j = 1,2,\cdots 2l+1, \tag{382}$$

and

$$U_{l_i;l_j}(t,t') = u_{l_i;l_j}(t,t') \exp\left[-i\int_t^{t'} E_l(\tau)d\tau\right], \qquad l \neq 0. \tag{383}$$

Here $E_0(t)$ and $E_l(t)$ denote the energy of the diabatic states correlating to the 1s state of one electron target and to the Rydberg state of ion, respectively. The submatrix u(t,t') satisfies the equation:

$$i\frac{d}{dt}u(t,t') = V_{int}u(t,t'), \tag{384}$$

according to the Eq.(122),

$$u(t,t') = e^{i\theta(t,t')L_y}, \tag{385}$$

$$u_{l,m;l,0}(t,t') = < l,m|e^{i\theta(t,t')L_y}|l,0 >$$
$$= d^l_{m,0}(\theta(t,t')), \tag{386}$$

For the single n level, the angular quantum number $l = 0,1,2,\cdots,n-1$. The amplitude $A_{lm}(b)$ is

$$A_{nlm}(b) = C^f_{nl}d^l_{m,0}(\theta_f) + C^i_{nl}d^l_{m,0}(\theta_i), \tag{387}$$

where $\theta_f = \theta(\infty, t_f)$ is the angle of rotation of the internuclear axis during the time interval (∞, t_f), $\theta_i = \theta(\infty, t_i)$ is the angle of rotation of the internuclear axis during the time interval (∞, t_i), and $\theta_{fi} = \theta(t_f, t_i)$ is the angle of rotation of the internuclear axis during the time interval (t_f, t_i). I define the rotation functions $\bar{d}^l_{m,0}(\theta(t,t'))$ are

$$\bar{d}^l_{m,m'}(\theta(t,t')) = d^l_{m,m'}(\theta(t,t'))\exp[i\int_{t'}^{t}[E_0(\tau) - E_l(\tau)]d\tau]. \tag{388}$$

The functions C^f_{nl} and C^i_{nl} are

$$\begin{aligned} C^f_{nl} = {} & g_{n-1}g_{n-2}\cdots g_{l+1}\exp[-i\int_{-\infty}^{t_{lf}} E_0(t)dt - i\int_{t_{lf}}^{\infty} E_l(t)]dt] \\ & \times\Big\{s^*_l g_l\Big[(g_{l-1}\cdots g_s)^2 + s^2_{l-1}\bar{d}^{l-1}_{0,0}(\theta_{(l-1)fi}) \\ & + (s_{l-2}g_{l-1})^2\bar{d}^{l-2}_{0,0}(\theta_{(l-2)fi}) + \cdots \\ & + (s_s g_1 g_2\cdots g_{l-1})^2\bar{d}^0_{0,0}(\theta_{Sfi})\Big] - s_l(g_l - 1)\bar{d}^l_{0,0}(\theta_{lfi})\Big\}, \end{aligned} \tag{389}$$

$$\begin{aligned} C^i_{nl} = {} & -s_l g_{n-1}g_{n-2}\cdots g_{l+1}\exp[-i\int_{-\infty}^{t_{li}} E_0(t)dt - i\int_{t_{li}}^{\infty} E_l(t)]dt], \\ & 1 \le l \le n-1, \end{aligned} \tag{390}$$

where the subscript s denotes the s-state. The rotation function $d^0_{0,0}(\theta) = 1$, this means that there is no rotation coupling in the s-state. Then the amplitude for populating s-state is

$$\begin{aligned} A_s(b) = {} & g_s g_1 g_2\cdots g_{n-1}\exp[-i\int_{-\infty}^{t_{sf}} E_0(t)dt - i\int_{t_{sf}}^{\infty} E_s(t)dt] \\ & \times\Big\{s^*_s - s_s\exp[i\int_{t_{si}}^{t_{sf}}[E_0(t) - E_s(t)]dt]\Big\}. \end{aligned} \tag{391}$$

The probability $P_{l,m}$(b)

$$\begin{aligned} P_{l,m}(b) = {} & |C^f_{n,l}|^2|d^l_{m,0}(\theta_f)|^2 + |C^i_{n,l}|^2|d^l_{m,0}(\theta_i)|^2 \\ & + \Big[C^f_{n,l}C^{*i}_{n,l}d^l_{m,0}(\theta_f)d^{*l}_{m,0}(\theta_i) + c.c.\Big]. \end{aligned} \tag{392}$$

where *c.c.* denotes complex conjugate. In the low velocities region, the term $\cos\int_{t_{li}}^{t_{lf}}[E_0(\tau)-E_l(\tau)]d\tau$ varys very rapidly so that I can drop it. Then I obtain

$$\begin{aligned}
P_{l,m}(b) = (1-p_l)p_{l+1}p_{l+2}\cdots p_{n-1}\Big\{\Big[&p_l(p_{l-1}p_{l-2}\cdots p_s)^2 \\
&+(1-p_s)^2(p_1\cdots p_{l-1})^2+(1-p_1)^2(p_2\cdots p_{l-1})^2|d^1_{0,0}(\theta_{1fi})|^2 \\
&+\cdots+(1-p_{l-2})^2p_{l-1}^2|d^{l-2}_{0,0}(\theta_{(l-2)fi})|^2 \\
&+(1-p_{l-1})^2|d^{l-1}_{0,0}(\theta_{(l-1)fi})|^2 \\
&+(\sqrt{p_l}-1)^2|d^l_{0,0}(\theta_{lfi})|^2\Big]\,|d^l_{m,0}(\theta_{lf})|^2+|d^{l_k}_{m_k,0}(\theta_{ki})|^2 \\
&-(\sqrt{p_l}-1)\left[d^l_{m,0}(\theta_{lf})d^{*l}_{m,0}(\theta_{ki})d^l_{0,0}(\theta_{lfi})+c.c.\right]\Big\}, \\
&1\le l\le n-1,
\end{aligned} \tag{393}$$

$$\begin{aligned}
P_s(b) = &\,2(1-p_s)p_sp_1p_2\cdots p_{n-1} \\
&\times[1+\sin(2\phi_s+2<Ea>)].
\end{aligned} \tag{394}$$

If I drop the term with rapidly varying factor $\sin(2\phi_s+2<Ea>)$, then

$$P_s(b) = 2(1-p_s)p_sp_1p_2\cdots p_{n-1}. \tag{395}$$

Using the group property of the rotation functions in Eq. (54) and summing over m to obtain P_l(b), I have

$$P_l(b) = |C^f_{n,l}|^2+|C^i_{n,l}|^2+\left[C^f_{n,l}C^{*i}_{n,l}P_l(\theta_{fi})+c.c.\right], \tag{396}$$

where $P_l(\theta_{fi})$ is a Legendre Polynomial.

Appendix F

The nonlinear Hamilton

In the neighbor of the branch point R_c, usually we can expand the Hamilton H as

$$H(R) = H_0(R_c) + a(R_c)(R - R_c) + b(R_c)(R - R_c)^2 + \cdots, \tag{397}$$

where $a(R_c)$ and $b(R_c)$ are constants. For the first approximation, the Hamilton H is linear function of R. H is

$$H(R) = H_0(R_c) + a(R_c)(R - R_c). \tag{398}$$

As I show in Sec.3.3, for $C^{3+} + H$ collision system, the Landau-Zener crossing radius of $3s$ state is close to the radius of the top-of-barrier. There is an interaction between them so that the Hamilton H becomes an nonlinear function of R. We can write the nonlinear Hamilton H as[52]

$$H(R) = H_0(R_c) + a(R_c)(R - R_c)^{\alpha}. \tag{399}$$

Appendix G

The represention of the Matrix $< j, m' | e^{iJ_x\phi} | j, m >$

From appendix B,

$$e^{i\phi\hat{n}.\vec{J}} = e^{i\alpha J_Z} e^{i\beta J_Y} e^{i\gamma J_Z}, \tag{400}$$

where

$$\vec{n} = n_x\vec{i} + n_y\vec{j} + n_z\vec{k}, \tag{401}$$

in present case

$$\begin{aligned} n_x &= 1, \\ n_y &= n_z = 0. \end{aligned} \tag{402}$$

For $\vec{J} = \frac{1}{2}\vec{\sigma} = \vec{S}$, where $\vec{\sigma}$ is the Pauli's matrix. I have

$$e^{i\frac{1}{2}\phi\hat{n}.\vec{\sigma}} = e^{i\frac{\alpha}{2}\sigma_z} e^{i\frac{\beta}{2}\sigma_y} e^{i\frac{\gamma}{2}\sigma_z}, \tag{403}$$

The left side of Eq.(405) is equal to

$$\begin{aligned} e^{i\frac{1}{2}\phi\sigma_x} &= \cos\frac{\phi}{2} + i\sigma_x \sin\frac{\omega}{2} \\ &= \begin{pmatrix} \cos\frac{\phi}{2} & i\sin\frac{\phi}{2} \\ i\sin\frac{\phi}{2} & \cos\frac{\phi}{2} \end{pmatrix}, \end{aligned} \tag{404}$$

The right side of Eq.(405) is equal to

$$e^{i\frac{\alpha}{2}\sigma_z} e^{i\frac{\beta}{2}\sigma_y} e^{i\frac{\gamma}{2}\sigma_z} = \begin{pmatrix} \cos\frac{\beta}{2}e^{\frac{i}{2}(\alpha+\gamma)} & \sin\frac{\beta}{2}e^{\frac{i}{2}(\alpha-\gamma)} \\ -\sin\frac{\beta}{2}e^{-\frac{i}{2}(\alpha-\gamma)} & \cos\frac{\beta}{2}e^{-\frac{i}{2}(\alpha+\gamma)} \end{pmatrix}, \tag{405}$$

and I get

$$\cos\frac{\beta}{2}\cos\frac{(\alpha+\gamma)}{2}=\cos\frac{\phi}{2},$$
$$\cos\frac{\beta}{2}\sin\frac{(\alpha+\gamma)}{2}=0,$$
$$\sin\frac{\beta}{2}\sin\frac{(\alpha-\gamma)}{2}=\sin\frac{\phi}{2}. \tag{406}$$

I find

$$\alpha=-\gamma=\frac{\pi}{2},$$
$$\phi=\beta. \tag{407}$$

Then the matrix $< j,m'|e^{iJ_x\phi}|j,m >$ is

$$\begin{aligned} < j,m'|e^{iJ_x\phi}|j,m > &= < j,m'|e^{i\alpha J_Z}e^{i\beta J_Y}e^{i\gamma J_Z}|j,m > \\ &= e^{i\frac{\pi}{2}m'}e^{-i\frac{\pi}{2}m}d^j_{m',m}(\beta) \\ &= e^{i\frac{\pi}{2}(m-m')}d^j_{m',m}(\phi). \end{aligned} \tag{408}$$

Vitae

Xingyuan Dong was born on February 16, 1946, in Zhejiang Province, P.R.China. She is the oldest child in the family and has a younger brother. When she was two and a half years old and her brother was only three months, her mother died. Her father and grandmother and her whole extended family took care of them so that the poor little girl could get a chance to go to school.

She graduated from high school in 1964, ranking the top of the entire senior class. Even though her father never married again and the family needed a woman to care for everyone, he still firmly supported her to pursue higher education. In the fall of 1964, she was accepted by Nankai University, one of the prestigious universities in China. In 1966, the Cultural Revolution began. She and all the other students were forced to quit studying and go to the countryside for reeducation. By the end of 1969, she was able to go back to Nankai University and started research under professor Guozhu Ho and professor Guoguang Mo. From 1973 to 1979, except another two years reeducation to the countryside of the northeast part of China, she worked as an instructor to teach electronmagnetic course and lab and finished all the undergraduate courses study.

With the encouragement from professor Guozhu Ho and Hanzhao Liu, she finished her Master's degree in 1982 while teaching Advanced Mathematics, the Methods of Physical Mathematics, Complex Variables, Thermodynamics and Statistical Mechanics, Quantum Mechanics and Classical Electrodynamics. With the support and inspiration from professor Guozhu Ho, she passed the English examination in 1985 and came to the United States in 1986. She did theoretical solid research work in Western Michigan University under professor A. R. McGurn for one year. In

September 1987, she joined theoretical atomic physics group directed by Dr. Joseph H. Macek at University of Nebraska, Lincoln. After Dr. Macek came to the University of Tennessee as a distinguished professor, she came to Knoxville in September in 1988. With the support of Dr. Macek, she passed TOEFL (the Test of English as a Foreign Language) in April 1990. In Summer of 1990, she started her study toward a Ph.D degree. She is expecting to get her Ph.D in Physics from University of Tennessee in January, 1994.